Department of Physics and Astronomy
University of Heidelberg

Intersecting D6-Brane Models On $\left(\mathbf{T^2} \times \mathbf{T^2} \times \mathbf{T^2}\right) / \left(\overline{\sigma} \times \mathbf{\Omega}\right)$ And $\left(\mathbf{T^2} \times \mathbf{T^2} \times \mathbf{T^2}\right) / \left(\mathbb{Z}_\mathbf{2} \times \mathbb{Z}_\mathbf{2} \times \overline{\sigma} \times \mathbf{\Omega}\right)$ Orientifolds

Bachelor Thesis in Physics
submitted by

Martin Bies

2012

This Bachelor Thesis has been carried out by
Martin Bies
at the Institut für Theoretische Physik
under the supervision of
Priv.-Doz. Dr. T. Weigand

Intersecting D6-Brane Models

The objective of this thesis is to analyize the structure of intersecting D6-brane models on the orientifolds $\mathcal{M}/(\overline{\sigma} \times \Omega) = (T^2 \times T^2 \times T^2)/(\overline{\sigma} \times \Omega)$ as well as $\mathcal{O}/(\overline{\sigma} \times \ \Omega) = (T^2 \times T^2 \times T^2)/(\mathbb{Z}_2 \times \mathbb{Z}_2 \times \overline{\sigma} \times \Omega)$.

The first part of this thesis adresses particles in intersecting D6-brane models, toroidal compactification of such models as well as supersymmetry conditions.

The second part then applies this knowledge to a class of non-supersymmetric models built on $\mathcal{M}/(\overline{\sigma} \times \Omega)$. It will be shown that the massless fermionic spectrum in one-to-one correspondance with the Standard Model matter particles. Also it will be demonstrated that Higgs particles appear and that a massless $U(1)$ gauge boson gives rise to the Standard Model hypercharge.

In the third part a supersymmetric three family model built on $\mathcal{O}/(\overline{\sigma} \times \Omega)$ is discussed. It will be shown that its massless fermionic spectrum contains all the matter particles in the Standard Model but also exotic matter. Subsequently a supersymmetric GUT model is presented, thereby demonstrating that a massless $U(1)$ gauge boson remains. So one can hope to obtain the Standard Model hypercharge after splitting the Georgi-Glashow $U(5)$ gauge group.

The final part then focuses on classifications of D6-branes. In particular bounds on the wrapping numbers of D6-branes forming supersymmetric models on $\mathcal{O}/(\Omega \times \overline{\sigma})$ will be derived.

Intersektionierende D6-Brane Modelle

Das Ziel dieser Arbeit ist die Analyse der Struktur von intersektionierenden D6-Brane Modellen auf den Orientierungsfaltigkeiten $\mathcal{M}/(\overline{\sigma} \times \Omega) = (T^2 \times T^2 \times T^2)/(\overline{\sigma} \times \Omega)$ und $\mathcal{O}/(\overline{\sigma} \times \Omega) = (T^2 \times T^2 \times T^2)/(\mathbb{Z}_2 \times \mathbb{Z}_2 \times \Omega \times \overline{\sigma})$.

Der erste Teil dieser Arbeit behandelt die Teilchen in intersektionierenden D6-Brane Modellen, torische Kompaktifizierung und Supersymmetriebedingungen.

Im zweiten Teil wird eine Familie nicht-supersymmetrischer Modelle auf der Orientierungsfaltigkeit $\mathcal{M}/(\overline{\sigma} \times \Omega)$ behandelt. Es wird gezeigt, dass das masselose fermionische Spektrum dieser Modellklasse in 1:1-Beziehung zu den Masseteilchen des Standardmodelles steht. Auch wird demonstriert, dass Higgs-Teilchen in diesen Modellen auftreten und dass durch ein masseloses $U(1)$ Eichboson die Hyperladung des Standardmodelles erhalten werden kann.

Im dritten Teil wird ein supersymmetrisches 3-Generationen-Modell auf der Orientierungsfaltigkeit $\mathcal{O}/(\overline{\sigma} \times \Omega)$ diskutiert. Es wird gezeigt, dass alle Masseteilchen des Standardmodelles im masselosen fermionischen Spektrum dieses Modelles enthalten sind, dass aber auch weitere exotische Materie auftritt. Nachfolgend wird ein supersymmetrisches GUT-Modell analysiert, wobei aufzeigt wird, dass in diesem Modell ein masseloses $U(1)$ Eichboson existiert. Daher kann man hoffen nach Spaltung der Georgi-Glashow $U(5)$ Eichgruppe die korrekte Hyperladung des Standardmodelles zu erhalten.

Der abschließende Teil dieser Arbeit beschäftigt sich mit der Klassifizierung verschiedener D6-Branen. Dabei werden Schranken für die Wicklungszahlen von D6-Branen, welche supersymmetrische Modelle auf der Orientierungsfaltigkeit $\mathcal{O}/(\overline{\sigma} \times \Omega)$ realisieren, hergeleitet.

Contents

0. Introduction

0.1. Task

The objective of this thesis is to analyize the structure of intersecting D6-brane models on the following two orientifolds

$$\begin{aligned} \mathcal{M}/\left(\overline{\sigma}\times\Omega\right) &= \left(T^2\times T^2\times T^2\right)/\left(\overline{\sigma}\times\Omega\right) \\ \mathcal{O}/\left(\overline{\sigma}\times\Omega\right) &= \left(T^2\times T^2\times T^2\right)/\left(\mathbb{Z}_2\times\mathbb{Z}_2\times\Omega\times\overline{\sigma}\right) \end{aligned} \tag{0.1}$$

In particular we face phenomenological questions whereof the most important are to realize the Standard Model matter particles and gauge bosons in terms of intersecting D6-brane models, to obtain the correct Standard Model hypercharge and to integrate Higgs doublets into such models.

0.2. Basic Concepts

During the first part of this thesis we develop the basic tools to adress this task. We start off by a brief revision of the Standard Model in chapter 1. After that intersecting D6-branes on the internal space $\mathbb{R}^2\times\mathbb{R}^2\times\mathbb{R}^2$ are considered. In particular we develop the mass formula for open strings in such models. This is presented in chapter 2. In order to obtain a four-dimensional theory we need to compactify the ten-dimensional superstring theory. In this text we focus on toroidal compactifications, in which case intersecting D6-branes become 3-cycles in the internal space and are described by homology classes. This description is introduced in chapter 3 where we also briefly discuss KK-states and winding states. We conclude this part with chapter 4 where we discuss the supersymmetry conditions that a setup of intersecting D6-branes has to satisfy in order to preserve at least $\mathcal{N}=1$ supersymmetry.

0.3. Non-Supersymmetric Models

The second part of this thesis will specialize the concepts introduced in the first part to the orientifold $\mathcal{M}/\left(\overline{\sigma}\times\Omega\right)$. Therefore we discuss the structure of this orientifold as well as R-R tadpole and K-theory constraints in chapter 5. Subsequently we present the anomaly cancelation by means of the generalized Green-Schwarz mechanism in chapter 6. We conclude this part with chapter 7, where we apply this knowledge to

a class of non-supersymmetric models that was first published in [21]. We will show that the massless fermionic spectrum is in one-to-one correspondance to the matter particles in the Standard Model. Furthermore we point out that there is a massless $U(1)$ gauge boson which allows to obtain the hypercharge of the Standard Model. Finally we discuss the multiplicities of Higgs doublets, the masses of the associated Higgs bosons and then conclude this discussion by presenting an overview over the Yukawa couplings.

0.4. Supersymmetric Models

Taking the orientifold $\mathcal{M}/(\overline{\sigma} \times \Omega)$ and requiring the massless fermionic spectrum to be in one-to-one correspondance with the Standard Model matter particles the authors of [21] derived the class of models that we discussed in the second part. This class of models is non-supersymmetric. Therefore it will in general suffer from uncanceled NS-NS tadpoles [7] which rend the model unstable. Therefore it is desirable to build supersymmetric models. Consequently one is lead to consider different orientifolds to built supersymmetric models on, which give rise to the Standard Model mattter particles.
In this thesis we choose to consider the orientifold $\mathcal{O}/(\overline{\sigma} \times \Omega)$. The structure of that orientifold as well as R-R tadpole and K-theory constraints will be discussed in chapter 8. We then apply this knowledge to a supersymmetric three family model in chapter 9 that was first published in [13]. Again we discuss the massless fermionic spectrum to show that it can account for the matter particles in the Standard Model. In contrast to the class of non-supersymmetric models discussed in chapter 7 we will also find additional exotic matter. Nevertheless there is again a massless $U(1)$ gauge boson that allows to obtain the Standard Model hypercharge. Furthermore Higgs doublets appear in this setup.
We conclude the third part by the discussion of a supersymmetric GUT model. This discussion is presented in chapter 10 and points out that there exists a massless $U(1)$ gauge boson. For that reason one can hope to obtain the Standard Model hypercharge after splitting the Georgi-Glashow $U(5)$ gauge group in order to obtain the Standard Model gauge group $U(3) \times U(2) \times U(1)$.

0.5. Number Of Supersymmetric Models

The final part of this thesis presents a classification of D6-branes in chapter 12. This classification was first published in [15] and allows to show that for a set of branes on $\mathcal{O}/(\overline{\sigma} \times \Omega)$, which is supersymmetric and satisfies both R-R tadpole and K-theory constraints, the wrapping numbers for these branes are bounded. This conclusion is presented in chapter 13.
In particular we will find that these bounds are independent of the moduli j, k and l. In order to obtain the supersymmetric model for a given number of brane stacks,

one can therefore proceed in the following manner. First one counts the number of intersecting D6-brane models which satisfy R-R tadpole cancelation and K-theory constraints and whose wrapping numbers in addition satisfy the bounds found in chapter 13. In the second step one specifies the moduli j, k and l to check the jsut-found brane configurations for supersymmetry.
To demonstrate this apporach we designed a C++ program which counts the number of one-brane models which undersaturate the R-R tadpole constraint but satisfy the K-theory constraints [1]. This is discussed in chapter 14. For further reference the major part of the code as well as the exact number of such brane configurations for $T \leq 20$ is presented in Appendix C.

[1] As pointed out in [15] such models can be completed to models satisfying R-R tadpole cancelation by adding C-type branes.

Part I.

Basic Concepts

1. The Standard Model

1.1. Particles In The Standard Model

The Standard Model contains matter particles, gauge bosons and the Higgs particle. The matter particles are chiral fermions. We list them in Table 1.1 and introduce group theoretical notations for them in Table 1.2. The latter also contains the Higgs doublets. The gauge bosons mediate the corresponding forces between matter particles and have their origin in the Standard Model gauge group $SU(3)_C \times SU(2)_W \times U(1)_Y$. For that reason there are

- 8 gauge bosons of the strong force - the gluons.
- 3 gauge bosons of the weak force - the $W^{\pm}$ and Z gauge bosons.
- 1 gauge boson of the electromagnetic force - the photon.

	Generation			Charge	Feels the force of		
	1^{st}	2^{nd}	3^{rd}	Units of e	Strong	Weak	EM
U-Type Quarks	u	c	t	$+\frac{2}{3}$	✓	✓	✓
D-Type Quarks	d	s	b	$-\frac{1}{3}$	✓	✓	✓
Charged Leptons	e	μ	τ	-1		✓	✓
Neutral Leptons	ν_e	ν_μ	ν_τ	0			✓

Table 1.1.: The matter particles in the Standard Model of particle physics.

1.2. Family Replication In The Standard Model

All matter particles appear in replicas, which carry the same charge under all forces but differ in mass. Such replicas are termed generations. To date it is not clear why precisely three generations of matter particles appear. [1] Still this is an important feature of the Standard Model. Consequently a string theory model should account for it.

[1] In order to include a $U(3)$ gauge theory into an intersecting D-brane model one needs a stack of three coincident D-branes. Oftentimes these branes are refered to as *color branes*. It has been pointed out in [21] that there is an attractive relation between the number of color branes and the number of generations of matter particles.

Symbol	Particle	Type	Chirality	Representation	Q_{em}	Q_Y
Q	quarks	fermion	L	$\left(3,\overline{2},1\right)$	$+\frac{2}{3}, -\frac{1}{3}$	$\frac{1}{6}$
U	up-quarks	fermion	R	$\left(3,\overline{1},1\right)$	$\frac{2}{3}$	$\frac{2}{3}$
D	down-quarks	fermion	R	$\left(3,\overline{1},1\right)$	$-\frac{1}{3}$	$-\frac{1}{3}$
L	leptons	fermion	L	$\left(1,\overline{2},1\right)$	$-1, 0$	$-\frac{1}{2}$
E	charged leptons	fermion	R	$\left(1,\overline{1},1\right)$	-1	-1
N	neutral leptons	fermion	R	$\left(1,\overline{1},1\right)$	0	0
Q^c	quarks	fermion	R	$\left(\overline{3},2,1\right)$	$-\frac{2}{3}, \frac{1}{3}$	$-\frac{1}{6}$
U^c	up-quarks	fermion	L	$\left(\overline{3},1,1\right)$	$-\frac{2}{3}$	$-\frac{2}{3}$
D^c	down-quarks	fermion	L	$\left(\overline{3},1,1\right)$	$\frac{1}{3}$	$\frac{1}{3}$
L^c	leptons	fermion	R	$\left(\overline{1},2,1\right)$	$1, 0$	$\frac{1}{2}$
E^c	charged leptons	fermion	L	$\left(\overline{1},1,1\right)$	1	1
N^c	neutral leptons	fermion	L	$\left(\overline{1},1,1\right)$	0	0
H_U	Higgs doublet	boson	✗	$\left(1,\overline{2},1\right)$	0	$\frac{1}{2}$
H_D	Higgs doublet	boson	✗	$\left(1,\overline{2},1\right)$	0	$-\frac{1}{2}$

Table 1.2.: Group theoretical notation for the matter particles and Higgs doublets in the Standard Model. The representations are written as $SU\left(3\right)_C \times SU\left(2\right)_W \times U\left(1\right)_Y$. Furthermore ^{c} denotes charge conjugation.

1.3. Chirality Of The Matter Particles

If the direction of motion of a particle and its spin are parallel, then that particle is right-handed. Conversely, if spin direction and direction of motion are antiparallel, then the particle is left-handed. The properties left- and right-handed are refered to as helicity or handedness.
For massive particles helicity is not well-defined, because there will always exist a Lorentz boost that inverts the direction of motion of the particle but does not affect its spin. Therefore such boosts turn left-handed particles into right-handed particles and vice versa. However, massless particles move at the speed of light. Therefore no such Lorentz boost exists and helicty is a well-defined property. It then coincides with chirality. For that reason we use these two concepts synonymously for massless particles. In particular this applies to the massless fermionic spectrum.
All matter particles in the Standard Model are massless until the electroweak theory is broken by the Higgs effect. So in particular the matter particles have well-defined helicity. The weak force acts chiraly, by which we mean that it only affects left-handed particles. Consequently chirality is a very important feature of the Standard Model and a string theory model has to account for it.

2. Factorizable D6-Brane Setup On $\mathbb{R}^6$ Internal Space

2.1. The Setup

2.1.1. String Theory Background

To describe the structure of the Standard Model a theory with both fermions and bosons is needed. So a possible candidate theory is superstring theory. In this thesis we will furthermore restrict attention to type IIA superstring theory, so that D6-branes are stable as they carry $C^{(7)}$ Ramond charge. It is also widely known that stacks of coincident Dp-branes carry $U(N)$ gauge groups [1] which makes Dp-branes natural candidates to embed the Standard Model gauge group into a string theory model.
In the subsequent sections we will also find that chiral fermions arise at the intersections of Dp-branes. Furthermore we present a natural mechanism for family replication of these string states in chapter 3. Consequently a setup of Dp-brane stacks is a very tempting candidate to set up a string theory model of the Standard Model of particle physics.

2.1.2. Spacetime Background

During this chapter we focus on a flat ten-dimensional Minkowski spacetime background $\mathbb{R}^{1,9}$ which we decompose into *external* and *internal* space as

$$\mathbb{R}^{1,9} = \mathbb{R}^{1,3} \times \mathbb{R}^6 \tag{2.1}$$

Furthermore we decompose the internal space $\mathbb{R}^6$ as

$$\mathbb{R}^6 = \mathbb{R}^2 \times \mathbb{R}^2 \times \mathbb{R}^2 \tag{2.2}$$

2.1.3. Factorizable Branes

We will consider Dp-brane setups that are made up of D6-branes only. All D6-branes are placed in the ten-dimensional spacetime such that they cover the entire external space $\mathbb{R}^{1,3}$. Therefore these branes are three-dimensional in the internal space. If

[1] In orientifold theories also $USp(2N, \mathbb{C})$ and $SO(N)$ gauge groups are possible.

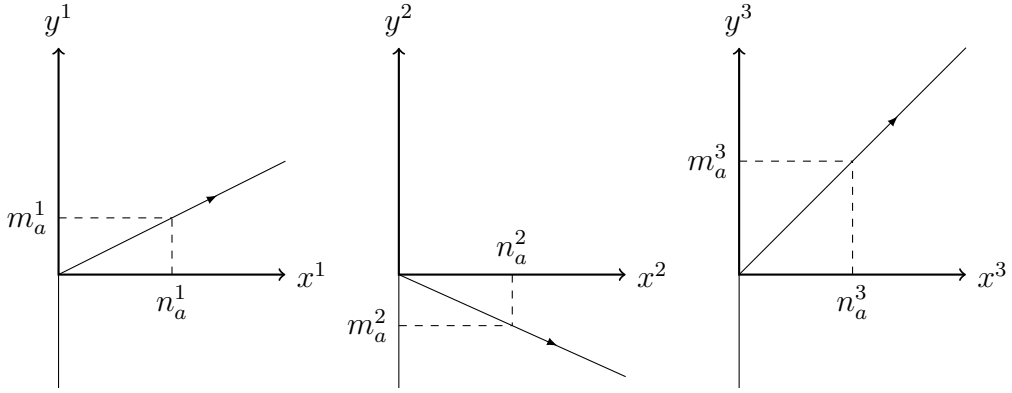

Figure 2.1.: Factorizable D6-brane a in the internal space.

furthermore this three dimensional space separates into three one-dimensional subspaces such that each subspace belongs to a different R^2, then the D6-brane is termed *factorizable*. Our analysis will focus on factorizable D6-brane stacks only.
A factorizable D6-brane stack a is completely specified by its properties in the internal space, which in turn are completely specified by the orientation of the brane stack in each $\mathbb{R}^2$ factor. We can describe this orientation in the I-th $\mathbb{R}^2$ factor by two real numbers $\left(n_a^I, m_a^I\right)$ $(I = 1, 2, 3)$. We term these numbers the *real wrapping numbers* [2]. The situation is illustrated in Figure 2.1.
By definition open strings start and end on Dp-branes. Therefore we may classify open strings according to whether they start and end on the same brane stack or start and end on different brane stacks. We term the open strings that start and end on the same brane stack the aa-sector, whilst strings stretching between different brane stacks a and b are referred to as the ab-sector. Finally there is also the closed string sector which is hardly affected by the D6-brane setup. Consequently we will focus on a discussion of the aa-sector and the ab-sector.

2.2. The ab-Sector

2.2.1. Intersection Angles

We consider two distinct, factorizable branes a and b that are given by

$$\begin{aligned} \pi_a &= \left(n_a^1 x^1 + m_a^1 y^1\right) \times \left(n_a^2 x^2 + m_a^2 y^2\right) \times \left(n_a^3 x^3 + m_a^3 y^3\right) \\ \pi_b &= \left(n_b^1 x^1 + m_b^1 y^1\right) \times \left(n_b^2 x^2 + m_b^2 y^2\right) \times \left(n_b^3 x^3 + m_b^3 y^3\right) \end{aligned} \tag{2.3}$$

[2] Later on we will perform toroidal compcatification on a $T^2 \times T^2 \times T^2$ internal space, which implies that factorizable D6-branes become 3-cycles in $H_3\left(T^2 \times T^2 \times T^2, \mathbb{Z}\right)$. The latter implies that factorizable D6-branes are then described in terms of three pairs of coprime integers, which we will term the wrapping numbers. To differ these integers from the real numbers considered during this chapter, we term the latter *real* wrapping numbers.

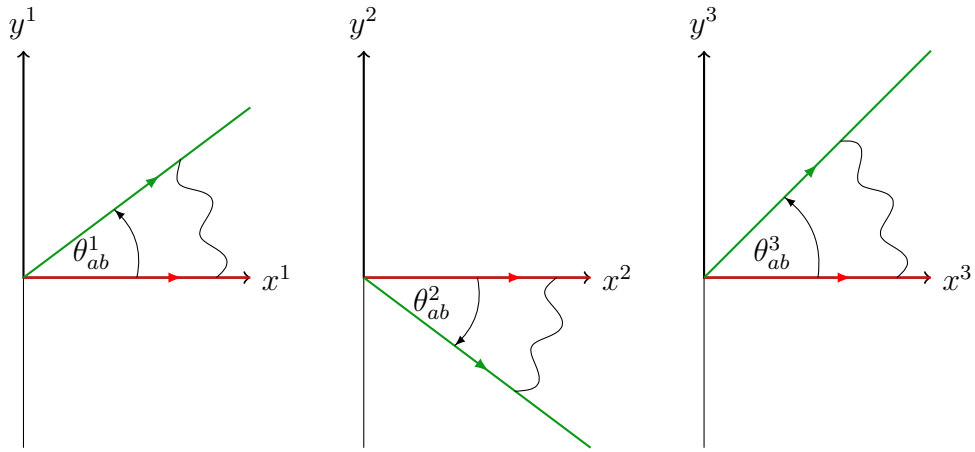

Figure 2.2.: String stretching between brane a (red) and brane b (green). For the pictured situation the intersection angles in the first and third $\mathbb{R}^2$ are positive, whilst the intersection angle in the second $\mathbb{R}^2$ is negative.

The ab-sector is then made of strings starting on brane a and ending on brane b. Without loss of generality we may align brane a with the x^I axis. This situation is pictured in Figure 2.2. We define the intersection angle between brane a and brane b in the I-th two-torus in the following way: [3]

- If brane a can be rotated into brane b by a counter-clockwise rotation about an angle α^I of or less than $\frac{\pi}{2}$, then the intersection angle is the absolute value of that angle α^I. In particular it is positive.
- If this is not possible, then brane a can be rotated into brane b by a clockwise rotation about an angle α^I of less than $\frac{\pi}{2}$. Then the intersection angle is given by the negative of the absolute value of α^I, so it is negative.

This convention implies

$$-\frac{\pi}{2} < \Theta^I_{ab} \leq \frac{\pi}{2} \tag{2.4}$$

We will first restrict our attention to intersection angles $0 < \Theta^I_{ab} < \frac{\pi}{2}$, but will find generalizsations momentarily. Finally let us define for later convenience

$$\vartheta^I_{ab} = \frac{\Theta^I_{ab}}{\pi} \tag{2.5}$$

2.2.2. Boundary Conditions

For simplicity we consider the boundary conditions for the bosonic string field only, but generalizations to the fermionic string fields are straight forward. We introduce the following notation for the bosonic string field.

[3] Note that for this definition branes are considered the same if they cover the same subspace of the spacetime. In particular parallel and anti-parallel branes are then considered the same.

- The bosonic string field in the external space is denote by X^μ.
- In the internal space we use X^I $(I = 1, 2, 3)$ for the components of the bosonic string field along the x^I directions and Y^I for the fields along the y^I directions.

In the external space the bosonic open string fields are subject to (NN) boundary conditions at both ends. In the internal space the situation is slightly more complicated because the string starts on brane a and ends on brane b. The entire situation translates into the following boundary conditions [4] [7]

- External space: $\partial_\sigma X^\mu|_{\sigma=0,\pi} = 0$
- Internal space:

$$\begin{aligned} \sigma = 0\colon &\quad 0 = \partial_\tau Y^I = \partial_\sigma X^I \\ \sigma = \pi\colon &\quad 0 = \partial_\tau \left[Y^I - \tan\left(\theta^I_{ab}\right) \cdot X^I\right] = \partial_\sigma \left[X^I + \tan\left(\theta^I_{ab}\right) Y^I\right] \end{aligned} \tag{2.6}$$

2.2.3. Mode Expansions

Solving the equation of motion

$$\partial_+\partial_- X^\mu = \partial_+\partial_- X^I = \partial_+\partial_- Y^I = 0 \tag{2.7}$$

subject to the boundary conditions in Equation 2.6 one finds the mode expansion for the bosonic string fields. In [3] the mode expnansions for both fermionic an bosonic string fields in the internal space were derived. The mode expansions in the external space can be found in [4]. To match conventions a further dressing by $\sqrt{\alpha'}$ was added to the bosonic string fields in the internal space.

Bosonic Part

We define $n_\pm := n \pm \vartheta^I_{ab}$. Then it holds [5]

$$\begin{aligned} X^\mu &= x^\mu + 2\alpha' p^\mu \tau + i\sqrt{2\alpha'} \sum_{n\in\mathbb{Z}, n\neq 0} \frac{\alpha^\mu_n}{n} e^{-in\tau} \cos(n\sigma) \\ X^I &= i\sqrt{\alpha'} \sum_{n\in\mathbb{Z}} \left[\frac{\alpha^I_{n_+}}{n_+} e^{-in_+\tau} \cos(n_+\sigma) + \frac{\alpha^I_{n_-}}{n_-} e^{-in_-\tau} \cos(n_-\sigma)\right] \\ Y^I &= i\sqrt{\alpha'} \sum_{n\in\mathbb{Z}} \left[\frac{\alpha^I_{n_+}}{n_+} e^{-in_+\tau} \sin(n_+\sigma) - \frac{\alpha^I_{n_-}}{n_-} e^{-in_-\tau} \sin(n_-\sigma)\right] \end{aligned} \tag{2.8}$$

The non-vanishing Poisson-brackets are

$$\left\{\alpha^I_{n_\pm}, \alpha^J_{n'_\mp}\right\}_{\text{P.B.}} = -in_\pm \delta_{n+n',0}\delta^{IJ}, \qquad \{\alpha^\mu_n, \alpha^\nu_{n'}\}_{\text{P.B.}} = -in\delta_{n+n',0}\eta^{\mu\nu} \tag{2.9}$$

[4] The string length has been set to π.

[5] Note that the boundary conditions force center of mass position and total momentum of the string fields in the internal space to vanish. For that reason the position of these strings is fixed in the internal space to the intersection point of the branes a and b. Thus neither KK nor winding states can appear in the ab-sector after toroidal compactification, as noted in [2].

Fermionic Part In The Ramond Sector

Here we have [6] [3]

$$\begin{aligned}
\psi^\mu &= \sum_{n\in\mathbb{Z}} \left[d_n^\mu e^{-in(\tau+\sigma)} + d_n^\mu e^{-in(\tau-\sigma)} \right] \\
\psi^I_{+,x} &= \frac{1}{\sqrt{2}} \sum_{n\in\mathbb{Z}} \left[d^I_{n_+} e^{-in_+(\tau+\sigma)} + d^I_{n_-} e^{-in_-(\tau+\sigma)} \right] \\
\psi^I_{-,x} &= \frac{1}{\sqrt{2}} \sum_{n\in\mathbb{Z}} \left[d^I_{n_+} e^{-in_+(\tau-\sigma)} + d^I_{n_-} e^{-in_-(\tau-\sigma)} \right] \\
\psi^I_{+,y} &= \frac{1}{\sqrt{2}} \cdot i \sum_{n\in\mathbb{Z}} \left[d^I_{n_+} e^{-in_+(\tau+\sigma)} - d^I_{n_-} e^{-in_-(\tau+\sigma)} \right] \\
\psi^I_{-,y} &= \frac{1}{\sqrt{2}} \cdot (-i) \sum_{n\in\mathbb{Z}} \left[d^I_{n_+} e^{-in_+(\tau-\sigma)} - d^I_{n_-} e^{-in_-(\tau-\sigma)} \right]
\end{aligned} \tag{2.10}$$

The non-vanishing Poisson bracket relations are

$$\left\{ d^I_{n_\pm}, d^J_{n'_\mp} \right\}_{\text{P.B.}} = -i\delta_{n+n',0}\delta^{IJ}, \qquad \{ d^\mu_n, d^\nu_{n'} \}_{\text{P.B.}} = -i\delta_{n+n',0}\eta^{\mu\nu} \tag{2.11}$$

Fermionic Part In The Neveu-Schwarz Sector

Here we first define $r := n + \frac{1}{2}, \qquad r_\pm := r \pm \vartheta^I_{ab}$. Then the mode expansions are [3]

$$\begin{aligned}
\psi^\mu &= \sum_{n\in\mathbb{Z}+\frac{1}{2}} \left[b^\mu_r e^{-ir(\tau+\sigma)} + b^\mu_r e^{-ir(\tau-\sigma)} \right] \\
\psi^I_{+,x} &= \frac{1}{\sqrt{2}} \sum_{n\in\mathbb{Z}} \left[b^I_{r_+} e^{-ir_+(\tau+\sigma)} + b^I_{r_-} e^{-ir_-(\tau+\sigma)} \right] \\
\psi^I_{-,x} &= \frac{1}{\sqrt{2}} \sum_{n\in\mathbb{Z}} \left[b^I_{r_+} e^{-ir_+(\tau-\sigma)} + b^I_{r_-} e^{-ir_-(\tau-\sigma)} \right] \\
\psi^I_{+,y} &= \frac{1}{\sqrt{2}} \cdot i \sum_{n\in\mathbb{Z}} \left[b^I_{r_+} e^{-ir_+(\tau+\sigma)} - b^I_{r_-} e^{-ir_-(\tau+\sigma)} \right] \\
\psi^I_{-,y} &= \frac{1}{\sqrt{2}} \cdot (-i) \sum_{n\in\mathbb{Z}} \left[b^I_{r_+} e^{-ir_+(\tau-\sigma)} - b^I_{r_-} e^{-ir_-(\tau-\sigma)} \right]
\end{aligned} \tag{2.12}$$

with non-vanishing Poisson brackets given by

$$\left\{ b^I_{r_\pm}, b^J_{r'_\mp} \right\}_{\text{P.B.}} = -i\delta_{r+r',0}\delta^{IJ}, \qquad \{ b^\mu_r, b^\nu_{r'} \}_{\text{P.B.}} = -i\delta_{r+r',0}\eta^{\mu\nu} \tag{2.13}$$

[6] The prefactor $\frac{1}{\sqrt{2}}$ is included for normalization purposes. The indices + and - refer to light-cone coordinates. So $\psi^I_{+,x}$ is the fermionic string field along the x^I direction which depends on ξ^+ only.

2.2.4. Masses For The Strings

We perform light-cone quantization. Then the masses of the strings in the ab-sector are given by [3]

$$\alpha' M^2 = N_{\perp,\nu} + \frac{Y^2}{4\pi^2\alpha'} + \nu \cdot \sum_{I=1}^{3} \vartheta^I_{ab} - \nu \tag{2.14}$$

where

- Y^2 measures the length of the string.
  For intersection angles $0 < \Theta^I_a < \frac{\pi}{2}$ the branes must intersect (as opposed to vanishing intersection angles, which would allow the branes to be parallel). Then the tension of a string forces it to be located at the intersection point. This can be seen on the mode expansion in Equation 2.8. Consequently Y^2 vanishes for such strings and we could drop the associated term here.
  However this term will be present for strings stretching between parallel branes. So we find it more natural to keep things general at this stage and to include Y^2 in the mass formula presented in Equation 2.14.

- $\nu = \begin{cases} 0 & \text{Ramond sector} \\ \frac{1}{2} & \text{Neveu-Schwarz sector} \end{cases}$

- $N_{\perp,\nu}$ is the number operator. In the Ramond sector it is given by

$$\begin{aligned} N_{\perp,0} = &\sum_{n>0} \left(\alpha^i_{-n}\alpha^i_n + n d^i_{-n} d^i_n \right) \\ &+ \sum_{n>0} \left(\alpha^I_{-n_+}\alpha^I_{n_+} + \alpha^I_{-n_-}\alpha^I_{n_-} \right) + \alpha^I_{-\vartheta^I_{ab}}\alpha^I_{\vartheta^I_{ab}} \\ &+ \sum_{n>0} \left(n_+ d^I_{-n_+} d^I_{n_+} + n_- d^I_{-n_-} d^I_{n_-} \right) + \vartheta^I_{ab} d^I_{-\vartheta^I_{ab}} d^I_{\vartheta^I_{ab}} \end{aligned} \tag{2.15}$$

  whilst in the Neveu-Schwarz sector one has

$$\begin{aligned} N_{\perp,\frac{1}{2}} = &\sum_{n>0} \left(\alpha^i_{-n}\alpha^i_n + r b^i_{-r} b^i_r \right) + \frac{1}{2} b^i_{-\frac{1}{2}} b^i_{\frac{1}{2}} \\ &+ \sum_{n>0} \left(\alpha^I_{-n_+}\alpha^I_{n_+} + \alpha^I_{-n_-}\alpha^I_{n_-} \right) + \alpha^I_{-\vartheta^I_{ab}}\alpha^I_{\vartheta^I_{ab}} \\ &+ \sum_{n\geq 0} \left(r_+ b^I_{-r_+} b^I_{r_+} + r_- b^I_{-r_-} b^I_{r_-} \right) \end{aligned} \tag{2.16}$$

  Note that the summation over I is implicit and that $i = 1, 2$ in the external space, due to our choice of light-cone quantization.

2.2.5. Ground States

Ramond Sector Ground State

We define the Ramond sector ground state via [7]

$$\alpha^i_{-n}\left|0\right\rangle_R = \alpha^I_{-n_\pm}\left|0\right\rangle_R = d^i_{-n}\left|0\right\rangle_R = d^I_{-n_\pm} = 0 \quad \forall n \in \mathbb{N} \tag{2.17}$$

So far we focused on intersection angles with $0 < \theta^I_{ab} < \frac{\pi}{2}$. Therefore the degeneracy of the Ramond sector ground states has its origin in the zero modes d^i_0 that appear in the external space.
Before light-cone quantization there are four such zero modes d^μ_0 in the external space. Their anticommutation relations match (up to a prefactor of 2) with the Clifford algebra. For that reason we conclude that the Ramond sector ground state is a Dirac spinor in the four-dimensional external space. Light-cone quantization as well as the supercurrent zero-mode constraint then imply [8]

$$\left|0\right\rangle_R = \left(\frac{1}{2}, \mathbf{1}\right) \oplus \left(\frac{1}{2}, \mathbf{1'}\right) \tag{2.18}$$

So the Ramond sector ground state is a priori a sum of positive and negative chirality spinors. However, by definition the GSO projection will keep only one chirality.

Neveu-Schwarz Sector Ground State

We define the Neveu-Schwarz sector ground state by

$$\alpha^i_{-r}\left|0\right\rangle_{NS} = \alpha^I_{-r_\pm}\left|0\right\rangle_{NS} = b^i_{-r}\left|0\right\rangle_{NS} = b^I_{-r_\pm}\left|0\right\rangle_{NS} = 0 \quad \forall r, r_\pm > 0 \tag{2.19}$$

It is not degenerate. Therefore all excitations in the NS sector are bosons.

2.2.6. GSO Projection

Ramond Sector

In the Ramond sector we define the G-parity by

$$G_R = \Gamma\,(-1)^{F_R} \tag{2.20}$$

where

$$F_R = \sum_{n=1}^{\infty} d^i_{-n} d^i_n + \sum_{n>0}^{\infty} d^I_{-n_-} d^I_{n_-} + \sum_{n=0}^{\infty} d^I_{-n_+} d^I_{n_+} \tag{2.21}$$

In this sector we keep states that have an **even fermion number**. As pointed out in [4] we can either project to states with positive or negative chirality. Our choice is here to keep states with negative chirality, i.e. the ground state in the Ramond sector obeys

$$\Gamma\left|0\right\rangle_R = -\left|0\right\rangle_R \tag{2.22}$$

[7] Our convention is that $\mathbb{N}$ does not include 0.

[8] $\left(\frac{1}{2}, 1\right)$ is a one-dimensional spinor with $s_0 = \frac{1}{2}$ and positive chirality. Correspondingly $\left(\frac{1}{2}, 1'\right)$ describes a one-dimensional spinor with $s_0 = \frac{1}{2}$ but negative chirality. More details on spinors can be found in [25].

Excitation	$\alpha'\text{Mass}^2$	Bosonic Notation
$b^1_{-t^1}\|0\rangle_{NS}$	$\frac{1}{2}(-\vartheta^1_{ab}+\vartheta^2_{ab}+\vartheta^3_{ab})$	$(-1+\vartheta^1_{ab},\vartheta^2_{ab},\vartheta^3_{ab},0)$
$b^2_{-t^2}\|0\rangle_{NS}$	$\frac{1}{2}(\vartheta^1_{ab}-\vartheta^2_{ab}+\vartheta^3_{ab})$	$(\vartheta^1_{ab},-1+\vartheta^2_{ab},\vartheta^3_{ab},0)$
$b^3_{-t^3}\|0\rangle_{NS}$	$\frac{1}{2}(\vartheta^1_{ab}+\vartheta^2_{ab}-\vartheta^3_{ab})$	$(\vartheta^1_{ab},\vartheta^2_{ab},-1+\vartheta^3_{ab},0)$
$b^1_{-t^1}b^2_{-t^2}b^3_{-t^3}\|0\rangle_{NS}$	$1-\frac{1}{2}(\vartheta^1_{ab}+\vartheta^2_{ab}+\vartheta^3_{ab})$	$(-1+\vartheta^1_{ab},-1+\vartheta^2_{ab},-1+\vartheta^3_{ab},0)$

Table 2.1.: The lightest NS states in the ab-sector. The bosonic notation is introduced in subsection 2.2.9. Furthermore we set $t^I=\frac{1}{2}-\vartheta^I_{ab}$.

Neveu-Schwarz Sector

In the Neveu-Schwarz sector we define the G-parity by

$$G_{NS}=(-1)^{F_{NS}+1} \tag{2.23}$$

where

$$F_{NS}=\sum_{n=0}^{\infty} b^i_{-r}b^i_r+\sum_{n=0}^{\infty} b^I_{-r_-}b^I_{r_-}+\sum_{n=0}^{\infty} b^I_{-r_+}b^I_{r_+} \tag{2.24}$$

The GSO-projection dictates to only keep those states in the NS sector which have positive G_{NS}-parity [4]. Those are the **states with odd fermion number** F_{NS}.

2.2.7. Lightest States In The Spectrum

Ramond Sector

The GSO projection keeps the Ramond sector ground state which has negative chirality. From Equation 2.14 it follows that the Ramond sector ground state is massless. So it is a left-handed, massless fermion.

Neveu-Schwarz Sector

The NS ground state is projected out by the GSO projection. The lightest states kept by the GSO projection are displayed in Table 2.1.

2.2.8. Comment On Angles

Negative Intersection Angles

Let us now relax our restrictions on the intersection angles and let us consider the situation of negative intersection angles. Following the path outlined above it turns out that the situation remains unchanged, except from the fact that the labels of the oscillator modes are shifted by a negative angle. The bosonic oscillator modes are therefore given by

$$\alpha^I_{n+\vartheta^I_{ab}}=\alpha^I_{n-|\vartheta^I_{ab}|},\quad \alpha^I_{n-\vartheta^I_{ab}}=\alpha^I_{n+|\vartheta^I_{ab}|} \tag{2.25}$$

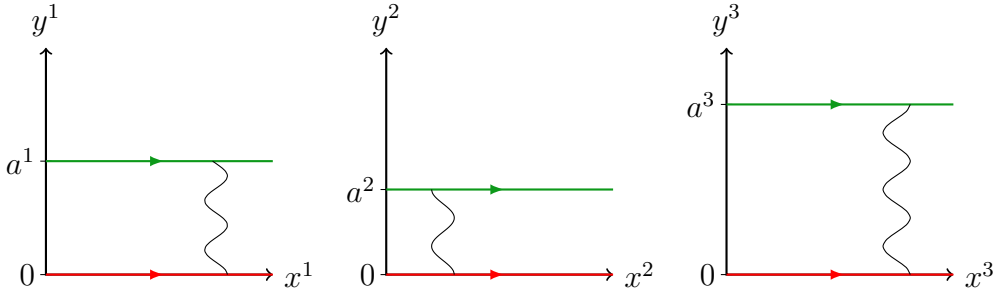

Figure 2.3.: String stretching between parallel branes a (red) and b (green). For simplicity we have placed brane a (red) on top of the x^I axis.

Obviously those modes are the same as the ones that were obtained for positive intersection angles. For fermionic modes the same logic applies.

The intersection angles $\left\vert\vartheta^I_{ab}\right\vert$ and $-\left\vert\vartheta^I_{ab}\right\vert$ give rise to the same oscillator modes.

So in particular the masses of the strings should depend on $\left\vert\vartheta^I_{ab}\right\vert$ only. Hence the mass formula generalizes to

$$\alpha' M^2 = N_{\perp,\nu} + \frac{Y^2}{4\pi^2\alpha'} + \nu \cdot \sum_{I=1}^{3} \left\vert\vartheta^I_{ab}\right\vert - \nu \tag{2.26}$$

Parallel And Orthogonal Branes

Finally we are left to discuss parallel and orthogonal branes. For simplicity we focus on bosonic strings and start off by considering parallel branes. This situation is pictured in Figure 2.3.
In the external space the situation remains unchanged. However the boundary conditions in the internal space change. Fields along the X^I directions are now subject to (NN) boundary conditions and the Y^I fields have to satisfy (DD) boundary conditions. The corresponding mode expansions for the bosonic string fields are [4]

$$\begin{aligned}
X^\mu(\tau,\sigma) &= x^\mu + 2\alpha' p^\mu \tau + i\sqrt{2\alpha'} \sum_{n\in\mathbb{Z},n\neq 0} \frac{\alpha^\mu_n}{n} e^{-in\tau} \cos(n\sigma) \\
X^I(\tau,\sigma) &= x^I + 2\alpha' p^I \tau + i\sqrt{2\alpha'} \sum_{n\in\mathbb{Z},n\neq 0} \frac{\alpha^I_{n,x}}{n} e^{-in\tau} \cos(n\sigma) \\
Y^I(\tau,\sigma) &= \frac{a^I}{\pi}\cdot\sigma + \sqrt{2\alpha'} \sum_{n\in\mathbb{Z},n\neq 0} \frac{\alpha^I_{n,y}}{n} e^{-in\tau} \sin(n\sigma)
\end{aligned} \tag{2.27}$$

The mode expansions for the fermionic string fields as well as the mass of the corresponding strings in light-cone quantization are easily obtained. It turns out that Equation 2.26 describes their mass, if the intersection angles ϑ^I_{ab} varnish and one sets $Y^2 = a^I a^I$.

Orthogonal Branes

For orthogonal branes the strings fields in the external space again have to satisfy (NN) boundary conditions. In the internal space (DN) and (ND) boundary conditions need to be satisfied. The corresponding mode expansion can be found in [4]. For this situation the oscillator modes in the internal space are shifted by $\frac{1}{2}$. Again it turns out that Equation 2.26 describes this situation for $\left|\vartheta_{ab}^I\right| = \frac{1}{2}$.

Summary

The result of the above analysis on the intersection angles is that for two branes intersecting at generic intersection angles $-\frac{1}{2} < \vartheta_{ab}^I \leq \frac{1}{2}$, the mass of the strings in the ab-sector are described by

$$\alpha' M^2 = N_{\perp,\nu} + \frac{Y^2}{4\pi^2\alpha'} + \nu \cdot \sum_I \left|\vartheta_{ab}^I\right| - \nu \tag{2.28}$$

2.2.9. Bosonic Language

In [1] it was pointed out that it is possible to describe the spectrum in the ab-sector (and the aa-sector also) in a bosonic language. To this end one introduces

$$\boldsymbol{v}_{\vartheta_{ab}} = \left(\vartheta_{ab}^1, \vartheta_{ab}^2, \vartheta_{ab}^3, 0\right)^t, \qquad \boldsymbol{r} = \left(r^1, r^2, r^3, r^4\right)^t \tag{2.29}$$

Then the states kept by the GSO projection are labeled by $\boldsymbol{v}_{\vartheta_{ab}} + \boldsymbol{r}$ where

$$r^i \in \begin{cases} \mathbb{Z} & \text{in the NS-sector} \\ \mathbb{Z} + \frac{1}{2} & \text{in the R-sector} \end{cases}, \qquad \sum_{i=1}^4 r^i = \begin{cases} \text{odd} & \text{in the NS-sector} \\ \text{even} & \text{in the R-sector} \end{cases} \tag{2.30}$$

With this notation the mass formula for the states in the ab-sector becomes

$$\alpha' M_{ab}^2 = \frac{Y^2}{4\pi^2\alpha'} + N_{\perp,\text{bos}} + \frac{(r+v)^2}{2} - \frac{1}{2} + E_{ab} \tag{2.31}$$

where

$$E_{ab} = \frac{1}{2} \cdot \sum_{I=1}^3 \left|\vartheta_{ab}^I\right| \cdot \left(1 - \left|\vartheta_{ab}^I\right|\right) \tag{2.32}$$

2.3. The aa-Sector

2.3.1. Initial Consideration

We now consider strings that start and end on the same brane. Instead of writing down the boundary conditions and solving them in order to obtain the mode expansions for the strings it is much easier to reapply the knowledge from the ab-sector. The key insight is that a string starting and ending on the same brane is equivalent to a string stretching between parallel branes with vanishing separation a^I. This is evident from Figure 2.3.

Excitation	$\alpha'\text{Mass}^2$	Bosonic Notation
$b^1_{-\frac{1}{2}} \left\|0\right\rangle_{NS}$	0	$(-1,0,0,0)$
$b^2_{-\frac{1}{2}} \left\|0\right\rangle_{NS}$	0	$(0,-1,0,0)$
$b^3_{-\frac{1}{2}} \left\|0\right\rangle_{NS}$	0	$(0,0,-1,0)$
$b^1_{-\frac{1}{2}} b^2_{-\frac{1}{2}} b^3_{-\frac{1}{2}} \left\|0\right\rangle_{NS}$	1	$(-1,-1,-1,0)$

Table 2.2.: Lightest NS states in the aa-sector.

2.3.2. Masses For The Strings

This immediately yields

$$\alpha' M^2 = \frac{Y^2}{4\pi^2\alpha'} + N_{\perp,\nu} - \nu \tag{2.33}$$

where the number operator $N_{\perp,\nu}$ in the Ramond and Neveu-Schwarz sector, respectively, is given by [9]

$$\begin{aligned} N_0 &= \sum_{n>0} (\alpha^\mu_{-n}\alpha_{n,\mu} + n d^\mu_{-n} d_{n,\mu}) \\ N_{\frac{1}{2}} &= \sum_{n>0} (\alpha^\mu_{-n}\alpha_{n,\mu} + r d^\mu_{-r} d_{r,\mu}), \qquad r = n + \frac{1}{2} \end{aligned} \tag{2.34}$$

2.3.3. Lightest States In The Spectrum

Ramond Sector

The GSO projection keeps the Ramond sector ground state, which is massless and has negative chirality. So the lightest state in the Ramond sector is a left-handed, massless fermion.

Neveu-Schwarz Sector

The NS ground state is projected out by the GSO projection. The lightest states kept by the GSO projection are displayed in Table 2.2. The three massless excitations will later become the massless gauge bosons in the Standard Model. In this context the massless fermionic groundstate in the Ramond sector, has an interpretation as supersymmetry partner of the gauge bosons.

[9] Note that here $\mu = 0, 1, 2, \ldots, 9$.

3. Toroidal Compactification

3.1. Introduction

3.1.1. The Need For Compactification

So far we have considered a ten-dimensional spacetime, where all ten dimensions are not compact. However, our aim is to built a string theory model that can give a description of the Standard Model of particle physics. The latter is formulated as four-dimensional quantum field theory. For that reason we need to compactify the six dimensions that form the internal space.

3.1.2. Ansatz

For the ten-dimensional spacetime $\mathcal{S}$ we make the ansatz $\mathcal{S} = \mathcal{N} \times \mathcal{M}$ such that

- the four-dimensional external space $\mathcal{N}$ is maximally symmetric. [1]
- the internal space $\mathcal{M}$ is six-dimensional.

To obtain stable D-brane models one should ensure the cancelation of R-R and NS-NS tadpoles. The cancelation of the former will be discussed during the next part. Moreover it was checked in [10] and [6] that in overall supersymmetric D-brane models the NS-NS tadpoles cancel precisely if the R-R tadpoles do. As we are interested in stable models we thus have to ensure the cancelation of R-R tadpoles and wish to preserve at least $\mathcal{N} = 1$ supersymmetry. It was shown in [4], that the latter leads to

- $\mathcal{N} = \mathbb{R}^{1,3}$, i.e. the external space is flat, four-dimensional Minkowski spacetime.
- $\mathcal{M}$ is a Calabi-Yau three-fold.

Compactifying finally requires to restrict attention to compact internal spaces, i.e. compact three-dimensional Calabi-Yau manifolds $\mathcal{M}$. To date it is not decided whether their number is finite [4]. Therefore such compactifications are by no means unique. However there is a particularly simple choice for such a compact Calabi-Yau three-fold, namely

$$\mathcal{M} = T^6 \tag{3.1}$$

Since we are interested in factorizable branes we decompose T^6 as

$$\mathcal{M} = T^2 \times T^2 \times T^2 \tag{3.2}$$

[1] By this we mean a space that is both homogeneous and isotropic.

Let us finally note that not every factorizable D6-brane on this internal space is supersymmetric. Rather there are additional constraints to be discussed in chapter 4.

3.1.3. From $\mathbb{R}^2 \times \mathbb{R}^2 \times \mathbb{R}^2$ to $\mathbf{T^2 \times T^2 \times T^2}$

Taking the internal space $\mathbb{R}^2 \times \mathbb{R}^2 \times \mathbb{R}^2$, that we discussed in chapter 2, as our starting point we can easily obtain a $T^2 \times T^2 \times T^2$ internal manifold by rolling up the six internal dimensions on cycles. Thus we make the identifications

$$x^I \sim x^I + 2\pi R_x^I, \qquad y^I \sim y^I + 2\pi R_y^I \tag{3.3}$$

Note that the radii are not necessarily the same.

3.2. Description Of Branes By Homology

On $T^2 \times T^2 \times T^2$ factorizable D6-brane stacks wrap 3-cycles - a 1-cycle on each two-torus. The latter are classified by the homology group $H_1\left(T^2, \mathbb{Z}\right)$ with [23]

$$H_1\left(T^2, \mathbb{Z}\right) = \mathbb{Z} \oplus \mathbb{Z}, \qquad b_1 = 2 \tag{3.4}$$

Therefore there are precisely two fundamental 1-cycles on each T^2. Let us denote the homology classes of these cycles by $\left[a^I\right]$ and $\left[b^I\right]$ (where $I = 1, 2, 3$). This allows to describe a 1-cycle on the I-th two-torus by

$$\pi_a^{(1)} = n_a^I \left[a^I\right] + m_a^I \left[b^I\right] \tag{3.5}$$

Consequently 3-cycles wrapped by factorizable branes are classified by

$$H_1\left(T^2, \mathbb{Z}\right) \times H_1\left(T^2, \mathbb{Z}\right) \times H_1\left(T^2, \mathbb{Z}\right) \subset H_3\left(T^6, \mathbb{Z}\right) \tag{3.6}$$

Hence 3-cycles wrapped by factorizable branes can be described by

$$\pi_a = \prod_{I=1}^{3} \left(n_a^I \left[a^I\right] + m_a^I \left[b^I\right]\right) \tag{3.7}$$

The integers n_a^I, m_a^I are called the **wrapping numbers** [2]. To obtain a one-to-one mapping between this description and the homology group these integers have to be coprime [27] [3]. Hence a brane with wrapping numbers $(1,1) \times (2,1) \times (1,1)$ is in agreement with this convention and can be investigated in Figure 3.1. Note in particular that topologically

$$T^2 \cong S^1 \times S^1 \tag{3.8}$$

This was used in Figure 3.1 to display the two-tori as squares.

[2] They can be seen as the analogue of the real numbers that were used in chapter 2 to describe a brane in the internal space $\mathbb{R}^2 \times \mathbb{R}^2 \times \mathbb{R}^2$.

[3] Two integers a, b are coprime precisely if the only positive integer that evenly divides both is 1.

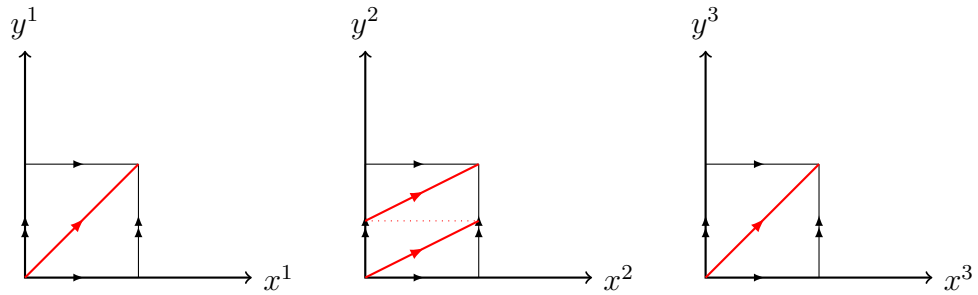

Figure 3.1.: Brane with wrapping numbers $(1,1)\times(2,1)\times(1,1)$ in $\mathcal{M} = T^2\times T^2\times T^2$ background.

3.3. Intersection Number

As we have learned in the previous chapter, chiral fermions appear in the ab-sector and are therefore located at the intersections of the factorizable D6-branes. Accordingly multiple intersections of two D6-brane stacks are a natural mechanism to integrate family replication into intersecting D-brane models. For that reason the topological intersection number between two 3-cycles is of primary interest.
We define the topological intersection numbers between fundamental 1-cycles as

$$\left[a^I\right]\circ\left[b^J\right] = -\left[b^J\right]\circ\left[a^I\right] = \delta^{IJ}, \qquad \left[a^I\right]\circ\left[a^J\right] = \left[b^I\right]\circ\left[b^J\right] = 0 \tag{3.9}$$

Then one readily checks that for two 3-cycles π_a and π_b one has [4]

$$I_{ab} := \pi_a\circ\pi_b = \prod_{I=1}^{3}\left(n_a^I m_b^I - n_b^I m_a^I\right) \tag{3.10}$$

3.4. Tilted Tori

3.4.1. The Involution

On each T^2 we can define a complex coordinate $z^I := x^I + i\cdot y^I$. By using these complex coordinates we can then define

$$\overline{\sigma}\colon T^2\times T^2\times T^2 \to T^2\times T^2\times T^2\ ,\ \left(z^1,z^2,z^3\right)\mapsto\left(\overline{z}^1,\overline{z}^2,\overline{z}^3\right) \tag{3.11}$$

This mapping $\overline{\sigma}$ is an anti-holomorphic, isometric involution. Throughout this thesis we will always use this very involution $\overline{\sigma}$. In particular we will discuss in the next chapter the need for an orientifold theory. Its construction will include (among others) dividing out by $\overline{\sigma}$.

[4] A more bottom-up derivation of this formula can be found in [27].

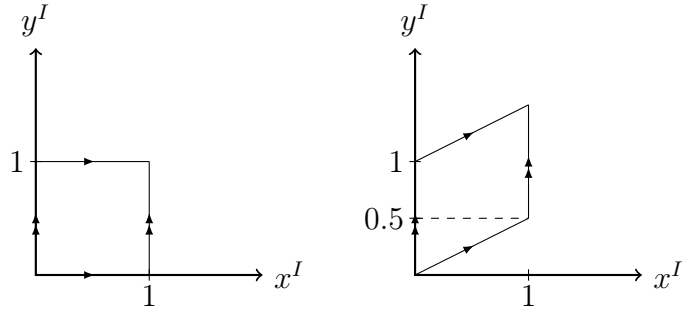

(a) Rectangular torus. (b) Tilted torus.

Figure 3.2.: The rectangular and tilted torus are invariant under the involution $\overline{\sigma}$.

3.4.2. Invariant Two-Tori

In Equation 3.11 we have assumed that $\overline{\sigma}$ maps the original two-tori to themselves. For a rectangular two-torus, as displayed in Figure 3.1, this is in fact the case. However rectangular tori are not the only two-tori that are invariant under $\overline{\sigma}$. To see this consider a two-torus spanned by

$$\boldsymbol{l}_1^I = \left[b^I\right], \qquad \boldsymbol{l}_2^I = \left[a^I\right] + \epsilon \left[b^I\right] \tag{3.12}$$

where we can focus on $\epsilon \in [0, 1)$ owing to $T^2 \cong S^1 \times S^1$. Then $\overline{\sigma}$ maps these vectors to

$$\overline{\sigma}\left(\boldsymbol{l}_1^I\right) = -\left[b^I\right] \sim \left[b^I\right], \qquad \overline{\sigma}\left(\boldsymbol{l}_2^I\right) = \left[a^I\right] - \epsilon \left[b^I\right] \sim \left[a^I\right] + (1-\epsilon)\left[b^I\right] \tag{3.13}$$

where again $T^2 \cong S^1 \times S^1$ was used - this time to make the above identifications. Enforcing invariance finally dictates

$$\epsilon = 0 \quad \vee \quad \epsilon = 1 - \epsilon \tag{3.14}$$

The case $\epsilon = 0$ yields the rectangular torus whilst $\epsilon = \frac{1}{2}$ gives a tilted torus. [5] Both are pictured in Figure 3.2.

3.4.3. Conversion Between Rectangular And Tilted Tori

It is possible to describe 3-cycles in the fundamental bases of both tilted and rectangular tori. For reasons of consistency and simplicity however, we decide to use the fundamental cycles on the rectangular tori only. Consequently we must find the

[5] This is in agreement with [7], where it has been pointed out that there exist precisely two choices for the complex structure on a two-torus, which are compatible with the involution $\overline{\sigma}$.

conversion between 1-cycles on a tilted torus and such on a rectangular torus. From Figure 3.2 one immediately reads of

$$\begin{aligned}\pi_a &= n^I_{a,\text{tilted}}\left[a^I_{\text{tilted}}\right] + m^I_{a,\text{tilted}}\left[b^I_{\text{tilted}}\right] \\ &= n^I_{a,\text{tilted}}\left[a^I\right] + \left(m^I_{a,\text{tilted}} + \frac{n^I_{a,\text{tilted}}}{2}\right)\left[b^I\right]\end{aligned} \tag{3.15}$$

Therefore let us define the NS background field as

$$b^I := \begin{cases} 0 & \text{rectangular tori} \\ \frac{1}{2} & \text{tilted tori} \end{cases} \tag{3.16}$$

which allows to define [6]

$$\widetilde{m}^I_a := m^I_a + b^I n^I_a \tag{3.17}$$

Then we can describe a cycle on both rectangular and tilted tori in terms of the fundamental cycles on a rectangular torus as

$$\pi_a = \prod_{I=1}^{3}\left(n^I_a\left[a^I\right] + \widetilde{m}^I_a\left[b^I\right]\right) \tag{3.18}$$

The topological intersection number generalizes to

$$I_{ab} = \pi_a \circ \pi_b = \prod_{I=1}^{3}\left(n^I_a\widetilde{m}^I_b - n^I_b\widetilde{m}^I_a\right) \tag{3.19}$$

3.5. Summary On States

Even in toroidal compactification the analysis from chapter 2 remains valid. Nonetheless there appear further states - the KK tower and winding states. As our primary interest in this thesis lies in the open string sector we follow [2], where more details can also be found.

3.5.1. The aa-Sector

KK States

The KK-tower of massive states appears in the aa-sector. For a 3-cycle π_a let us denote by π^I_a the corresponding 1-cycle on the I-th two-torus. Then the mass of these KK states is given by

$$M_{\text{KK}} = \frac{K_1}{|\pi^1_a|} + \frac{K_2}{|\pi^2_a|} + \frac{K_3}{|\pi^3_a|} \tag{3.20}$$

[6] Note that for tilted tori $\widetilde{m}^I_a$ is half-integer multiple.

where K_1, K_2 and K_3 are non-negative integers and the length of the 1-cycle π_a^I is given by [7]

$$\left|\pi_a^I\right| = \sqrt{\left(n_a^I R_x^I\right)^2 + \left(\widetilde{m}_a^I R_y^I\right)^2} \tag{3.21}$$

Winding States

Also winding states appear in the aa-sector. Their mass is given by

$$M_{\text{winding}} = \frac{1}{\alpha'} \cdot \left(\frac{A^1}{|\pi_a^1|} \cdot p_1 + \frac{A^2}{|\pi_a^2|} \cdot p_2 + \frac{A^3}{|\pi_a^3|} \cdot p_3 \right) \tag{3.22}$$

where $A^I = (2\pi)^2 R_x^I R_y^I$ is the area of the I-th two-torus [8] and p_1, p_2, p_3 are non-negative integers.

3.5.2. The ab-Sector

The strings in the ab-sector are located at the intersection of two D6-branes. Consequently they propagate in the external space $\mathbb{R}^{1,3}$ only. This prevents both winding states and KK states to appear in the ab-sector. Hence this sector remains unchanged with respect to chapter 2.
As we will discuss in the subsequent chapter, supersymmetry of a 3-cycle will impose a condition on the intersection angles Θ_a^I. Given enough supersymmetry the lightest bosonic excitations in the ab-sector can become massless. In that case they are supersymmetry partners of the chiral fermionic groundstate in the Ramond sector. Consequently the (would-be) supersymmetry partners of leptons and quarks are termed sleptons and squarks.
Let us note that in addition to these strings states, further excitations can appear in the ab-sector which are not located at the intersection point of the branes a and b. Such states are refered to as gonions.

3.5.3. The ba-Sector

The ba-sector is related to the ab-sector by parity transformation. After toroidal compactification T-duality arises, which implies that a parity transformation reverses chirality [4]. Therefore strings in the ab-sector and those in the ba-sector have opposite chirality, relating the two sectors by a particle-antiparticle mapping.

[7] Not only do we describe cycles exclusively in terms of the fundamental cycles of rectangular tori, but also do we use the metric on rectangular tori only. The latter is diagonal and therefore allows for a neat expression for the length of a 1-cycle. The reader may wish to compare [2], where a description in terms of the metric on tilted tori is presented.

[8] Note that this applies to both rectangular and tilted tori since we agreed to use the metric on the rectangular torus. Thus Cavalieri's principle implies equal areas for tilted and rectangular tori.

3.5.4. Massless States

From the above considerations we conclude that there are three sets of massless states in intersecting D6-brane models, namely chiral fermions in the ab-sector, gauge bosons as well as massless fermionic excitations in the aa-sector. In [21] it has been noted that the latter acquire masses due to quantum corrections. For that reason the massless spectrum will be made of the chiral fermions in the ab-sector and the gauge bosons in the aa-sector only. [9]

[9] For a more detailed discussion of massive states beyond the Standard Model particles we refer the reader to [2] and [21].

4. Supersymmetry Conditions

4.1. Introduction

As we pointed out in chapter 3 we will eventually focus on building supersymmetric models, since in such models we can ensure the cancelation of both NS-NS and R-R tadpoles. This then guaranties stability of the model. Accordingly our goal is now to discuss constraints on intersecting D6-brane models such that they preserve at least $\mathcal{N} = 1$ supersymmetry.
Let us therefore consider the general situation of an internal space given by a Calabi-Yau three-fold. As pointed out in [7] there exists a covariantly constant holomorphic 3-form Ω_3 and a Kähler 2-form J, which in local coordinates z^1, z^2 and z^3 can be expressed as

$$\Omega_3 = dz^1 \wedge dz^2 \wedge dz^3, \qquad J = i \sum_{I=1}^{3} \left(dz^I \wedge d\overline{z}^I \right) \tag{4.1}$$

The supersymmetry condition will be a constraint on the restriction of these forms to the 3-cycles wrapped by the D6-branes forming the model under consideration.

4.2. Genernal Supersymmetry Constraints

As pointed out in [7] a setup of D6-branes preserves at least one unbroken supersymmetry if every brane in the setup satisfies the following constraints.

- Constraint I: $J|_{\pi_a} = 0$
- Constraint II: $\Im\left(\Omega_3\right)|_{\pi_a} = 0$
- Constraint III: $\Re\left(\Omega_3\right)|_{\pi_a} > 0$

4.3. Analysis Of The Constraints

4.3.1. Constraint I

On a 3-cycle π_a we have

$$dy^I\Big|_{\pi_a} = \frac{\widetilde{m}_a^I}{n_a^I} \cdot u^I \; dx^I\Big|_{\pi_a} \tag{4.2}$$

where $u^I := \frac{R_y^I}{R_x^I}$. So we find $dx^I\Big|_{\pi_a} \wedge dy^I\Big|_{\pi_a} = 0$. But since $dz^I \wedge d\overline{z}^I = 2i dy \wedge dx$ this implies that $J|_{\pi_a} = 0$ is trivially satisfied for each 3-cycles π_a.

4.3.2. Constraint II

By use of $dz^I = dx^I + idy^I$ one can write

$$\Im\left(\Omega_3\right) = dx^1 \wedge dx^2 \wedge dy^3 + dx^1 \wedge dy^2 \wedge dx^3 + dy^1 \wedge dx^2 \wedge dx^3 - dy^1 \wedge dy^2 \wedge dy^3 \quad (4.3)$$

Now we use Equation 4.2 to rewrite this expression as

$$\Im\left(\Omega_3\right) = dx^1 \wedge dx^2 \wedge dx^3 \cdot \left(- \prod_{I=1}^{3} \widetilde{m}_a^I + \sum_{I \neq J \neq K \neq I} \widetilde{m}_a^I \cdot \frac{n_a^J n_a^K}{u^J u^K} \right) \quad (4.4)$$

The supersymmetry constraint II requires that this expression vanishes. So we must have

$$0 = \prod_{I=1}^{3} \widetilde{m}_a^I - \sum_{I \neq J \neq K \neq I} \widetilde{m}_a^I \cdot \frac{n_a^J n_a^K}{u^J u^K} \quad (4.5)$$

4.3.3. Constraint III

Equation 4.2 also allows to rewrite the third supersymmetry consraint. Thereby one obtains

$$\prod_{I=1}^{3} n_a^I - \sum_{I \neq J \neq K \neq I} n_a^I \widetilde{m}_a^J \widetilde{m}_a^K u^J u^K > 0 \quad (4.6)$$

4.4. Constraint On Angles

The angles that a 3-cycle π_a includes with the x^I axis are Θ_a^I [1]. We first restrict our attention to branes with $-\frac{\pi}{2} < \Theta_a^I < \frac{\pi}{2}$. Then $n_a^I \neq 0$ and we can write

$$\tan\left(\theta_a^I\right) = \frac{\widetilde{m}_a^I \cdot R_y^I}{n_a^I \cdot R_x^I} \cdot u^I \quad (4.7)$$

By using this relation we rewrite the two non-trivial supersymmetry constraints in terms of the angles Θ_a^I. This yields

$$\begin{aligned} 0 &= \sum_{I=1}^{3} \tan\left(\Theta_a^I\right) - \prod_{I=1}^{3} \tan\left(\Theta_a^I\right) := \xi_1 \\ 0 &< 1 - \tan\left(\Theta_a^1\right)\tan\left(\Theta_a^2\right) - \tan\left(\Theta_a^1\right)\tan\left(\Theta_a^3\right) - \tan\left(\Theta_a^2\right)\tan\left(\Theta_a^3\right) := \xi_2 \end{aligned} \quad (4.8)$$

Let us now define

$$\Gamma := \sum_{I=1}^{3} \Theta_a^I \quad (4.9)$$

[1] Put differently, consider the brane $\pi = \left[a^1\right]\left[a^2\right]\left[a^3\right]$. Then we consider the intersection angles between this brane π and π_a as introduced in chapter 2.

Then it holds

$$\exp(i\Gamma) = \prod_{I=1}^{3} \exp\left(i\Theta_a^I\right) \tag{4.10}$$

Let us now make use of the identity $\exp\left(i\Theta_a^I\right) = \cos\left(\Theta_a^I\right) + i\sin\left(\Theta_a^I\right)$ to expand the right-hand side of Equation 4.10. This yields [2]

$$\frac{\exp(i\Gamma)}{\prod_{I=1}^{3}\cos\left(\Theta_a^I\right)} = \xi_2 + i\xi_1 \tag{4.11}$$

But we know from Equation 4.8 $\xi_1 = 0$ and $\xi_2 > 0$. Consequently we must have

$$\Gamma = \sum_{I=1}^{3} \Theta_a^I = n \cdot 2\pi, \quad n \in \mathbb{Z} \tag{4.12}$$

The above analysis can also be applied to the remaining cases in which at least one angle Θ_a^I equals $\frac{\pi}{2}$. [3] This analysis is not difficult but lengthy. For that reason we skip it here, but encourage the interested reader to check that the above result applies in those situations.

4.5. Summary

Given a setup of factorizable D6-branes each brane has to satisfy

$$\Theta_a^1 + \Theta_a^2 + \Theta_a^3 = 0 \bmod 2\pi \tag{4.13}$$

to ensure that the complete brane setup preserves at least one unbroken supersymmetry. In addition to this constraint it should be noted [7] that the brane setup preserves $\mathcal{N} = 1$ supersymmetry if for all branes $\Theta_a^1, \Theta_a^2, \Theta_a^3 \neq 0$. If some angles vanish the setup either preserves $\mathcal{N} = 2$ supersymmetry or the maximal $\mathcal{N} = 4$ supersymmetry.

[2] The restriction $-\frac{\pi}{2} < \Theta_a^I < \frac{\pi}{2}$ implies $\cos\left(\Theta_a^I\right) \neq 0$.

[3] Recall that by our convention on intersection angles we have $-\frac{\pi}{2} < \Theta_a^I \leq \frac{\pi}{2}$ - for more details see chapter 2.

Part II.

Non-Supersymmetric Models

5. Orientifold And Constraints

5.1. The Need For Orientifolding

Our goal will be to built a string theory model of the Standard Model. In particular we want to obtain a massless fermionic spectrum as close as possible to the one of the Standard Model. Also the model should be stable. The latter needs cancelation of R-R and NS-NS tadpoles. Cancelation of R-R tadpoles is equivalent to consistency of the field equation of $G^{(8)}$, the field strength of the Ramond $C^{(7)}$ charge. From this consistency condition one obtains a condition on the homoloy class of the overall 3-cycle wrapped by all branes in the intersecting D6-brane setup. [1] This condition allows for non-trivial setups only in the presence of branes, whose Ramond $C^{(7)}$ charge is opposite to the one of the ordinary D6-branes.
As pointed out in [7] this in fact applies to an orientifold plane, e.g. an O6-plane has Ramond $C^{(7)}$ charge -4μ if μ denotes the $C^{(7)}$ charge of the D6-branes. Consequently we will consider models built on orientifolds which ensures the presence of one O6-plane.

5.2. Orientifold

5.2.1. Definition

Alltogether we decide to built a non-supersymmetric model on the orientifold

$$\mathcal{O} = \mathcal{M}/\left(\overline{\sigma} \times \Omega\right) \tag{5.1}$$

where

- $\overline{\sigma}$ is our isometric, anti-holomorphic involution which in local patches takes the form of complex conjugation.
- Ω is the parity operator.

In order to derive the gauge groups on the D6-branes one has to implement the action of $\overline{\sigma} \times \Omega$ into the Chan-Paton factors. We will not discuss this in detail but cite the corresponding results. For a detailed analysis on this implementation we refer the interested reader to [5].

[1] We present more details on this in section 5.4.

5.2.2. An Intuitive Picture For The Orientifold

After dividing out by $\overline{\sigma} \times \Omega$ we have to consider a quotient space, i.e. a set of equivalence classes. However, this is not very intuitive and we therefore prefer to consider the situation in the intuitive picture of $T^2 \times T^2 \times T^2$. Then we must consider brane configurations such that, when considered as a whole, they are invariant under the action of $\overline{\sigma}$. Consequently for each D6-brane π_a we have to include its image brane

$$\pi_a' := \overline{\sigma}\left(\pi_a\right) \tag{5.2}$$

Moreover there are points in the internal space that are invariant under the involution $\overline{\sigma}$. The set of all these points forms the orientifold plane which we denote by π_{O6}.

5.2.3. Orientifold Plane

To derive the orientifold plane in $\mathcal{M}/\left(\overline{\sigma} \times \Omega\right)$ we consider a general cycle π_a with

$$\pi_a = \prod_{i=I}^{3} \left(n_a^I \left[a^I\right] + \widetilde{m}_a^I \left[b^I\right]\right) \tag{5.3}$$

The involution acts on the tori as reflection about the x^I axis. Therefore we obtain

$$\overline{\sigma}\left(\pi_a\right) = \prod_{I=1}^{3} \left(n_a^I \left[a^I\right] - \widetilde{m}_a^I \left[b^I\right]\right) \tag{5.4}$$

We require that the 1-cycles on each T^2 are invariant under the involution. This implies

$$\widetilde{m}_a^I = m_a^I + b^I n_a^I = 0, \qquad I = 1, 2, 3 \tag{5.5}$$

For rectangular tori this requires $m_a^I = 0$. In particular there are two distinct invariant 1-cycles on a rectangular torus. For a tilted torus however, we have $b^I = \frac{1}{2}$ and invariance of π_a implies $n_a^I = -2 \cdot m_a^I$. So in particular n_a^I is even [2] and there exists only a single brane that is invariant under $\overline{\sigma}$, namely $2\left[a^I\right]$. We illustrate the $\overline{\sigma}$ invariant 1-cycles on rectangular and tilted tori in Figure 5.1.
Independent of whether or not certain tori are tilted we consequently obtain

$$\pi_{O6} = 8 \prod_{I=1}^{3} \left[a^I\right] \tag{5.6}$$

[2] A different way to find this requirement is to realized that $\left[a^I\right]$ is not closed on a tilted torus, rather one has to consider $2\left[a^I\right]$.

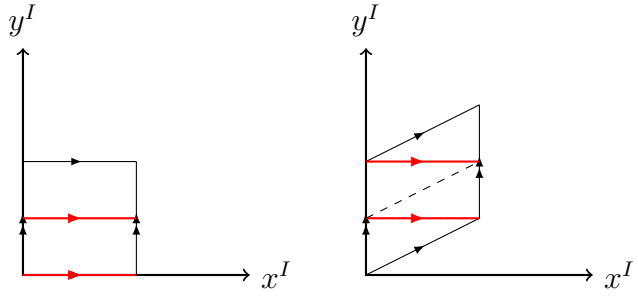

(a) Rectangular torus. (b) Tilted torus.

Figure 5.1.: The $\overline{\sigma}$-invariant 1-cycles on rectangular tori and tilted tori. Note that on tilted tori the points connected by the dashed line are identified, so that there exists only a single $\overline{\sigma}$ invariant 1-cycle on tilted tori.

5.3. Massless Fermionic Spectrum

After toroidal compactification, there are chiral fermions in the ab-sector (c.f. subsection 3.5.4). Orbifolding by $\overline{\sigma} \times \Omega$ introduces chiral fermions in the aa′-sector and ab′-sector as well. So these sectors give rise to massless fermionic states, which we will now discuss in further detail.
A D6-brane that is not invariant under $\overline{\sigma}$ will always carry a $U(N)$ gauge group. Therefore chiral fermions appearing at the intersection of such branes will transform in bifundamental, symmetric or antisymmetric representations of $U(N)$ [7].
Moreover a D6-brane setup may include brane stacks that are invariant under the involution $\overline{\sigma}$. Such a brane stack of N_a coincident branes may either carry $USp(2N_a, \mathbb{C})$ or $SO(N_a)$ gauge group. We specify the orientifold projection such that any invariant brane stack carries $USp(2N, \mathbb{C})$ gauge group. [3] In particular this implies that chiral fermions transforming under $U(N) - USp(2N, \mathbb{C})$ bifundamental representations appear in a general intersecting D6-brane setup on $\mathcal{M}/(\overline{\sigma} \times \Omega)$.
For later convenience we agree on denoting a brane π_a with $U(N_a)$ gauge group by π_a^U. Similarly π_a^{USp} is a brane with $USp(2N_a, \mathbb{C})$ gauge group. The original notation π_a then refers to brane stacks with either $U(N)$ or $USp(2N, \mathbb{C})$ gauge group.
Note that chiral fermions transforming under symmetric and antisymmetric representations of $USp(2N, \mathbb{C})$ can never appear on $\mathcal{M}/(\overline{\sigma} \times \Omega)$. Such strings would have to be located at aa′ intersections for a brane π_a^{USp}. But $\pi_a^{\mathrm{USp}} = \overline{\sigma}\left(\pi_a^{\mathrm{USp}}\right)$, so the topological intersection number $\pi_a^{\mathrm{USp}} \circ \pi_a^{\mathrm{USp}\prime}$ vanishes. Hence no matching intersection exist. We summarize our findings in Table 5.1.
Let us finally note that [22] and [13] use $USp(2N, \mathbb{C})$ gauge groups, whilst [7] [12] [11] revisited the result of [13] but used $Sp(2N, \mathbb{C})$ gauge group. Therefore we want

[3] It is a priori not clear that we can do this. However in [7] four K-theory constraints are stated, which implicitely justifies our choice.

Non-Abelian Representation	$U(1)$ Charges	Multiplicity
$\square\square_a^U$	(2_a)	$\frac{1}{2}\left(\pi_a^{U\prime}\circ\pi_a^U-\pi_{O6}\circ\pi_a^U\right)$
$\begin{smallmatrix}\square\\\square\end{smallmatrix}_a^U$	(2_a)	$\frac{1}{2}\left(\pi_a^{U\prime}\circ\pi_a^U+\pi_{O6}\circ\pi_a^U\right)$
$\left(\overline{\square}_a^U,\square_b^U\right)$	$(-1_a,1_b)$	$\pi_a^U\circ\pi_b^U$
$\left(\square_a^U,\square_b^U\right)$	$(1_a,1_b)$	$\pi_a^{U\prime}\circ\pi_b^U$
$\left(\overline{\square}_a^U,\square_a^{USp}\right)$	$\left(-1_a,\text{✗}\right)$	$\pi_a^U\circ\pi_b^{\mathrm{USp}}$
$\left(\square_a^U,\square_a^{USp}\right)$	$\left(1_a,\text{✗}\right)$	$\pi_a^{U\prime}\circ\pi_b^{\mathrm{USp}}$

Table 5.1.: Massless fermionic spectrum for intersecting D6-brane setups on $\mathcal{M}/(\overline{\sigma}\times\Omega)$. Note in particular that there is no $U(1)$ generator on the π_a^{USp} branes. More details on $Sp(2N,\mathbb{C})$ and $USp(2N,\mathbb{C})$ are presented in Appendix A.

to point out that our choice of $USp(2N,\mathbb{C})$ gauge groups is based on the fact that $USp(2N,\mathbb{C})$ has Hermitian generators. In contrast the generators of $Sp(2N,\mathbb{C})$ are Hamiltonian matrices. More information on both groups is presented in Appendix A.

5.4. R-R Tadpole Cancelation

The $C^{(7)}$ Ramond charge couples naturally to a setup of intersecting D6-branes via the Chern-Simons action.

$$\begin{aligned} S_{CS} = &\underbrace{-\frac{1}{4k^2}\int\limits_{\mathbb{R}^{3,1}\times\mathcal{M}} dC^{(7)}\wedge\star dC^{(7)}}_{=S_{\text{kin}}} \\ &\underbrace{+\mu_6\sum_a N_a\int\limits_{\mathbb{R}^{3,1}\times\pi_a} C^{(7)}+\mu_6\sum_a N_a\int\limits_{\mathbb{R}^{3,1}\times\pi_a'} C^{(7)}-4\mu_6\int\limits_{\mathbb{R}^{3,1}\times\pi_{O6}} C^{(7)}}_{S_{\text{coup}}} \end{aligned} \tag{5.7}$$

Note that the kinetic term is integrated over the entire ten-dimensional spacetime, whilst the remaining brane-coupling terms are integrated over the seven-dimensional branes only. To ensure that the action is composed of integrals over the entire ten-dimensional spacetime only, we use the Poincaré duals of π_a, π_a' and π_{O6}. Then we can rewrite the action as

$$\begin{aligned} S_{CS} = &-\frac{1}{4k^2}\int\limits_{\mathbb{R}^{3,1}\times\mathcal{M}} dC^{(7)}\wedge\star dC^{(7)}+\mu_6\sum_a N_a\int\limits_{\mathbb{R}^{3,1}\times\mathcal{M}} C^{(7)}\wedge p(\pi_a) \\ &+\mu_6\sum_a N_a\int\limits_{\mathbb{R}^{3,1}\times\mathcal{M}} C^{(7)}\wedge p(\pi_a')-4\mu_6\int\limits_{\mathbb{R}^{3,1}\times\mathcal{M}} C^{(7)}\wedge p(\pi_{O6}) \end{aligned} \tag{5.8}$$

where p indicates the mapping that assigns to a 3-cycle the corresponding Poincaré dual 3-form. [4] We require the variation of the action S_{CS} with respect to $C^{(7)}$ to vanish. This implies

$$\frac{1}{4k^2}\frac{\delta\left(dC^{(7)}\wedge\star dC^{(7)}\right)}{\delta C^{(7)}} = \mu_6\sum_a N_a\left(p\left(\pi_a\right)+p\left(\pi_a'\right)\right)-4\mu_6 p\left(\pi_{O6}\right) \tag{5.9}$$

The left-hand-side is proportional to $d\left(\star dC^{(7)}\right)=d\left(\star G^{(8)}\right)$ and is therefore exact. By using linearity and injectivity of p one then arrives at

$$[0]=\sum_a N_a\left(\pi_a+\pi_a'\right)-4\pi_{O6} \tag{5.10}$$

This constraint is easily expressed in terms of the wrapping numbers of the D6-branes in our setup, namely one obtains [5]

$$\begin{aligned}&\sum_a N_a\prod_{I=1}^{3}n_a^I=16\\&\sum_a N_a n_a^I\widetilde{m}_a^J\widetilde{m}_a^K=0,\qquad I\neq J\neq K\neq I\end{aligned} \tag{5.11}$$

5.5. K-Theory Constraints

It has been pointed out in [7] and [26] that the Ramond charges of D-branes are classified by K-theory groups rather than homology classes. Therefore there may exist uncanceled K-theory charges even if Equation 5.10 is imposed.
Heuristically one can ensure cancelation of such charges by introducing probe D6-branes that carry $USp\left(2,\mathbb{C}\right)$ gauge group and then requiring that the total number of fundamental representations of $USp\left(2,\mathbb{C}\right)$ in the world volume of these probe branes is even [22]. By our choice of the orientifold projection every brane invariant under $\overline{\sigma}$ carries $USp\left(2,\mathbb{C}\right)$ gauge group. The wrapping numbers of these probe D6-branes are [6]

$$\begin{aligned}\pi_1^{\mathrm{USp}}&=2^{2b^1}2^{2b^2}2^{2b^3}\cdot(1,0)\times(1,0)\times(1,0)\\\pi_2^{\mathrm{USp}}&=2^{2b^1}\cdot(1,0)\times(0,1)\times(0,1)\\\pi_3^{\mathrm{USp}}&=2^{2b^2}\cdot(0,1)\times(1,0)\times(0,1)\\\pi_4^{\mathrm{USp}}&=2^{2b^3}\cdot(0,1)\times(0,1)\times(1,0)\end{aligned} \tag{5.12}$$

These probe branes then give rise to the following K-theory constraints [7]

$$\begin{aligned}2^{2b^1}2^{2b^2}2^{2b^3}\cdot\sum_a N_a\widetilde{m}_a^1\widetilde{m}_a^2\widetilde{m}_a^3&\in 2\mathbb{Z}\\2^{2b^I}\cdot\sum_a N_a\widetilde{m}_a^I n_a^J n_a^K&\in 2\mathbb{Z},\qquad I\neq J\neq K\neq I\end{aligned} \tag{5.13}$$

[4] Note that this mapping is linear and injective.
[5] No summation over image branes.
[6] For tilted tori the 1-cycle $(1,0)$ is not closed (c.f. Figure 5.1). This makes it necessary to consider the 1-cycle $(2,0)$ for tilted tori, which is done by including the prefactor 2^{2b^I}.
[7] No summation over image branes.

6. Anomalies And Anomaly Cancelation

6.1. Anomalies

6.1.1. Introduction

A gauge symmetry with associated Noether current that is not conserved is by definition anomalous. The gauge theories that we encounter in the context of intersecting D6-brane models on $\mathcal{M}/(\overline{\sigma} \times \Omega)$ are $U(N) = SU(N) \times U(1)$ and $USp(2N, \mathbb{C})$. For that reason we will have to discuss the associated anomalies and their cancelation by means of the generalized Green-Schwarz mechanism. For a detailed analysis on these two topics in terms of Lagrangian field theory we point the reader to [9], whilst here we focus on its application to intersecting D6-brane models.

6.1.2. Notation

Throughout this text we use the following notation for the Lie groups $U(1)$, $SU(N)$ and $USp(2N, \mathbb{C})$.

Abelian Gauge Field

- The Abelian $U(1)_a$ gauge field on the brane stack a is denoted by C_μ^a.
- Q^a is the charge operator of the $U(1)_a$ symmetry on brane stack a. It is proportional to the identity matrix $\mathbb{1}_{d\times d}$ with d the dimension of the corresponding representation of $SU(N_a)$. The proportionality constant is the $U(1)$ charge of the representation under consideration.
- The $U(1)$ field strength is given by

$$C_{\mu\nu}^a = \partial_\mu C_\nu^a - \partial_\nu C_\mu^a \tag{6.1}$$

Non-Abelian Gauge Field

- On the brane stack a there is a non-Abelian gauge group G - either we have $G = SU(N_a)$ or $G = USp(2N_a, \mathbb{C})$. The generators of these groups are denoted by $(T^a)^A$ where $A = 1, \ldots, \dim(G)$. Note that by our choice of $USp(2N, \mathbb{C})$ gauge groups, every generator is Hermitian. Moreover the generators of $SU(N)$

are tracelsss [24]. This is also true for $USp(2N,\mathbb{C})$ (c.f. Appendix A). As $SU(N)$ and $USp(2N,\mathbb{C})$ are the only non-Abelian gauge groups that we will face throughout this text, for our purposes generators $(T^a)^A$ are always traceless.

- There will be $\dim(G)$ non-Abelian gauge fields on the brane stack a. We denote them by $\left(A^a_\mu\right)^A$.
- The non-Abelian field strength is given by

$$F^a_{\mu\nu} = \left(\partial_\mu \left(A^a_\nu\right)^A\right) T^A - \left(\partial_\nu \left(A^a_\mu\right)^A\right) T^A + \left(A^a_\mu\right)^A \left(A^a_\nu\right)^B \left[T^A, T^B\right] \tag{6.2}$$

  Note that the summation over repeated capitalised indicies is implicit.

6.1.3. Anomalies

It has been pointed out in [9], that there are the following $U(1)$ anomalies in intersecting D6-brane models on $\mathcal{M}/(\overline{\sigma}\times\Omega)$. [1]

- $U(1)_a - SU(N_b)^2$ anomalies are proportional to $\mathcal{A}^{abb} = \mathrm{tr}\left(Q^a \left(T^b\right)^A \left(T^b\right)^B\right)$.
- $U(1)_a - USp(2N_b)^2$ anomalies are proportional to $\mathcal{A}^{abb} = \mathrm{tr}\left(Q^a \left(T^b\right)^A \left(T^b\right)^B\right)$.
- $U(1)_a - U(1)_b - U(1)_c$ anomalies are proportional to $\mathcal{A}^{abc} = \mathrm{tr}\left(Q^a Q^b Q^c\right)$.
- $U(1)_a$ − gravitation anomalies are proportional to $\mathcal{A}^{agg} = \mathrm{tr}\left(Q^a\right)$.

The Feynman diagram for the $U(1)_a - U(1)_b - U(1)_c$ anomaly is given in figure 6.1a.

6.1.4. Meaning Of The Trace

Let us now specify the meaning of the trace in more detail. First note that in general Q^a and $\left(T^b\right)^A$ are matrices of different dimension, so that $Q^a \left(T^b\right)^A \left(T^b\right)^B$ is in general not defined. Also $Q^aQ^bQ^c$ suffers from this lack of matching dimensionalities. Therefore we agree on splitting the argument of the trace into pieces of matching dimensionality and then to perform the trace over these pieces individually.
Furthermore the trace is meant to be a sum over all massless fermionic states given in Table 5.1 that are charged under the participating fields.

[1] The $U(1)_a - USp(2N_b,\mathbb{C})^2$ anomalies were not given in [9] because the authors focused on $U(N)$ gauge groups in the corresponding section.

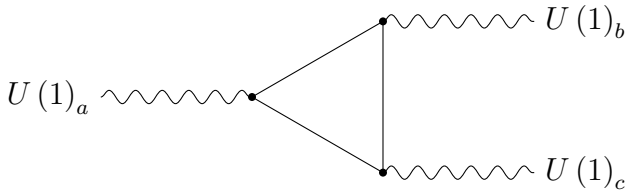

(a) Origin of the $\widetilde{\mathcal{A}}^{abc}$ anomaly.

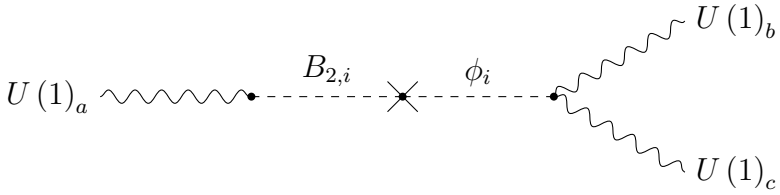

(b) The counterterm of the $\widetilde{\mathcal{A}}^{abc}$ anomaly

Figure 6.1.: Feynman diagrams for the $\widetilde{\mathcal{A}}^{abc}$ anomaly. For the $U(1)_a - U(1)_b^2$ anomaly it holds $S = 2! = 2$, whilst for $U(1)_a^3$ one has $S = 3! = 6$.

6.1.5. Further Anomalies

In addition to the $U(1)$ anomalies given in subsection 6.1.3 one could a priori have anomalies of the following types

- $U(1)_a^2 - SU(N_a)$
- $U(1)_a^2 - USp(2N_b, \mathbb{C})$
- $SU(N_a) - USp(2N_b, \mathbb{C})^2$
- $SU(N_a)^2 - USp(2N_b, \mathbb{C})$.

But note that these anomalies all vanish after splitting the trace, since the generators of $SU(N_a)$ and $USp(2N_b, \mathbb{C})$ are traceless. Nevertheless cubic anomalies of the type $SU(N_a)^3$ or $USp(2N_b, \mathbb{C})^3$ can appear and do not vanish a priori. Therefore we will calculate these anomalies now.

6.2. Calculation Of Cubic Anomalies

6.2.1. SU(N)-SU(N)-SU(N) Anomaly

Let us compute the $SU(N_a)^3$ anomaly for the fermionic spectrum given in Table 5.1. One has

$$\mathcal{A}^{aaa} = \mathrm{tr}\left((T^a)^A \left\{(T^a)^B, (T^a)^C\right\}\right) \tag{6.3}$$

Representation r	$D(r)$	$Q(r)$	$C(r)$	$A(r)$
F	N	1	$\frac{1}{2}$	1
$\overline{F}$	N	-1	$\frac{1}{2}$	-1
S	$\frac{N(N+1)}{2}$	2	$\frac{N+2}{2}$	$N+4$
$\overline{S}$	$\frac{N(N+1)}{2}$	-2	$\frac{N+2}{2}$	$-N-4$
A	$\frac{N(N-1)}{2}$	2	$\frac{N+2}{2}$	$N-4$
$\overline{A}$	$\frac{N(N-1)}{2}$	-2	$\frac{N+2}{2}$	$-N+4$

Table 6.1.: Properties of fundamental F, symmetric S and antisymmetric A representations of $SU(N)$ [22]. The dimension of the representations is denoted by $D(r)$. $Q(r)$ is the $U(1)$ charge under the decomposition $U(N) = SU(N) \times U(1)$. The quadratic and cubic Casimir coefficients are denoted by $C(r)$ and $A(r)$, respectively.

As noted above the trace is meant to be a sum over the traces of the various fermionic representations that are charged under $SU(N_a)$. Therefore we find

$$\begin{aligned}\mathcal{A}^{aaa} = &\frac{1}{2}\left(\pi_a^{U\prime}\circ\pi_a^U - \pi_{O6}\circ\pi_a^U\right)\mathrm{tr}_S\left((T^a)^A\left\{(T^a)^B,(T^a)^C\right\}\right)\\ &+\frac{1}{2}\left(\pi_a^{U\prime}\circ\pi_a^U + \pi_{O6}\circ\pi_a^U\right)\mathrm{tr}_A\left((T^a)^A\left\{(T^a)^B,(T^a)^C\right\}\right)\\ &+\sum_{b\neq a}N_b\cdot\left(\pi_a^U\circ\pi_b\right)\mathrm{tr}_{\overline{F}}\left((T^a)^A\left\{(T^a)^B,(T^a)^C\right\}\right)\\ &+\sum_{b\neq a}N_b\cdot\left(\pi_a^{U\prime}\circ\pi_b\right)\mathrm{tr}_F\left((T^a)^A\left\{(T^a)^B,(T^a)^C\right\}\right)\end{aligned} \tag{6.4}$$

We now need to evaluate the traces. We do so by using the information provided in Table 6.1. Then we find

$$\begin{aligned}\mathcal{A}^{aaa} = &\frac{N_a+4}{2}\left(\pi_a^{U\prime}\circ\pi_a^U - \pi_{O6}\circ\pi_a^U\right)\xi^{ABC}\\ &+\frac{N_a-4}{2}\left(\pi_a^{U\prime}\circ\pi_a^U + \pi_{O6}\circ\pi_a^U\right)\xi^{ABC}\\ &-\sum_{b\neq a}N_b\cdot\left(\pi_a^U\circ\pi_b\right)\xi^{ABC}\\ &+\sum_{b\neq a}N_b\cdot\left(\pi_a^{U\prime}\circ\pi_b\right)\xi^{ABC}\\ = &-\pi_a^U\circ\left(\sum_b N_b\left(\pi_b+\pi_b'\right)-4\pi_{O6}\right)\xi^{ABC}\end{aligned} \tag{6.5}$$

But recall that R-R tadpole cancelation gave us the constraint

$$\sum_b N_b\left(\pi_b+\pi_b'\right) = 4\pi_{O6} \tag{6.6}$$

So the $SU(N_a)^3$ anomaly vanishes if we impose R-R tadpole cancelation.

Anomaly	Label	Formula
$U(1)_a - SU(N_b)^2$	$\mathcal{A}^{abb}$	$\frac{N_a}{2}\left(-\pi_a^U + \pi_a^{U\prime}\right) \circ \pi_b^U$
$U(1)_a - USp(2N_b,\mathbb{C})^2$	$\mathcal{A}^{aUSpUSp}$	$\frac{N_a}{2}\left(-\pi_a^U + \pi_a^{U\prime}\right) \circ \pi_b^{\mathrm{USp}}$
$U(1)_a - U(1)_b^2$	$\widetilde{\mathcal{A}}^{abb}$	$N_a N_b \left(\pi_a^U + \pi_a^{U\prime}\right) \circ \pi_b^U$
$U(1)_a - RR$	$\mathcal{A}^{agg}$	$3N_a \pi_{O6} \circ \pi_a^U$

Table 6.2.: The $U(1)$ anomalies for the massless fermionic spectrum given in Table 5.1, which do neither vanish trivially nor upon imposing R-R tadpole cancelation. Note that the above results are valid for $a = b$ and $a \neq b$.

6.2.2. $\mathbf{USp(2N,\mathbb{C}) - USp(2N,\mathbb{C}) - USp(2N,\mathbb{C})}$ Anomaly

Given a brane π_a^{USp} one similarly computes the $USp(2N_a,\mathbb{C})^3$ anomaly. It is given by [2]

$$\begin{aligned}\mathcal{A}^{USpUSpUSp} &= \sum_{b\neq a} \pi_b^U \circ \pi_a^{\mathrm{USp}} \cdot \mathrm{tr}_F\left((T^a)^A\left\{(T^a)^B(T^a)^C\right\}\right) \\ &\quad + \sum_{b\neq a} \pi_b^{U\prime} \circ \pi_a^{\mathrm{USp}} \cdot \mathrm{tr}_F\left((T^a)^A\left\{(T^a)^B(T^a)^C\right\}\right) \\ &= \sum_{b\neq a}\left(\pi_b^U + \pi_b^{U\prime}\right) \circ \pi_a^{\mathrm{USp}} \cdot \mathrm{tr}_F\left((T^a)^A\left\{(T^a)^B(T^a)^C\right\}\right)\end{aligned} \tag{6.7}$$

But for any 3-cycle π_b^U on $\mathcal{M}/(\overline{\sigma}\times\Omega)$, the sum $\pi_b^U + \pi_b^{U\prime}$ is parallel to the orientifold plane. As π_b^{USp} carries $USp(2N_b,\mathbb{C})$ gauge group also π_b^{USp} is parallel to π_{O6}. As a consequence we have

$$\left(\pi_b^U + \pi_b^{U\prime}\right) \circ \pi_a^{\mathrm{USp}} = 0 \tag{6.8}$$

So we finally conclude that $\mathcal{A}^{USpUSpUSp}$ vanishes.

6.2.3. Summary On Anomalies

By similar arguments all $U(1)$ anomalies can be calculated. We give the details of these derivations in Appendix B, to which we refer the interested reader. Here it suffices it to state the results, which we list in Table 6.2.

6.3. Anomaly Cancelation

For a detailed discussion of anomaly cancelation by means of the generalized Green-Schwarz mechanism in terms of Lagrangian field theory we point the reader to [9]. Here we are more interested in its application to intersecting D6-brane models. Therefore we basically follow [1] in this section.

[2] Note that $(T^a)^A$ now denotes the $USp(2N_a)$ generators.

6.3.1. Definition Of Axion $\phi_{\mathbf{i}}$ And 2-Form Field $\mathbf{B_{2,i}}$

So far we described 3-cycles as

$$\pi_a = \prod_{I=1}^{3} \left(n_a^I \left[a^I \right] + \widetilde{m}_a^I \left[b^I \right] \right) \tag{6.9}$$

If we expand this product we obtain a sum of 3-cycles dressed by integer prefactors. For that reason we can switch to a different notation for a 3-cycle by using a 3-cycle basis of $H_1\left(T^2, \mathbb{Z}\right) \times H_1\left(T^2, \mathbb{Z}\right) \times H_1\left(T^2, \mathbb{Z}\right)$. For the remaining part of this section we will consider two such bases $[\Sigma^i]$ and $[\Lambda^i]$ $(i = 1, 2, \ldots, 8)$ that are dual. By the latter we mean

$$\left[\Sigma^i\right] \circ \left[\Lambda^j\right] = \delta^{ij} \tag{6.10}$$

Now recall that the democratic formulation of type IIA superstring theory not only includes the $C^{(7)}$ Ramond field, but also $C^{(3)}$ and $C^{(5)}$. We use these two to define

- the axion ϕ_i by $\phi_i := \int\limits_{\Lambda^i} C^{(3)}$.
- the 2-form field $B_{2,i}$ by $B_{2,i} := \int\limits_{\Sigma^i} C^{(5)}$.

6.3.2. Couplings And 4-Dimensional Reduction

Consider a three cycles π_a and let $\widetilde{F}_a$ denote a field strength on π_a [3]. Then there exist the following couplings between $C^{(3)}$, $C^{(5)}$ and $\widetilde{F}_a$.

$$\begin{aligned} S_{\text{coup 1}} &= \int\limits_{\mathbb{R}^{1,3}\times\pi_a} C^{(3)} \wedge \operatorname{tr}\left(\widetilde{F}_a \wedge \widetilde{F}_a\right) = \sum_i p_{ai} \int\limits_{\mathbb{R}^{1,3}} \phi_i \wedge \operatorname{tr}\left(\widetilde{F}_a \wedge \widetilde{F}_a\right) \\ S_{\text{coup 2}} &= \int\limits_{\mathbb{R}^{1,3}\times\pi_a} C^{(5)} \wedge \operatorname{tr}\left(\widetilde{F}_a\right) = \sum_i r_{ai} \int\limits_{\mathbb{R}^{1,3}} B_{2,i} \wedge \operatorname{tr}\left(\widetilde{F}_a\right) \end{aligned} \tag{6.11}$$

In the second step we assumed that the field strength $\widetilde{F}_a$ does only depend on the external space, which is a sensible choice for compactifications. Thereby we reduced ten-dimensional couplings to four-dimensional couplings and made our way to the arena of four dimensional quantum field theory.

[3] It may either refer to the Abelian or non-Abelian field strength on π_a. For now we like to keep things general, and therefore introduce this notion.

6.3.3. Cancelation Of U(1) - SU(N) - SU(N) Anomalies

We will now demonstrate how to cancel the $U(1)_a$ - $SU(N_b)^2$ anomalies. The corresponding couplings are [4]

$$\begin{aligned} S_{SU(N_b)} &= \sum_i p_{bi} \int_{\mathbb{R}^{1,3}} \phi_i \wedge \mathrm{tr}\left(F^b \wedge F^b\right), \quad S_{SU(N_b)'} = \sum_i p'_{bi} \int_{\mathbb{R}^{1,3}} \phi_i \wedge \mathrm{tr}\left(F^b \wedge F^b\right) \\ S_{U(1)_a} &= N_a \sum_i r_{ai} \int_{\mathbb{R}^{1,3}} B_{2,i} \wedge C^a, \qquad\qquad S_{U(1)'_a} = -N_a \sum_i r'_{ai} \int_{\mathbb{R}^{1,3}} B_{2,i} \wedge C^a \end{aligned} \tag{6.12}$$

Taking all these couplings into account we find

$$\begin{aligned} S_{U(1)_a - SU(N_b)^2} = N_a \sum_i &\left(r_{ai} p_{bj} + r_{ai} p'_{bj} - r'_{ai} p_{bj} - r'_{ai} p'_{bj}\right) \\ &\times \int_{\mathbb{R}^{3,1}} B_{2,i} \wedge C^a \cdot \int_{\mathbb{R}^{3,1}} \phi_i \wedge \mathrm{tr}\left(F^b \wedge F^b\right) \end{aligned} \tag{6.13}$$

But note that due to our choice of dual bases $[\Lambda^i]$ and $[\Sigma^i]$ we have

$$\sum_{i=1}^{8} r_{ai} p_{bi} = \sum_{i,j=1}^{8} r_{ai} p_{bj} \delta^{ij} = \sum_{i,j=1}^{8} r_{ai} p_{bj} \left[\Sigma^i\right] \circ \left[\Lambda^j\right] = \pi_a \circ \pi_b \tag{6.14}$$

Thus we find [5]

$$S_{U(1)_a - SU(N_b)^2} \sim N_a \left(\pi_a^U \circ \pi_b^U + \pi_a^U \circ \pi_b^{U\prime} - \pi_a^{U\prime} \circ \pi_b^U - \pi_a^{U\prime} \circ \pi_b^{U\prime}\right) \tag{6.15}$$

It is easy to verify $\pi_a \circ \pi'_b = -\pi'_a \circ \pi_b$ and $\pi'_a \circ \pi'_b = -\pi_a \circ \pi_b$. Taking this into account one can rewrite the coupling as

$$S_{U(1)_a - SU(N_b)^2} \sim 2N_a \left(\pi_a^U - \pi_a^{U\prime}\right) \circ \pi_b^U \tag{6.16}$$

Therefore this counterterm is of the form needed to cancel the $U(1)_a$ - $SU(N_b)^2$ anomaly given in Table 6.2. For $a = b$ it also reduces to the correct form to cancel the $U(1)_a - SU(N_a)^2$ anomaly.

6.3.4. Cancelation Of The Remaining Anomalies

All other anoamlies can be canceled in precisely the same way. We abondon an in-detail analysis here, but encourage the interested reader to verify this result. Note also that Feynman diagram giving rise to the counterterm for the $\tilde{\mathcal{A}}^{abc}$ anomalies is given in figure 6.1b.

[4] Recall the notation introduced in subsection 6.1.2. The prefactor N_a appears due to appropriate normalization of the $U(1)_a$ generator. Note also that on the image brane one has $C^{a\prime} = -C^a$.

[5] Note that the integrals in Equation 6.13 carry an i index and are therefore summed over. Nevertheless we drop these terms for demonstrational purposes.

6.4. Mass Generation

6.4.1. General Feature

As we have already seen there are couplings between the $U(1)_a$ field strength C^a and the two-form field $B_{2,i}$ of the form

$$S = N_a \cdot \sum_i (r_{ai} - r'_{ai}) \cdot \int_{\mathbb{R}^{3,1}} B_{2,i} \wedge C^a \tag{6.17}$$

These coupling allows for an interpretation in terms of a mass^2 matrix M^2. For k factorizable D-brane stacks this matrix M^2 is given by

$$M^2 := \begin{pmatrix} N_1(r_{11} - r'_{11}) & N_2(r_{21} - r'_{21}) & \dots & N_k(r_{k1} - r'_{k1}) \\ N_1(r_{12} - r'_{12}) & N_2(r_{22} - r'_{22}) & \dots & N_k(r_{k2} - r'_{k2}) \\ \vdots & \vdots & \ddots & \vdots \\ N_1(r_{18} - r'_{18}) & N_2(r_{28} - r'_{28}) & \dots & N_k(r_{k8} - r'_{k8}) \end{pmatrix} \tag{6.18}$$

The kernel of this matrix will determine the $U(1)$ combinations that remain massless.

6.4.2. Explicit Form

For later convenience we choose a basis of $H_1(T^2, \mathbb{Z}) \times H_1(T^2, \mathbb{Z}) \times H_1(T^2, \mathbb{Z})$, namely

$$\begin{aligned} \Sigma^1 &= \left[b^1\right]\left[b^2\right]\left[b^3\right], & \Sigma^2 &= \left[b^1\right]\left[a^2\right]\left[a^3\right] \\ \Sigma^3 &= \left[a^1\right]\left[b^2\right]\left[a^3\right], & \Sigma^4 &= \left[a^1\right]\left[a^2\right]\left[b^3\right] \\ \Sigma^5 &= \left[a^1\right]\left[a^2\right]\left[a^3\right], & \Sigma^6 &= \left[a^1\right]\left[b^2\right]\left[b^3\right] \\ \Sigma^7 &= \left[b^1\right]\left[a^2\right]\left[b^3\right], & \Sigma^8 &= \left[b^1\right]\left[b^2\right]\left[a^3\right] \end{aligned} \tag{6.19}$$

Then the matrix M^2 is given by

$$M^2 := \begin{pmatrix} 2N_1 m_1^1 m_1^2 m_1^3 & 2N_2 m_2^1 m_2^2 m_2^3 & \dots & 2N_K m_K^1 m_K^2 m_K^3 \\ 2N_1 m_1^1 n_1^2 n_1^3 & 2N_2 m_2^1 n_2^2 n_2^3 & \dots & 2N_K m_K^1 n_K^2 n_K^3 \\ 2N_1 m_1^2 n_1^1 n_1^3 & 2N_2 m_2^2 n_2^1 n_2^3 & \dots & 2N_K m_K^2 n_K^1 n_K^3 \\ 2N_1 n m_1^3 n_1^1 n_1^2 & 2N_2 n_2^3 n_2^1 n_2^2 & \dots & 2N_K n_K^3 n_K^1 n_K^2 \\ 0 & 0 & \dots & 0 \\ 0 & 0 & \dots & 0 \\ 0 & 0 & \dots & 0 \\ 0 & 0 & \dots & 0 \end{pmatrix} \tag{6.20}$$

In writing out this explicit form we have used that the image branes are obtained by changing the sign of the $[b^i]$ cycles. This implies that $r_{ai} = r'_{ai}$ for $i = 5, 6, 7, 8$ and so the last four lines of M^2 become trivial.

It is crucial to note that not only anomalous, but also anomaly-free $U(1)$ gauge bosons can aquire mass due to the $B_{2,i} \wedge C^a$ couplings [7]. Yet the hypercharge should remain massless. Thus we should expect further constraints arising from this requirement.

7. Class Of Non-Supersymmetric Models

By now we have gathered all the knowledge needed to discuss non-supersymmetric models. Under general assumptions an entire class of such models was derived and first published in [21]. We will now discuss this class of non-supersymmetric models, thereby following closely to the original literature.

7.1. General Features Of The Setup

7.1.1. The Branes

We consider the orientifold $\mathcal{M}/\left(\overline{\sigma}\times\Omega\right)$ with the third torus tilted. Therefore there is an NS background $b^3=\frac{1}{2}$ on the third torus. In this background we consider the class of intersecting D6-brane models listed in Table 7.1. Among others they depend on

$$\beta^i = 1 - b^i \in \left\{\frac{1}{2}, 1\right\}, \qquad i=1,2 \tag{7.1}$$

This tells us that in some of these models further tori are tilted. Hence it would be counter-intuitive to apply the $\widetilde{m}$ notation, which is why we do not apply it during the discussion of this class of models.
As discussed in subsection 5.2.3 the orientifold plane is given by

$$\pi_{\text{O6}} = 8\left[a^1\right]\left[a^2\right]\left[a^3\right] \tag{7.2}$$

7.1.2. Intersection Numbers And Brane Picture

With the wrapping numbers as specified in Table 7.1 it is possible to compute the topological intersection numbers between the various 3-cycles in the setup via

$$I_{ab} = \pi_a \circ \pi_b = \prod_{I=1}^{3}\left(n_a^I\widetilde{m}_b^I - n_b^I\widetilde{m}_a^I\right) \tag{7.3}$$

We display their absolute value in the brane picture given in Figure 7.1. Their sign is incoded in the displayed strings via the following convention.

- $I_{ab}>0$, then **left-handed, massless** fermions stretch from b to a.
- $I_{ab}<0$, then **left-handed, massless** fermions stretch from a to b.

Brane	Wrapping Numbers	Gauge Group	$U(1)$ gauge boson
$N_a = 3$ $N'_a = 3$	$\left(\frac{1}{\beta^1}, 0\right) \times (n_a^2, \epsilon\beta^2) \times \left(\frac{1}{\rho}, \frac{1}{2}\right)$ $\left(\frac{1}{\beta^1}, 0\right) \times (n_a^2, -\epsilon\beta^2) \times \left(\frac{1}{\rho}, -\frac{1}{2}\right)$	$U(3)$	Q_a
$N_b = 2$ $N'_b = 2$	$(n_b^1, -\epsilon\beta^1) \times \left(\frac{1}{\beta^2}, 0\right) \times \left(1, \frac{3\rho}{2}\right)$ $(n_b^1, \epsilon\beta^1) \times \left(\frac{1}{\beta^2}, 0\right) \times \left(1, -\frac{3\rho}{2}\right)$	$U(2)$	Q_b
$N_c = 1$ $N'_c = 1$	$(n_c^1, 3\rho\epsilon\beta^1) \times \left(\frac{1}{\beta^2}, 0\right) \times (0, 1)$ $(n_c^1, -3\rho\epsilon\beta^1) \times \left(\frac{1}{\beta^2}, 0\right) \times (0, -1)$	$U(1)$	Q_c
$N_d = 1$ $N'_d = 1$	$\left(\frac{1}{\beta^1}, 0\right) \times \left(n_d^2, -\frac{\beta^2\epsilon}{\rho}\right) \times \left(1, \frac{3\rho}{2}\right)$ $\left(\frac{1}{\beta^1}, 0\right) \times \left(n_d^2, \frac{\beta^2\epsilon}{\rho}\right) \times \left(1, -\frac{3\rho}{2}\right)$	$U(1)$	Q_d

Table 7.1.: Branes, image branes and gauge groups in the non-supersymmetric three family model first published in [21]. Note that the parameters that specifiy the wrapping numbers obey the relations $\epsilon = \pm 1$, $\rho = \frac{1}{3}, 1$, $\beta^1, \beta^2 = \frac{1}{2}, 1$. The remaining n_a^2, n_b^1, n_c^1 and n_d^2 are integers.

7.1.3. Proof Of Non-Supersymmetry

Let us now proof that this class of models is not supersymmetric.

Brane Stack a

If the brane stack a was supersymmetric, it would satisfy Equation 4.5 and Equation 4.6. Applied to brane stack a these conditions become

$$n_a^2 = -\frac{2u^2\epsilon\beta^2}{\rho u^3}, \qquad 0 < \frac{n_a^2}{\rho} - \frac{\epsilon\beta^2 u^2 u^3}{2} \tag{7.4}$$

Using the equation for n_a^2 we obtain

$$0 < \underbrace{\left(\frac{2u^2}{\rho^2 u^3} + \frac{u^2 u^3}{2}\right) \cdot \beta^2}_{>0} \cdot (-\epsilon) \tag{7.5}$$

Therefore we must have $\epsilon = -1$.

Brane Stack c

Similarly we can apply Equation 4.5 and Equation 4.6 to brane stack c. From Equation 4.5 we obtain $0 = \frac{n_c^1}{\beta^2 u^1 u^2}$, which implies $n_c^1 = 0$. Then Equation 4.6 gives the condition

$$0 < \underbrace{\frac{\beta^1 u^1 u^3}{\beta^2}}_{>0} \cdot \epsilon \tag{7.6}$$

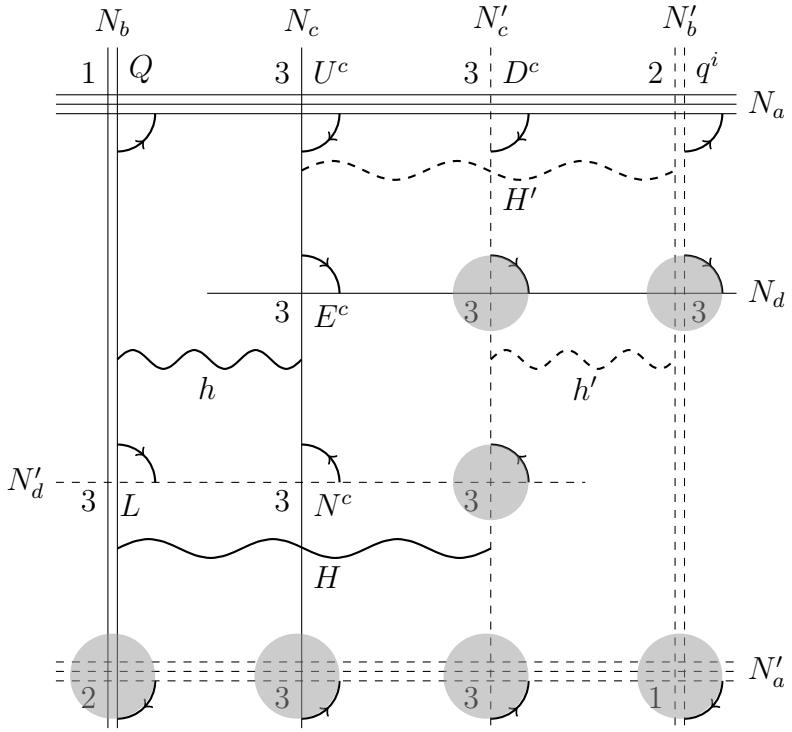

Figure 7.1.: Brane picture for the class of non-supersymmetric models first published in [21]. The branes of these models are specified in Table 7.1. The oriented arcs indicate the strings that give rise to massless, left-handed fermions. The corresponding matter particles in the Standard Model are also indicated. In addition the strings that allow for an interpretation in terms of the Higgs doublets are drawn.

But supersymmetry of brane stack a requires $\epsilon = -1$, as outlined above. Therefore we find a contradition from which we conclude that this class of intersecting D6-brane models is never supersymmetric.

7.1.4. Check Of The Various Constraints

The Constraints

This class of non-supersymmetric models has to satisfy two sets of constraints, namely

- R-R tadpole constraints.
- K-theory constraint.

It is readily checked that the model satisfies the K-theory constraints given in Equation 5.13, which leaves the R-R tadpole constraints to be checked. Recall that these

constraints are

$$\begin{aligned} &\sum_a N_a \prod_{I=1}^{3} n_a^I = 16 \\ &\sum_a N_a n_a^I \widetilde{m}_a^J \widetilde{m}_a^K = 0, \quad I \neq J \neq K \neq I \end{aligned} \tag{7.7}$$

It is not difficult to check that $\sum_a N_a n_a^I \widetilde{m}_a^J \widetilde{m}_a^K = 0$ holds trivially for this model. The remaining constraint however is not trivially satisfied, but leads to the requirement

$$\frac{3n_a^2}{\beta^1 \rho} + \frac{2n_b^1}{\beta^2} + \frac{n_d^2}{\beta^1} = 16 \tag{7.8}$$

This is a constraint on the so-far unconstraint integers n_a^2, n_b^1, n_d^2.

'Hidden' Branes

It is possible to weaken the R-R tadpole constraints by adding further N_h D6-branes with $\widetilde{m}_h^I = 0$. These branes are parallel to the orientifold plane. An explicit calculation reveals that these branes have vanishing intersection number with all the other branes in Table 7.1. For that reason these branes do not change the massless fermionic bifundamentals and are hidden in this sense. [1]
In the presence of such hidden branes the R-R tadpole constraints are weakend, as they change to

$$\begin{aligned} &\sum_a N_a \prod_{i=I}^{3} n_a^I + N_h n_h^1 n_h^2 n_h^3 = 16 \\ &\sum_a N_a n_a^I \widetilde{m}_a^J \widetilde{m}_a^K = 0, \quad I \neq J \neq K \neq I \end{aligned} \tag{7.9}$$

7.2. Massless Spectrum And U(1) Gauge Bosons

7.2.1. Gauge Groups

All branes given in Table 7.1 are not invariant under the involution $\overline{\sigma}$. Therefore they all carry $U(N)$ gauge groups, which are listed in Table 7.1.

7.2.2. Massless Fermionic Spectrum

We discussed the massless fermionic spectrum in a general context in section 5.3 and summarized our findings in Table 5.1. Naturally this result can be applied to the current class of models. The so-obtained massless fermionic spectrum is given in Table 7.2. Note that we list the $U(1)$ charge

$$Q_x := \frac{1}{6}Q_a - \frac{1}{2}Q_c + \frac{1}{2}Q_d \tag{7.10}$$

Sector	Chirality	Representation	Q_a	Q_b	Q_c	Q_d	Q_x	Field
(ab)	L	$\left(3,\overline{2},1,1\right)$	1	-1	0	0	$\frac{1}{6}$	Q
	R	$\left(\overline{3},2,1,1\right)$	-1	1	0	0	$-\frac{1}{6}$	Q^c
(ab')	L	$2\times(3,2,1,1,)$	1	1	0	0	$\frac{1}{6}$	Q
	R	$2\times\left(\overline{3},\overline{2},1,1,\right)$	-1	-1	0	0	$-\frac{1}{6}$	Q^c
(ac)	L	$3\times\left(\overline{3},1,1,1\right)$	-1	0	1	0	$-\frac{2}{3}$	U^c
	R	$3\times\left(3,1,\overline{1},1\right)$	1	0	-1	0	$\frac{2}{3}$	U
(ac')	L	$3\times\left(\overline{3},1,\overline{1},1\right)$	-1	0	-1	0	$\frac{1}{3}$	D^c
	R	$3\times(3,1,1,1)$	1	0	1	0	$-\frac{1}{3}$	D
(bd')	L	$3\times\left(1,\overline{2},1,\overline{1}\right)$	0	-1	0	-1	$-\frac{1}{2}$	L
	R	$3\times(1,2,1,1)$	0	1	0	1	$\frac{1}{2}$	L^c
(cd)	L	$3\times\left(1,1,\overline{1},1\right)$	0	0	-1	1	1	E^c
	R	$3\times\left(1,1,1,\overline{1}\right)$	0	0	1	-1	-1	E
(cd')	L	$3\times(1,1,1,1)$	0	0	1	1	0	N^c
	R	$3\times\left(1,1,\overline{1},\overline{1}\right)$	0	0	-1	-1	0	N

Table 7.2.: Massless fermionic spectrum of the class of non-supersymmetric models first published in [21]. The brane picture for these models is depictured in Figure 7.1. Note that the representations are written as $SU(3)\times SU(2)\times U(1)_c\times U(1)_d$.

From the results in Table 7.2 one is tempted to identify Q_x with the hypercharge in the Standard Model. We will prove momentarily that this $U(1)$ combination in fact remains massless, which then justifies this identification.

7.2.3. Massless Bosonic Spectrum

Massless bosons arise as excitations of strings in the aa-sector, i.e. strings that start and end on the same brane stack. The corresponding string states will transform in the adjoint representation. Therefore they allow for an interpretation in terms of gauge bosons. We list these excitations in Table 7.3.

7.2.4. U(1) Gauge Bosons

Anomlous U(1) Gauge Bosons

The various $U(1)$ anomalies are listed in Table 6.2. They were calculated and the results are displayed in Table 7.4. From this table we deduce that Q_a+3Q_d and Q_c are anomaly free. Q_a-3Q_d and Q_b are anomalous. So we expect the latter

[1]Note however, that such branes lead to an extended gauge group. As a consequence additional gauge bosons will appear.

Sector	$U(3) \times U(2) \times U(1)_c \times U(1)_d$	Field
(aa)	$3 \times (8+1,1,1,1)$	Gluons , Q_a
(bb)	$3 \times (1,3+1,1,1)$	$W^{\pm}$, Z , Q_b
(cc)	$3 \times (1,1,1,1)$	Q_c
(dd)	$3 \times (1,1,1,1)$	Q_d

Table 7.3.: Massless bosons in the class of non-supersymmetric models first published in [21] and illustrated in Figure 7.1. The wrapping numbers are given in Table 7.1.

		Q_a	Q_b	Q_c	Q_d
$\mathcal{A}^{abb}$	a	0	-1	0	0
	b	$-\frac{9}{2}$	0	0	$\frac{3}{2}$
	c	9	0	0	-3
	d	0	3	0	0
$\widetilde{\mathcal{A}}^{abb}$	a	0	-6	0	0
	b	-18	0	0	6
	c	18	0	0	-6
	d	0	6	0	0
$\mathcal{A}^{agg}$		0	0	0	0

Table 7.4.: U(1) anomalies in the class of non-supersymmetric models first published in [21]. The anomalies were calculated by using Table 6.2 and the wrapping numbers for the branes specified in Table 7.1.

two to acquire mass upon anomaly cancelation by the generalized Green-Schwarz mechanism.

Masses For Anomalous U(1) Gauge Bosons

Therefore we compute the mass^2 matrix and obtain [2]

$$M^2 = \begin{array}{c} \begin{array}{cccc} Q_a & Q_b & Q_c & Q_d \end{array} \\ \left(\begin{array}{cccc} 0 & 0 & 0 & 0 \\ 0 & -\frac{2\epsilon\beta^1}{\beta^2} & 0 & 0 \\ \frac{3\epsilon\beta^2}{\rho\beta^1} & 0 & 0 & -\frac{\epsilon\beta^2}{\rho\beta^1} \\ \frac{3n_a^2}{2\beta^1} & \frac{6\rho n_b^1}{2\beta^2} & \frac{2n_c^1}{2\beta^2} & \frac{3\rho n_d^2}{2\beta^1} \end{array} \right) \end{array} \tag{7.11}$$

[2] Equation 6.20 was used. We dropped the last four rows, as they are always trivial.

It is easy to see that

$$\ker(M) = \text{span}\left[\begin{pmatrix} n_c^1 \\ 0 \\ -\frac{3\beta^2}{2\beta^1}\left(n_a^2 + 3\rho n_d^2\right) \\ 3n_c^1 \end{pmatrix}\right] \tag{7.12}$$

Thus we find that the following combination of $U(1)$ gauge fields remains massless

$$Q = n_c^1\left(Q_a + 3Q_d\right) - \frac{3\beta^2}{2\beta^1}\left(n_a^2 + 3\rho n_d^2\right)Q_c \tag{7.13}$$

Thus we obtain the correct hypercharge (up to rescaling) if we require

$$n_c^1 = \frac{\beta^2}{2\beta^1}\left(n_a^2 + 3\rho n_d^2\right) \tag{7.14}$$

Consequently we can now justify to identify Q_x with the Standard Model hypercharge.
The three remaining, linearly independent $U(1)$ combinations obtain masses of the string-scale. Therefore they correspond to perturbative global symmetries in the four-dimensional low energy effective theory [7].
Note that the massive $U(1)$ gauge bosons Q_a, Q_b and Q_d have the following interpretations (c.f. Table 7.2).

- Q_a corresponds to the baryon number.
- Q_d corresponds to the lepton number.
- Q_b is a Peccei-Quinn type $U(1)$ symmetry.

So the proton is stable in this class of models.

7.3. Massive States

7.3.1. Tachyons

In the ab-sector as well as the a′b-sector massive bosonic and fermionic excitations exist. The lightest bosonic excitations in the ab-sector are listed in Table 2.1.
As their mass depends on the intersection angles, it is possible that tachyons appear in the NS-sector. This would render the model unstable. However it has been pointed out in [21] that this class of non-supersymmetric models contains models, in which the intersection angles are such that no tachyons appear and the model is stabilized at this stage. For further details we refer the interested reader to the original literature [21].

Higgs Doublets	Representation	Q_b	Q_c	Q_Y
h_U	$(1,2,1)$	1	-1	$\frac{1}{2}$
h_D	$\left(1,\overline{2},1\right)$	-1	1	$-\frac{1}{2}$
H_U	$\left(1,\overline{2},1\right)$	-1	-1	$\frac{1}{2}$
H_D	$(1,2,1)$	1	1	$-\frac{1}{2}$

Table 7.5.: Higgs doublets in the class of non-supersymmetric models first published in [21].

7.3.2. Massive Particles Beyond the Standard Model

In the ab-sector, the ab$'$-sector and the aa-sector further massive states appear as higher excitations. We discussed these excitations and their masses in chapter 2.
In addition to these massive excitations one also obtains winding states and KK-states in the aa-sector, owing their existence to toroidal compactification. This was discussed in section 3.5.
For certain models the winding states and/or the KK-states can be lighter than the lightest massive excitations in the aa-sector, ab-sector and ab$'$-sector. In that case these winding states and/or KK-states would be the first particles beyond the Standard model to be observed at accelerators. More details on the appearance of these particles in the current class of non-supersymmetric models can be found in the original literature [21].

7.4. Higgs Doublets

7.4.1. Location And Quantum Numbers

The properties of the Higgs doublets are listed in Table 1.2. It is possible to realize such states in this class of non-supersymmetric model, as strings in the bc-sector and bc$'$-sector. These states are listed in Table 7.5 and are also indicated in Figure 7.1.

7.4.2. Mass For Higgs Particles

We give a schematic picture for the h_U and h_D strings in Figure 7.2 - they stretch between the branes b and c that are parallel in the second torus. With Equation 2.26 it is easy to write down the mass for the lightest bosonic excitations in the bc-sector, kept by the GSO projection. We list these states in Table 7.6. The masses for the other Higgs fields are obtained similarly. For further convenience we define

$$\begin{aligned} m^2_{H^\pm} &= \frac{Z^2_{bc'}}{4\pi^2\alpha'} \pm \frac{1}{2\alpha'}\left(\left|\vartheta^1_{bc'}\right| - \left|\vartheta^3_{bc'}\right|\right) := m^2_H \pm m^2_B \\ m^2_{h^\pm} &= \frac{Z^2_{bc}}{4\pi^2\alpha'} \pm \frac{1}{2\alpha'}\left(\left|\vartheta^1_{bc}\right| - \left|\vartheta^3_{bc}\right|\right) := m^2_h \pm m^2_b \end{aligned} \tag{7.15}$$

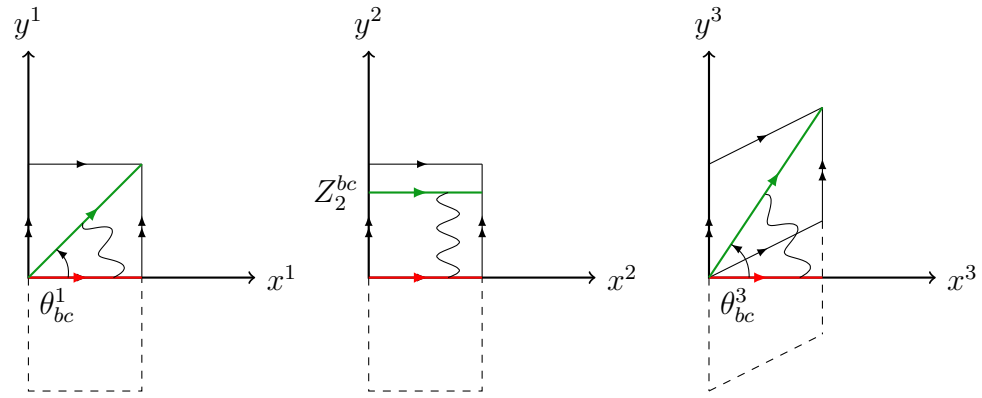

Figure 7.2.: Schematic picture for strings stretching between the branes b (red) and c (green) in the class of non-supersymmetric models first published in [21]. For simplicity we have chosen the first two tori to be rectangular. For the same reason we have aligned brane b (red) with the x^I axis.

Excitation	$\alpha'\text{Mass}^2$	Bosonic Notation
$b^1_{-\left(\frac{1}{2}-\vartheta^1_{cb}\right)}\left\|0\right\rangle_{NS}$	$\frac{Z_2^{cb}}{4\pi^2}+\frac{1}{2}\left(\left\|\vartheta^3_{cb}\right\|-\left\|\vartheta^1_{cb}\right\|\right)$	$(-1+\vartheta^1_{bc},0,\vartheta^3_{bc})$
$b^{6,7}_{-\frac{1}{2}}\left\|0\right\rangle_{NS}$	$\frac{Z_2^{cb}}{4\pi^2}+\frac{1}{2}\left(\left\|\vartheta^1_{cb}\right\|+\left\|\vartheta^3_{cb}\right\|\right)\right\|$	$(\vartheta^1_{bc},-1,\vartheta^3_{bc})$
$b^3_{-\left(\frac{1}{2}-\vartheta^3_{cb}\right)}\left\|0\right\rangle_{NS}$	$\frac{Z_2^{cb}}{4\pi^2}+\frac{1}{2}\left(\left\|\vartheta^1_{cb}\right\|-\left\|\vartheta^3_{cb}\right\|\right)$	$(\vartheta^1_{bc},0,-1+\vartheta^3_{bc})$

Table 7.6.: Lightest bosonic excitations in the bc-sector of the non-supersymmetric models first published in [21]. Note that this sector contains the h_U field.

7.4.3. Higgs Potential And Electroweak Symmetry Breaking

As was pointed out in [22], the scalar spectrum outlined in the previous subsection can be understood as arising from a mass term in the effective potential of the form

$$\begin{aligned} V &= m^2_{H^+}\left(H^+\right)^\star H^+ + m^2_{H^-}\left(H^-\right)^\star H^- + m^2_{h^+}\left(h^+\right)^\star h^+ + m^2_{h^-}\left(h^-\right)^\star h^- \\ &= \left(H_U^\star, H_D\right) M^2 \begin{pmatrix} H_U \\ H_D^\star \end{pmatrix} + \left(h_U^\star, h_D\right) m^2 \cdot \begin{pmatrix} h_U \\ h_D^\star \end{pmatrix} + \text{h.c.} \end{aligned} \tag{7.16}$$

where the mass^2 matrices M^2 and m^2 are given by

$$M^2 = \begin{pmatrix} m^2_H & m^2_B \\ m^2_B & m^2_H \end{pmatrix}, \quad m^2 = \begin{pmatrix} m^2_h & m^2_b \\ m^2_b & m^2_h \end{pmatrix} \tag{7.17}$$

and we defined

$$H^\pm = \frac{1}{2}\left(H_U^\star \pm H_D\right), \qquad h^\pm = \frac{1}{2}\left(h_U^\star \pm h_D\right) \tag{7.18}$$

The mass terms m_H and m_h depend von Z_2^{bc} and $Z_2^{bc'}$. For that reason these terms can be made arbitarily small in comparision with the string scale M_s. This however is not true for m_B^2 and m_b^2. The reason for this is that the masses of all sleptons and squarks in this class of models depend on six intersection angles only [22] [21]. For that reason lowering m_B^2 or m_b^2 implies lowering the mass of at least one slepton or squark. But for the latter two, there are experimental bounds. So it is not possible to lower m_B^2 and m_b^2 to arbitrarly small values compared to the strings scale M_s.
Finally let us highlight that for $m_H^2 \simeq m_B^2$ (or $m_h^2 \simeq m_b^2$), scalar flat directions along the vacuum expectation values $\langle H_U \rangle = \langle H_D \rangle$ (or $\langle h_U \rangle = \langle h_D \rangle$) arise [22]. In particular this may tripper electroweak symmetry breaking at scales well below the string scale. The latter requires $M_s = 1 - \text{few} TeV$ [21].

7.4.4. Multiplicity Of Higgs Doublets

H_U and H_D are given by strings stretching between brane b and brane c (see Figure 7.2). Therefore their multiplicity is given by the topological intersection number of the branes b and c in the first and third torus. Similarly the multiplicities for the h_U and h_D fields are obtained and one readily verifies

$$n_h = \beta^1 \cdot \left| 3\rho n_b^1 + n_c^1 \right|, \qquad n_H = \beta^1 \cdot \left| 3\rho n_b^1 - n_c^1 \right| \tag{7.19}$$

Minimal Higgs System

From the previous subsection we learn that the minimal number of Higgs doublets is obtained if

$$(n_h = 0,\ n_H = 1) \quad \vee \quad (n_h = 1,\ n_H = 0) \tag{7.20}$$

Let us discuss the first case in detail, i.e. we must satisfy

$$\beta^1 \cdot \left| 3\rho n_b^1 + n_c^1 \right| = 0, \qquad \beta^1 \cdot \left| 3\rho n_b^1 - n_c^1 \right| = 1 \tag{7.21}$$

From the first condition we conclude $3\rho n_b^1 = -n_c^1$. This allows to rewrite the second condition as $2\beta^1 \left| n_c^1 \right| = 1$. But note that $n_c^1 \in \mathbb{Z}$. Consequently this equation can only be satisfied for $\beta^1 = \frac{1}{2}$ and $n_c = \pm 1$.
These deducations allow to rewrite $n_h = 0$ as $3\rho n_b^1 = \mp 1$. Since $n_b^1 \in \mathbb{Z}$ this implies $\rho = \frac{1}{3}$ and $n_b^1 = \mp 1$. Finally recall that we need

$$n_c^1 = \frac{\beta^2}{2\beta^1} \left(n_a^2 + 3\rho n_d^2 \right) \tag{7.22}$$

to obtain the correct hypercharge in this class of models. By using the above results this condition gives

$$n_d^2 = \pm \frac{1}{\beta^2} - n_a^2 \tag{7.23}$$

The consideration $n_h = 1$ and $n_H = 0$ gives similar results. We summarize all these results in the upper half of Table 7.7.

Multiplicites		ρ	β^1	β^2	n_a^2	n_b^1	n_c^1	n_d^2	N_h
n_H	n_h								
1	0	$\frac{1}{3}$	$\frac{1}{2}$	β^2	n_a^2	± 1	∓ 1	$\pm\frac{1}{\beta^2} - n_a^2$	$4\beta^2\left(1-n_a^2\right)$
0	1	$\frac{1}{3}$	$\frac{1}{2}$	β^2	n_a^2	± 1	± 1	$\pm\frac{1}{\beta^2} - n_a^2$	$4\beta^2\left(1-n_a^2\right) - 1$
1	1	1	1	β^2	n_a^2	0	± 1	$\frac{1}{3}\left(\pm\frac{2}{\beta^2} - n_a^2\right)$	$\beta^2\left(8 - \frac{4n_a^2}{3}\right) \mp \frac{1}{3}$
1	1	$\frac{1}{3}$	$\frac{1}{2}$	β^2	n_a^2	0	± 1	$\pm\frac{2}{\beta^2} - n_a^2$	$\beta^2\left(8-4n_a^2\right) \mp 1$

Table 7.7.: The class of non-supersymmetric models first published in [21] contains models with one or two Higgs doublets. The models with minimal Higgs system are displayed in the upper half of this table, the ones with double Higgs system are listed in the lower half. The last column states the number of hidden branes that is needed to satisfy the R-R tadpole constraints in Equation 7.9 [21].

Double Higgs System

Similarly one can have $n_H^1 = n_H^2 = 1$. Then one finds four models which allow for this double Higgs system. We list the details of these models in the lower half of Table 7.7.

7.5. Yukawa Couplings

We list the possible Yukawa couplings among the Standard Model matter particles and the different Higgs doublets in Table 7.8.
Note that there are couplings with $Q_b = 0$ and such with $Q_b \neq 0$. Recall that Q_b became massive and therefore corresponds to a perturbative symmetry (of Peccei-Quinn type) in the low-energy effective theory. So only couplings with $Q_b = 0$ are possible. [3]
Note that in general the three interacting particles are located at different intersecting points. Therefore their interaction will be governed by a worldsheets, which has the form of a triangle in each of the three two-tori. Let A^I denote the area of this worldsheet in the I-th two-torus, then it holds [21] [7]

$$Y \sim \exp\left(-A^1\right) \cdot \exp\left(-A^2\right) \cdot \exp\left(-A^3\right) \tag{7.24}$$

This exponential behaviour can then account for the Hierarchy problem related to the masses of the Standard Model matter particles.

[3] However it has been pointed out in [21] that the strong force will break the $U(1)_b$ symmetry. After that also the couplings in the lower half of Table 7.8 are possible.

Fermion 1		Fermion 2		Higgs Doublet		Yukawa Coupling	$\sum Q_Y$	$\sum Q_b$
Q	$\frac{1}{6}$	$U^{c,j}$	$-\frac{2}{3}$	h_U	$\frac{1}{2}$	y_j^U	0	0
Q	$\frac{1}{6}$	$D^{c,j}$	$\frac{1}{3}$	H_D	$-\frac{1}{2}$	y_j^D	0	0
q^i	$\frac{1}{6}$	$U^{c,j}$	$-\frac{2}{3}$	H_U	$\frac{1}{2}$	y_{ij}^U	0	0
q^i	$\frac{1}{6}$	$D^{c,j}$	$\frac{1}{3}$	h_D	$-\frac{1}{2}$	y_{ij}^D	0	0
L^j	$-\frac{1}{2}$	$E^{c,k}$	1	H_D	$-\frac{1}{2}$	y_{jk}^L	0	0
L^j	$-\frac{1}{2}$	$N^{c,k}$	0	h_U	$\frac{1}{2}$	y_{jk}^N	0	0
Q	$\frac{1}{6}$	$U^{c,j}$	$-\frac{2}{3}$	H_U	$\frac{1}{2}$	y_j^U	0	-2
Q	$\frac{1}{6}$	$D^{c,j}$	$\frac{1}{3}$	h_D	$-\frac{1}{2}$	y_j^D	0	-2
q^i	$\frac{1}{6}$	$U^{c,j}$	$-\frac{2}{3}$	h_U	$\frac{1}{2}$	y_{ij}^U	0	2
q^i	$\frac{1}{6}$	$D^{c,j}$	$\frac{1}{3}$	H_D	$-\frac{1}{2}$	y_{ij}^D	0	2
L^j	$-\frac{1}{2}$	$E^{c,k}$	1	h_D	$-\frac{1}{2}$	y_{jk}^L	0	-2
L^j	$-\frac{1}{2}$	$N^{c,k}$	0	H_U	$\frac{1}{2}$	y_{jk}^N	0	-2

Table 7.8.: Possible Yukawa couplings in the class of non-supersymmetric models first published in [21]. Note that $i = 1, 2$ whilst $j, k = 1, 2, 3$.

7.6. Summary

In section 7.1 we discussed general properties of this model. The most important conclusion from ths section is the brane picture given in Figure 7.1, which gives an intuitive picture of the situation.
We then moved on to discuss the massless spectrum and the $U(1)$ gauge bosons in section 7.2. In particular we discussed the massless fermionic spectrum, which is given in Table 7.2 and pointed out that it is in one-to-one correspondance with the matter particles of the Standard Model. The discussion of $U(1)$ gauge bosons finally showed that for

$$n_c^1 = \frac{\beta^2}{2\beta^1}\left(n_a^2 + 3\rho n_d^2\right) \tag{7.25}$$

one obtains the Standard Model hypercharge and three massive $U(1)$ gauge bosons. The latter three then give rise to perturbative symmetries in the low-energy effective theory, corresponding to conservation of lepton and baryon number and also a Peccei-Quinn type symmetry. In particular note that therefore the proton is stable in this class of models.
Subsequently we considered light massive excitations in section 7.3. In particular we considered the appearance of tachyons. The corresponding discussion in [21] showed that one can choose the intersection angles in this class of models such, that no tachyons appear, and the corresponding models are stabilized at this stage. Note however that non-supersymmetric models in general suffer from uncanceled NS-NS tadpoles. This lack will be overcome when building supersymmetric models and imposing cancelation of R-R tadpoles [7]. Therefore we will discuss supersymmetric models during the next part.

Of high phenomenological interest is the possibility to embed Higgs doublets in this class of models. The appearance, mass and multiplicity of these particles were discussed in section 7.4. Thereby we found that models with minimal or double Higgs system can be obtained. We list the details of these models in Table 7.7 [4]. In particular note that for models with $\langle H_U \rangle = \langle H_D \rangle$ (or $\langle h_D \rangle = \langle h_U \rangle$), scalar flat direction appear in the Higgs potential and may then trigger electroweak symmetry breaking at scales well below the string scale. [22]
Finally we briefly discussed the Yukawa couplings in section 7.5. As long as the Peccei-Quinn like $U(1)_b$ symmetry remains unbroken only the couplings in the upper half of Table 7.8 are possible. This has phenomenological impact when discussing mass generation for the Standard Model matter particles. Note in particular that

$$Y \sim \exp\left(A^1\right) \cdot \exp\left(A^2\right) \cdot \exp\left(A^3\right) \tag{7.26}$$

This exponential dependence can then be used to solve the Hirarchy problem for the masses of the Standard Model matter particles. For a detailed discussion on the masses of the matter particles in the context of minimal and double Higgs systems, we refer the interested reader to the original literature [21] and also [22]. In these two references also a discussion of the gauge couplings can be found. For completeless let us therefore only state that the gauge couplings are given by

$$\begin{aligned} \alpha_{\mathrm{QCD}}^{-1} &:= \frac{4\pi}{g_a^2} = \frac{M_s}{\pi\lambda_{II}} \cdot |\pi_a| \\ \alpha_{\mathrm{W}}^{-1} &:= \frac{4\pi}{g_a^b} = \frac{M_s}{\pi\lambda_{II}} \cdot |\pi_b| \\ \alpha_{\mathrm{Y}}^{-1} &= \frac{M_s}{\pi\lambda_{II}} \cdot \left(\frac{|\pi_a|}{6} + \frac{|\pi_c|}{2} + \frac{|\pi_d|}{2} \right) \end{aligned} \tag{7.27}$$

where for the brane π_a its length is given by

$$|\pi_a|^2 = \prod_{I=1}^{3} \left(\left(n_a^I R_x^I \right)^2 + \left(\widetilde{m}_a^I R_y^I \right)^2 \right) \tag{7.28}$$

So not only the Yukawa couplings and the masses for the Higgs particles, but also the gauge couplings have an interpretation in geometric terms of the intersecting D6-brane model.

[4] Note in particular that the condition to obtain the correct Standard Model hypercharge was implemented in the derivation of these models.

Part III.

Supersymmetric Models

8. Orientifold And Constraints

8.1. The Need For A New Background

In the previous part we discussed a class of non-supersymmetric models. Built on

$$\mathcal{M} = T^2 \times T^2 \times T^2 \tag{8.1}$$

this class of models was derived in [21] under the constraint to obtain a massless fermionic spectrum in one-to-one correspondance to the Standard Model matter particles. We pointed out in subsection 7.1.3, that this class of models is never supersymmetric. So its stability will in general suffer from uncanceled NS-NS tadpoles. Stable models, in which both R-R and NS-NS tadpoles are canceled, can be achieved by building supersymmetric models and imposing R-R tadpole cancelation [7]. Therefore we want to focus on supersymmetric models, in which the massless fermionic spectrum is as close as possible to the Standard Model matter particles. As just noted, on the $\mathcal{M}$ orbifold models with massless fermionic spectrum in one-to-one correspondance with the Standard Model matter particles will in general not be supersymmetric. Therefore it is natural to consider a different orbifold to built supersymmetric models on. In the following we will therefore consider the orbifold

$$\mathcal{O} = \left(T^2 \times T^2 \times T^2\right) / \left(\mathbb{Z}_2 \times \mathbb{Z}_2\right) \tag{8.2}$$

8.2. Structure Of $\mathcal{M}$

The structure of $\mathcal{M}$ was already discussed in chapter 3. Let us therefore only briefly revisit this topic.

- On each T^2 we use coordinates x^I and y^I, which we use to define a complex coordinate $z^I = x^I + iy^I$. The involution $\overline{\sigma}$ is then chosen such that (in local patches)

$$\overline{\sigma}\left(z^I\right) = \overline{z}^I \tag{8.3}$$

- 3-cycles on $\mathcal{M}$ are described by

$$\pi_a = \prod_{I=1}^{3} \left(n_a^I \left[a^I\right] + \widetilde{m}_a^I \left[b^I\right]\right) \tag{8.4}$$

where n_a^I, m_a^I are integers, $\widetilde{m}_a^I = m_a^I + b^I n_a^I$ and b^I is the NS background field given by

$$b^I = \begin{cases} 0 & \text{rectangular torus} \\ \frac{1}{2} & \text{tilted torus} \end{cases} \tag{8.5}$$

A brane with wrapping numbers $(1,1) \times (2,1) \times (1,1)$ on three rectangular tori is displayed in Figure 3.1.

- The topological intersection numbers between the fundamental 1-cycles on rectangular tori are defined as

$$\left[a^I\right] \circ \left[b^J\right] = -\left[b^I\right] \circ \left[a^J\right] = \delta^{IJ} \,, \qquad \left[a^I\right] \circ \left[a^J\right] = \left[b^I\right] \circ \left[b^J\right] = 0 \tag{8.6}$$

This implies that for two 3-cycles π_a and π_b one has

$$\pi_a \circ \pi_b = \prod_{I=1}^{3} \left(n_a^I \widetilde{m}_b^I - n_b^I \widetilde{m}_a^I \right) \tag{8.7}$$

8.3. Structure Of $\mathcal{O}$

Let us now divide $\mathcal{M} = T^2 \times T^2 \times T^2$ by $\mathbb{Z}_2 \times \mathbb{Z}_2$ to obtain the orbifold

$$\mathcal{O} = \mathcal{M} / \left(\mathbb{Z}_2 \times \mathbb{Z}_2 \right) \tag{8.8}$$

To this end we implement the group $\mathbb{Z}_2 \times \mathbb{Z}_2 = \{id, \Theta, \Theta', \Theta\Theta'\}$ on $\mathcal{M}$ by [7]

$$\Theta \begin{pmatrix} z_1 \\ z_2 \\ z_3 \end{pmatrix} = \begin{pmatrix} -z_1 \\ -z_2 \\ z_3 \end{pmatrix}, \qquad \Theta' \begin{pmatrix} z_1 \\ z_2 \\ z_3 \end{pmatrix} = \begin{pmatrix} z_1 \\ -z_2 \\ -z_3 \end{pmatrix} \tag{8.9}$$

8.3.1. Bulk Cycles On $\mathcal{O}$

Given a cycle π_a on $\mathcal{M}$, we make the following identifications in $\mathcal{O}$

$$\pi_a \sim \Theta\left(\pi_a\right) \sim \Theta'\left(\pi_a\right) \sim \Theta\Theta'\left(\pi_a\right) \tag{8.10}$$

Consequently the associated bulk state in the orbifold $\mathcal{O}$ is given by

$$\pi_a^B = \pi_a + \Theta\left(\pi_a\right) + \Theta'\left(\pi_a\right) + \Theta\Theta'\left(\pi_a\right) \tag{8.11}$$

But note that

$$\begin{aligned} \Theta\left(\pi_a\right) &= \Theta\left(\prod_{I=1}^{3} \left(n_a^I \left[a^I\right] + \widetilde{m}_a^I \left[b^I\right] \right) \right) \\ &= \prod_{I=1}^{2} \left(-n_a^I \left[a^I\right] - \widetilde{m}_a^I \left[b^I\right] \right) \times \left(n_a^3 \left[a^3\right] + m_a^3 \left[b^3\right] \right) \\ &= \prod_{I=1}^{3} \left(n_a^I \left[a^I\right] + \widetilde{m}_a^I \left[b^I\right] \right) \\ &= \pi_a \end{aligned} \tag{8.12}$$

By similar arguments one can show that 3-cycles π_a on $\mathcal{M}$ are also invariant under Θ' as well as $\Theta\Theta'$. Consequently we find $\pi_a^B = 4 \cdot \pi_a$.

8.3.2. Fundamental Cycles On $\mathcal{O}$

We will have to carefully distinguish cycles on $\mathcal{M}$ and cycles on $\mathcal{O}$. Therefore we agree on the following notation.

- π_a^t is a 3-cycle on $\mathcal{M} = T^2 \times T^2 \times T^2$.
- π_a^o is a 3-cycle on $\mathcal{O} = \mathcal{M}/\left(\mathbb{Z}_2 \times \mathbb{Z}_2\right)$.

The topological intersection number of cycles π_a^o in $\mathcal{O}$ is given by [1]

$$\pi_a^o \circ_o \pi_b^o = \frac{1}{4}\left(4\pi_a^t \circ_t 4\pi_b^t\right) = 4\pi_a^t \circ_t \pi_b^t \tag{8.14}$$

On a rectangular torus the 1-cycles $\left[a^{I,t}\right]$ and $\left[b^{I,t}\right]$ are fundamental cycles in the sense that they intersect at most once and span the homology group. However the associated bulk cycles $4\left[a^{I,t}\right]$ and $4\left[b^{I,t}\right]$ do intersect up to 4 times. Consequently they are not fundamental cycles. Instead let us consider the following 1-cycles

$$\left[a^{I,o}\right] := 2\left[a^{I,t}\right], \qquad \left[b^{I,o}\right] := 2\left[b^{I,t}\right] \tag{8.15}$$

Their intersection numbers are

$$\left[a^{I,o}\right] \circ_o \left[b^{I,o}\right] = \frac{1}{4}\left(2\left[a^{I,t}\right] \circ_t 2\left[b^{I,t}\right]\right) = \left[a^{I,t}\right] \circ_t \left[b^{I,t}\right] \tag{8.16}$$

Therefore we use $\left[a^{I,o}\right]$ and $\left[b^{I,o}\right]$ as fundamental 1-cycles on $\mathcal{O}$.

8.4. The Orientifold Plane

The final theory will be built on the orientifold

$$\mathbb{O} = \mathcal{O}/\left(\overline{\sigma} \times \Omega\right) \tag{8.17}$$

Mathematically $\mathbb{O}$ is made of equivalence classes. Considering these equivalence classes does not allow for an intuitive picture of the situation. Therefore we prefer to work with the picture of $\mathcal{O}$ that we obtained in the previous section. Then, however, we have to consider intersecting D6-brane setups that are invariant under

[1] The group $\mathbb{Z}_2 \times \mathbb{Z}_2$ identifies points in $\mathcal{M}$ as

$$(z_1, z_2, z_3) \sim \Theta\,(z_1, z_2, z_3) \sim \Theta'\,(z_1, z_2, z_3) \sim \Theta\Theta'\,(z_1, z_2, z_3) \tag{8.13}$$

to form $\mathcal{O}$. So four distinct points in $\mathcal{M}$ become a single point in $\mathcal{O}$. Therefore we have to divide the topological intersection number in $\mathcal{M}$ by 4 to obtain the one in $\mathcal{O}$ [7].

$\overline{\sigma}$. This is easily arranged by including the image brane $\pi'_a = \overline{\sigma}(\pi_a)$ for each brane π_a in the setup. Furthermore we have to consider the orientifold plane, which is given by the fixpoint locus under $\overline{\sigma}$.
To obtain this fixpoint locus we go back to $\mathcal{M}$ and calculate the fixpoint locus under $\overline{\sigma} \times \mathbb{Z}_2 \times \mathbb{Z}_2$ in terms of 3-cycles on $\mathcal{M}$. Subsequently we convert these 3-cycles on $\mathcal{M}$ into a 3-cycles on $\mathcal{O}$, by the conversions outlined in the previous subsection.

8.4.1. Fixpoints Under $\overline{\sigma}$

As discussed in the context of the non-supersymmetric models, the fixpoint locus under this operation is given by [2]

$$\pi^t_{a,\overline{\sigma}} = 8\left[a^{1,t}\right]\left[a^{2,t}\right]\left[a^{3,t}\right] \tag{8.18}$$

8.4.2. Fixpoints Under $\overline{\sigma} \times \Theta$

It holds

$$(\overline{\sigma}\times\Theta)\begin{pmatrix} z_1 \\ z_2 \\ z_3 \end{pmatrix} = \overline{\sigma}\begin{pmatrix} -z_1 \\ -z_2 \\ z_3 \end{pmatrix} = \begin{pmatrix} -\overline{z_1} \\ -\overline{z_2} \\ \overline{z_3} \end{pmatrix} = \begin{pmatrix} -\Re(z_1) + i\Im(z_1) \\ -\Re(z_2) + i\Im(z_2) \\ \Re(z_3) - i\Im(z_3) \end{pmatrix} \tag{8.19}$$

Thus if applied to a general 3-cycle π^t_a with

$$\pi^t_a = \prod_{I=1}^{3}\left(n^I_a\left[a^I\right] + \widetilde{m}^I_a\left[b^I\right]\right) \tag{8.20}$$

we obtain

$$\begin{aligned}(\overline{\sigma}\times\Theta)\left(\pi^t_a\right) = &\left(-n^{1,t}_a\left[a^{1,t}\right] + \widetilde{m}^{1,t}_a\left[b^{1,t}\right]\right)\cdot\left(-n^{2,t}_a\left[a^{2,t}\right] + \widetilde{m}^{2,t}_a\left[b^{2,t}\right]\right)\\ &\times\left(n^{3,t}_a\left[a^{3,t}\right] - \widetilde{m}^{3,t}_a\left[b^{3,t}\right]\right)\end{aligned} \tag{8.21}$$

So if we enforce invariance of the three 1-cycles, we find that π^t_a has to satisfy [3]

$$\pi^t_a = \left(m^{1,t}_a\left[b^{1,t}\right]\right)\cdot\left(m^{2,t}_a\left[b^{2,t}\right]\right)\cdot\left(n^{3,t}_a\left[a^{3,t}\right]\right) \tag{8.22}$$

At this point it becomes important to differ rectangular and tilted tori.

- On a rectangular torus there are two 1-cycles that are both parallel to $\left[b^I\right]$ and invariant under $\overline{\sigma}\times\Theta$.
- On a tilted torus there exists only a single such 1-cycle.

This is outlined in Figure 8.1. Consequently we find

$$\pi^t_{a,\overline{\sigma}\times\Theta} = \frac{8}{2^{2b^1}\cdot 2^{2b^2}}\cdot\left[b^{1,t}\right]\left[b^{2,t}\right]\left[a^{3,t}\right] \tag{8.23}$$

[2] For more details see subsection 5.2.3.
[3] Vanishing n^I_a implies $\widetilde{m}^I_a = m^I_a + b^I n^I_a = m^I_a$.

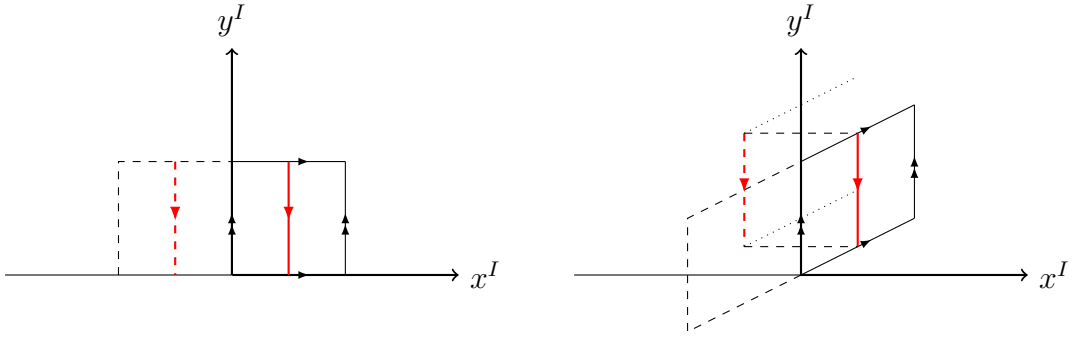

(a) Rectangular torus.

(b) Tilted torus.

Figure 8.1.: On both rectangular and tilted tori there is a 1-cycle which is placed on top of the y^I axis. This 1-cycle is both invariant under $\overline{\sigma} \times \Omega$ and parallel to $\left[b^I\right]$. In addition to this 1-cycle there exists a second 1-cycle on rectangular tori, which satisfies these criteria. This 1-cycle is displayed in red in figure 8.1a. The anaologue of this red 1-cycle on a tilted torus is displayed in figure 8.1b. It is not invariant, because the image cycle (dashed in red) must be identified along the dotted lines in a tilted torus. From this identification it becomes evident that image cycle and original cycle differ.

8.4.3. Fixpoints Under $\overline{\sigma} \times \Theta'$ And $\overline{\sigma} \times \Theta\Theta'$

By similar arguments one finds

$$\begin{aligned} \pi^t_{a,\overline{\sigma}\times\Theta'} &= \frac{8}{2^{2b^2} \cdot 2^{2b^3}} \left[a^{1,t}\right] \left[b^{2,t}\right] \left[b^{3,t}\right] \\ \pi^t_{a,\overline{\sigma}\times\Theta\times\Theta'} &= \frac{8}{2^{2b^1} \cdot 2^{2b^3}} \left[b^{1,t}\right] \left[a^{2,t}\right] \left[b^{3,t}\right] \end{aligned} \tag{8.24}$$

8.4.4. The Complete Orientifold Plane

An explicit calculation shows that $\pi^t_{a,\overline{\sigma}}$, $\pi^t_{a,\overline{\sigma}\times\Theta}$, $\pi^t_{a,\overline{\sigma}\times\Theta'}$ and $\pi^t_{a,\overline{\sigma}\times\Theta\times\Theta'}$ are invariant under all operations in $\overline{\sigma} \times \mathbb{Z}_2 \times \mathbb{Z}_2$. Therefore their sum forms the orientifold plane. Recall however that we wish to built a supersymmetric model. For that reason we choose the orientifold plane such that

$$\sum_{I=1}^{3} \Theta^I_a = 0 \bmod 2\pi \tag{8.25}$$

Baring this in mind and converting the above 3-cycles on $\mathcal{M}$ into 3-cycles on $\mathcal{O}$ one finds

$$\begin{aligned} \pi^o_{O6} = 4 \left[a^{1,o}\right] \left[a^{2,o}\right] \left[a^{3,o}\right] &- \frac{4}{2^{2b^1} \cdot 2^{2b^2}} \left[b^{1,o}\right] \left[b^{2,o}\right] \left[a^{3,o}\right] \\ - \frac{4}{2^{2b^1} \cdot 2^{2b^3}} \left[b^{1,o}\right] \left[a^{2,o}\right] \left[b^{3,o}\right] &- \frac{4}{2^{2b^2} \cdot 2^{2b^3}} \left[a^{1,o}\right] \left[b^{2,o}\right] \left[b^{3,o}\right] \end{aligned} \tag{8.26}$$

8.5. Massless Fermionic Spectrum

The massless fermionic spectrum is important to us, as this is where the matter particles of the Standard Model can appear. This spectrum was derived in [13] and organizes in the same way, as the spectrum for the models on the $\mathcal{M}/(\overline{\sigma} \times \Omega)$ orientifold does. The latter is listed in Table 5.1 and is easily converted into the spectrum of models on the $\mathcal{O}/(\overline{\sigma} \times \Omega)$ orientifold by the minor adjustment $\pi_a \to \pi_a^o$ [4].

Let us emphasize that in contrast to [13] we use the convention of [7]. This means that N coincident branes which are not invariant under $\overline{\sigma}$ carry $U(N)$ gauge group. Invariant brane stacks of N coincident branes carry $USp(2N, \mathbb{C})$ gauge group. Note in particular that the latter is a specification on our orientifold projection. It goes back to the original literature [13], where it was pointed out that such a projection is possible.

8.6. R-R Tadpole Cancelation

To obtain the R-R tadpole constraints one starts off by considering the Chern-Simon action. This analysis works on $\mathcal{O}$ in precisely the same way as it does on $\mathcal{M}$. The analysis on the latter was already discussed in section 5.4 and yields

$$0 = \sum_a N_a \left(\pi_a^o + \pi_a^{o\prime}\right) - 4\pi_{O6}^o \tag{8.27}$$

By using Equation 8.26 one can rewrite this constraint in terms of the wrapping numbers of an intersecting D6-brane model. One obtains

$$\begin{aligned} 8 &= \sum_a N_a \prod_{I=1}^{3} n_a^{I,o} \\ 8 &= -2^{2b^J} 2^{2b^K} \sum_a \left(N_a n_a^{I,o} \widetilde{m}_a^{J,o} \widetilde{m}_a^{K,o}\right), \qquad I \neq J \neq K \neq I \end{aligned} \tag{8.28}$$

8.7. K-Theory Constraints

Recall that the Ramond $C^{(7)}$ charges are actually classified by K-theory groups rather than homology groups. Therefore there exist torsion K-theory charges that are invisible to homology but still need cancelation.

As discussed in section 5.5, heuristically we can ensure this cancelation by enforcing an even number of fundamental representations of $USp(2, \mathbb{C})$. By our choice of

[4] It should be highlighted that the authors of [13] conventionally use an orientifold plane that is normalized differently than ours, given in Equation 8.26. Therefore in [13] a factor $\frac{4}{2^k}$ appears in the multiplicity of the symmetric and antisymmetric representations, where k is the number of tilted tori. Let us also highlight that our choice for the orientifold plane is in agreement with [7].

orientifolding, every brane stack that is invariant under $\overline{\sigma}$ carries $USp\,(2N, \mathbb{C})$ gauge group. So the probe branes with $USp\,(2, \mathbb{C})$ gauge group are [5]

$$\begin{aligned}
\pi_1^{\mathrm{USp}} &:= 2^{2b^1}2^{2b^2}2^{2b^3} \cdot (1,0) \times (1,0) \times (1,0) \\
\pi_2^{\mathrm{USp}} &:= 2^{2b^1} \cdot (1,0) \times (0,1) \times (0,1) \\
\pi_3^{\mathrm{USp}} &:= 2^{2b^2} \cdot (0,1) \times (1,0) \times (0,1) \\
\pi_4^{\mathrm{USp}} &:= 2^{2b^3} \cdot (0,1) \times (0,1) \times (1,0)
\end{aligned} \tag{8.29}$$

They give rise to the following K-theory constraints.

$$\begin{aligned}
&2^{2b^1}2^{2b^2}2^{2b^3} \sum_a \left(N_a \widetilde{m}_a^{1,o} \widetilde{m}_a^{2,o} \widetilde{m}_a^{3,o} \right) \in 2\mathbb{Z} \\
&2^{2b^I} \sum_a \left(N_a \widetilde{m}_a^{I,o} n_a^{J,o} n_a^{K,o} \right) \in 2\mathbb{Z}, \qquad I \neq J \neq K \neq I
\end{aligned} \tag{8.30}$$

[5] Recall again that the number of invariant 1-cycles may differ on tilted and rectangular tori. This is outlined in Figure 8.1 and is accounted for by including the prefactors 2^{2b^I}.

9. Supersymmetric Three Family Model

We will now discuss a three family supersymmetric model. This model is build on the orientifold

$$\mathbb{O} = \mathcal{O}/\left(\overline{\sigma} \times \Omega\right), \qquad \mathcal{O} = \mathcal{M}/\left(\mathbb{Z}_2 \times \mathbb{Z}_2\right) \tag{9.1}$$

with the third torus tilted. It was first published in [13]. [1]

9.1. General Features Of The Setup

9.1.1. The Branes

The branes that form this particular intersecting D6-brane model are listed in Table 9.1. Also the image branes are listed in this table. The orientifold plane is easily obtained from Equation 8.26. For $b^1 = b^2 = 0$ and $b^3 = \frac{1}{2}$ one finds

$$\pi^o_{O6} = 4\prod_{i=1}^{3}\left[a^{i,o}\right] - 2\left[a^{1,o}\right]\left[b^{2,o}\right]\left[b^{3,o}\right] - 2\left[a^{2,o}\right]\left[b^{1,o}\right]\left[b^{3,o}\right] - 4\left[a^{3,o}\right]\left[b^{1,o}\right]\left[b^{2,o}\right] \tag{9.2}$$

9.1.2. Intersection Numbers And Brane Picture

From the wrapping numbers given in Table 9.1 one can work out the intersection numbers. Their absolute value is given in the brane picture displayed in Figure 9.1. Note especially that the following convention is in use.

- $I_{ab} < 0$, then **left-handed, massless** fermions stretch from b to a.
- $I_{ab} > 0$, then **left-handed, massless** fermions stretch from a to b.

Finally let us point out that the brane stack A_2 is a 'hidden' brane stack. [2]

[1] Even though the authors of [13] term this particular model a three family model (and we therefore adopt this terminology), it will turn out that there are only two generations of right-handed matter particles.

[2] More information can be found in section 7.1.4.

Brane	N_a	$(n_a^1, m_a^1) \times (n_a^2, m_a^2) \times (n_a^3, \widetilde{m}_a^3)$	Gauge group	$U(1)$
A_1	4	$(0,1) \times (0,-1) \times \left(2, \widetilde{0}\right)$	$U(1) \times U(1)$	Q_8, Q'_8
A'_1	4	$(0,-1) \times (0,1) \times \left(2, \widetilde{0}\right)$		
A_2	1	$(1,0) \times (1,0) \times \left(2, \widetilde{0}\right)$	$USp(2,\mathbb{C})_A$	
A'_2	1	$(1,0) \times (1,0) \times \left(2, \widetilde{0}\right)$		
B_1	2	$(1,0) \times (1,-1) \times \left(1, \widetilde{\frac{3}{2}}\right)$	$SU(2) \times U(1)$	Q_2
B'_1	2	$(1,0) \times (1,1) \times \left(1, \widetilde{-\frac{3}{2}}\right)$		
B_2	1	$(1,0) \times (0,1) \times \left(0, \widetilde{-1}\right)$	$USp(2,\mathbb{C})_B$	
B'_2	1	$(1,0) \times (0,-1) \times \left(0, \widetilde{1}\right)$		
C_1	3+1	$(1,1) \times (1,0) \times \left(1, \widetilde{\frac{1}{2}}\right)$	$SU(3) \times U(1) \times U(1)$	Q_3, Q_1
C'_1	3+1	$(1,1) \times (1,0) \times \left(1, \widetilde{-\frac{1}{2}}\right)$		
C_2	2	$(0,1) \times (1,0) \times \left(0, \widetilde{-1}\right)$	$USp(4,\mathbb{C})$	
C'_2	2	$(0,-1) \times (1,0) \times \left(0, \widetilde{1}\right)$		

Table 9.1.: The branes, their image branes and the associated gauge groups in the three family supersymmetric setup first published in [13]. In the third column we introduce the notion for the $U(1)$ gauge bosons.

9.1.3. Check Of The Various Constraints

As this is a supersymmetric model, it has to satisfy three sets of constraints.

- The supersymmetry constraint.
- The R-R tadpole constraints.
- The K-theory constraints.

It is not difficult to verify that all these constraints are satisfied by this model. Therefore we skip an in-detail analysis, but encourage the interested reader to perform these checks explicitely.

9.2. Massless Spectrum And U(1) Gauge Bosons

9.2.1. Gauge Groups

The gauge groups on the various branes in this setup are listed in Table 9.1. Note that a priori the brane stack A_1 is invariant under $\overline{\sigma}$ and would therefore carry a $USp(8)$ gauge group. However it is neater to split A_1 into four individual branes and to move two of them away from the orientifold plane. The position of the remaining

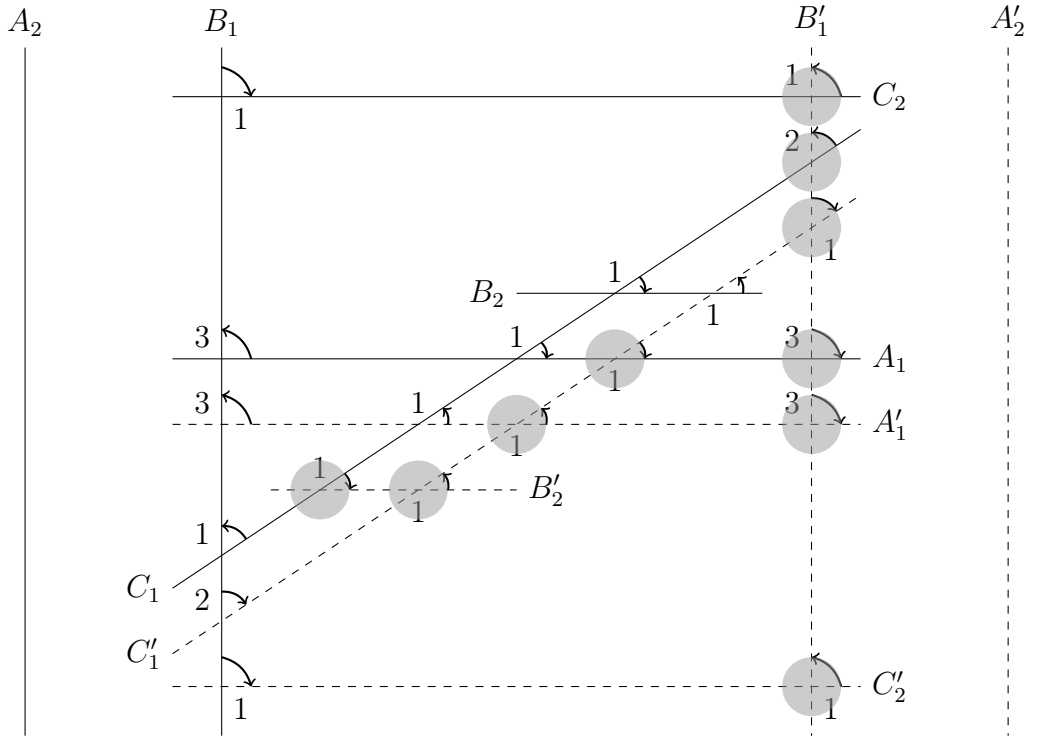

Figure 9.1.: Brane setup of the supersymmetric three family model first published in [13]. Arrows along arcs indicate the orientation of the open strings stretching between the corresponding branes and giving rise to left-handed fermions. Shadows indicate image particles.

two branes is then fixed by the requirement that the overall situation is invariant under $\overline{\sigma}$. In particular the gauge group along A_1 is reduced to $U(1) \times U(1)$. Thereby we obtain additional $U(1)$ gauge bosons that will be used to built the Standard Model hypercharge.
In principle this technique could also be applied to C_2, but the authors of [13] prefered not to do this. Note also that it is not possible to do this with B_2 or A_2, as the latter two are fractional branes.

9.2.2. Massless Fermionic Spectrum

We define [3]

$$Q_x := \frac{1}{6}Q_3 - \frac{1}{2}Q_1 + \frac{1}{2}\left(Q_8 + Q_8'\right) \tag{9.3}$$

[3]This combination of $U(1)$ gauge fields will turn out to be the hypercharge in this intersecting D6-brane model. However it is too early to claim this as we need to analyse the masses and anomalies of the various $U(1)$ gauge bosons in the model. Therefore we use the index x until we performed this analysis.

Sector	Chirality	Representation	$(Q_3, Q_1, Q_2, Q_8, Q'_8)$	Q_x	$Q_8 - Q'_8$	Field
A_1B_1	L	$3 \times \left(1, \overline{2}, 1, 1, 1\right)$	$(0, 0, -1, 1, 0)$	$\frac{1}{2}$	1	
	R	$3 \times (1, 2, 1, 1, 1)$	$(0, 0, 1, -1, 0)$	$-\frac{1}{2}$	-1	
	L	$3 \times \left(1, \overline{2}, 1, 1, 1\right)$	$(0, 0, -1, 0, 1)$	$\frac{1}{2}$	-1	
	R	$3 \times (1, 2, 1, 1, 1)$	$(0, 0, 1, 0, -1)$	$-\frac{1}{2}$	1	
$A_1B'_1$	L	$3 \times \left(1, \overline{2}, 1, 1, 1\right)$	$(0, 0, -1, -1, 0)$	$-\frac{1}{2}$	-1	
	R	$3 \times (1, 2, 1, 1, 1)$	$(0, 0, 1, 1, 0)$	$\frac{1}{2}$	1	
	L	$3 \times \left(1, \overline{2}, 1, 1, 1\right)$	$(0, 0, -1, 0, -1)$	$-\frac{1}{2}$	1	
	R	$3 \times (1, 2, 1, 1, 1)$	$(0, 0, 1, 0, 1)$	$\frac{1}{2}$	-1	
A_1C_1	L	$1 \times \left(\overline{3}, 1, 1, 1, 1\right)$	$(-1, 0, 0, 1, 0)$	$\frac{1}{3}$	1	D^c
	R	$1 \times (3, 1, 1, 1, 1)$	$(1, 0, 0, -1, 0)$	$-\frac{1}{3}$	-1	D
	L	$1 \times \left(\overline{3}, 1, 1, 1, 1\right)$	$(-1, 0, 0, 0, 1)$	$\frac{1}{3}$	-1	D^c
	R	$1 \times (3, 1, 1, 1, 1)$	$(1, 0, 0, 0, -1)$	$-\frac{1}{3}$	1	D
	L	$1 \times \left(\overline{1}, 1, 1, 1, 1\right)$	$(0, -1, 0, 1, 0)$	1	1	E^c
	R	$1 \times (1, 1, 1, 1, 1)$	$(0, 1, 0, -1, 0)$	-1	-1	E
	L	$1 \times \left(\overline{1}, 1, 1, 1, 1\right)$	$(0, -1, 0, 0, 1)$	1	-1	E^c
	R	$1 \times (1, 1, 1, 1, 1)$	$(0, 1, 0, 0, -1)$	-1	1	E
$A_1C'_1$	L	$1 \times \left(\overline{3}, 1, 1, 1, 1\right)$	$(-1, 0, 0, -1, 0)$	$-\frac{2}{3}$	-1	U^c
	R	$1 \times (3, 1, 1, 1, 1)$	$(1, 0, 0, 1, 0)$	$\frac{2}{3}$	1	U
	L	$1 \times \left(\overline{3}, 1, 1, 1, 1\right)$	$(-1, 0, 0, 0, -1)$	$-\frac{2}{3}$	1	U^c
	R	$1 \times (3, 1, 1, 1, 1)$	$(1, 0, 0, 0, 1)$	$\frac{2}{3}$	-1	U
	L	$1 \times \left(\overline{1}, 1, 1, 1, 1\right)$	$(0, -1, 0, -1, 0)$	0	-1	N^c
	R	$1 \times (1, 1, 1, 1, 1)$	$(0, 1, 0, 1, 0)$	0	1	N
	L	$1 \times \left(\overline{1}, 1, 1, 1, 1\right)$	$(0, -1, 0, 0, -1)$	0	1	N^c
	R	$1 \times (1, 1, 1, 1, 1)$	$(0, 1, 0, 0, 1)$	0	-1	N
B_1C_1	L	$1 \times \left(3, \overline{2}, 1, 1, 1\right)$	$(1, 0, -1, 0, 0)$	$\frac{1}{6}$	0	Q
	R	$1 \times \left(\overline{3}, 2, 1, 1, 1\right)$	$(-1, 0, 1, 0, 0)$	$-\frac{1}{6}$	0	Q^c
	L	$1 \times \left(1, \overline{2}, 1, 1, 1\right)$	$(0, 1, -1, 0, 0)$	$-\frac{1}{2}$	0	L
	R	$1 \times \left(\overline{1}, 2, 1, 1, 1\right)$	$(0, -1, 1, 0, 0)$	$\frac{1}{2}$	0	L^c
$B_1C'_1$	L	$2 \times (3, 2, 1, 1, 1)$	$(1, 0, 1, 0, 0)$	$\frac{1}{6}$	0	Q
	R	$2 \times \left(\overline{3}, \overline{2}, 1, 1, 1\right)$	$(-1, 0, -1, 0, 0)$	$-\frac{1}{6}$	0	Q^c
	L	$2 \times (1, 2, 1, 1, 1)$	$(0, 1, 1, 0, 0)$	$-\frac{1}{2}$	0	L
	R	$2 \times \left(1, \overline{2}, 1, 1, 1\right)$	$(0, -1, -1, 0, 0)$	$\frac{1}{2}$	0	L^c
B_1C_2	L	$1 \times \left(1, 2, 1, 1, \overline{4}\right)$	$(0, 0, 1, 0, 0)$	0	0	
	R	$1 \times \left(1, \overline{2}, 1, 1, 4\right)$	$(0, 0, -1, 0, 0)$	0	0	
$B_1C'_2$	L	$1 \times (1, 2, 1, 1, 4)$	$(0, 0, 1, 0, 0)$	0	0	
	R	$1 \times \left(1, \overline{2}, 1, 1, \overline{4}\right)$	$(0, 0, -1, 0, 0)$	0	0	

Sector	Chirality	Representation	$(Q_3, Q_1, Q_2, Q_8, Q_8')$	Q_x	$Q_8 - Q_8'$	Field
B_2C_1	L	$1 \times \left(\overline{3}, 1, 1, 2, 1\right)$	$(-1, 0, 0, 0, 0)$	$-\frac{1}{6}$	0	
	R	$1 \times \left(3, 1, 1, \overline{2}, 1\right)$	$(1, 0, 0, 0, 0)$	$\frac{1}{6}$	0	
	L	$1 \times (1, 1, 1, 2, 1)$	$(0, -1, 0, 0, 0)$	$\frac{1}{2}$	0	
	R	$1 \times \left(1, 1, 1, \overline{2}, 1\right)$	$(0, 1, 0, 0, 0)$	$-\frac{1}{2}$	0	
B_2C_1'	L	$1 \times (3, 1, 1, 2, 1)$	$(1, 0, 0, 0, 0)$	$\frac{1}{6}$	0	
	R	$1 \times \left(\overline{3}, 1, 1, \overline{2}, 1\right)$	$(-1, 0, 0, 0, 0)$	$-\frac{1}{6}$	0	
	L	$1 \times (1, 1, 1, 2, 1)$	$(0, 1, 0, 0, 0)$	$-\frac{1}{2}$	0	
	R	$1 \times \left(\overline{1}, 1, 1, \overline{2}, 1\right)$	$(0, -1, 0, 0, 0)$	$\frac{1}{2}$	0	

Table 9.2.: The massless fermionic spectrum in the three family supersymmetric model first published in [13]. The representations are written as $SU(3)_C \times SU(2)_W \times USp(2, \mathbb{C})_A \times USp(2, \mathbb{C})_B \times USp(4, \mathbb{C})$.

This $U(1)$ charge together with the massless fermionic spectrum are displayed in Table 9.2.
Note that one obtains three families of left-handed quarks and leptons in the B_1C_1 and B_1C_1' sector. But there are only two generations of right-handed matter particles. These can be found in the A_1C_1 and A_1C_1' sector.
The fermions that appear in the A_1B_1 and A_1B_1' sector transform in the same way as Higgs doublets do. They also have the appropriate Q_x charge. Therefore we will eventually identify the lightest bosonic excitations in these two sectors with Higgs doublets.

9.2.3. Massless Bosonic Spectrum

The massless bosonic excitations arise in the aa-sector. We list those excitations in Table 9.3. They transform in the adjoint representation of the corresponding gauge group and therefore correspond to the associated gauge bosons. Consequently the gluons arise as bosonic excitations in the C_1C_1 sector, whilst $W^{\pm}$ and Z gauge bosons appear in the B_1B_1 sector.

9.2.4. U(1) Gauge Bosons

Anomalous U(1) Gauge Bosons

The $U(1)$ anomalies are listed in Table 6.2. Baring this in mind one calculates the $U(1)$ anomalies given in Table 9.4. Thereby we find that Q_8, Q_8' and $Q_3 - 3Q_1$ are anomaly free. In particular this implies that Q_x is anomaly free.

Sector	$U(3)_C \times U(2)_W \times USp(2,\mathbb{C})_A \times USp(2,\mathbb{C})_B \times USp(4,\mathbb{C})$	Field
A_1A_1	$3 \times (1,1,1,1,1)$	Q_8
	$3 \times (1,1,1,1,1)$	Q_8'
A_2A_2	$3 \times (1,1,3,1,1)$	
B_1B_1	$3 \times (1,4,1,1,1)$	$W^{\pm}$, Z, Q_2
B_2B_2	$3 \times (1,1,1,3,1)$	
C_1C_1	$3 \times (9,1,1,1,1)$	Gluons, Q_3
	$3 \times (1,1,1,1,1)$	Q_1
C_2C_2	$3 \times (1,1,1,1,10)$	

Table 9.3.: Massless bosonic spectrum in the supersymmetric three family model first published in [13]. Note that these bosons transform in the adjoint representation. In particular note that we used $\dim_{\mathbb{R}}(USp(2N,\mathbb{C})) = N \cdot (2N+1)$ (see Appendix A for more details on $USp(2N,\mathbb{C})$).

Masses For Anomalous U(1) Gauge Bosons

Q_2 and $Q_3 + 3Q_1$ are anomalous $U(1)$ gauge bosons. Therefore we expect them to aquire masses in the course of anomaly cancelation by means of the generalized Green-Schwarz mechanism. To check this we calculate M^2 by using Equation 6.20. Thereby one obtains

$$M^2 = \begin{array}{c} \begin{array}{ccccc} Q_8 & Q_8' & Q_2 & Q_3 & Q_1 \end{array} \\ \left(\begin{array}{ccccc} 0 & 0 & 0 & 0 & 0 \\ 0 & 0 & 0 & -6 & -2 \\ 0 & 0 & -4 & 0 & 0 \\ 0 & 0 & 6 & 3 & 1 \end{array} \right) \end{array} \tag{9.4}$$

This matrix has

$$\ker(M) = \text{span}\left[\begin{pmatrix} 1 \\ 0 \\ 0 \\ 0 \\ 0 \end{pmatrix}, \begin{pmatrix} 0 \\ 1 \\ 0 \\ 0 \\ 0 \end{pmatrix}, \begin{pmatrix} 0 \\ 0 \\ 0 \\ 1 \\ -3 \end{pmatrix} \right] \widehat{=} \text{span}(Q_8, Q_8', Q_3 - 3Q_1) \tag{9.5}$$

Therefore Q_8, Q_8' and $Q_3 - 3Q_1$ remain massless. Note that in particular Q_x remains massless, and we can finally conclude that $Q_x = Q_Y$. But also note that Q_2 and $Q_3 + 3Q_1$ obtain masses, as expected.

Physical Significance Of Massive U(1) Gauge Bosons

Massive $U(1)$ gauge bosons serve as perturbative symmetries in the effective four-dimensional theory [7]. From Table 9.2 one easily concludes

		Q_8	Q'_8	Q_2	Q_3	Q_1
$\mathcal{A}^{abb}$	A_1	0	0	0	0	0
	B_1	0	0	0	$\frac{9}{2}$	$\frac{3}{2}$
	C_1	0	0	$\frac{3}{2}$	0	0
$\widetilde{\mathcal{A}}^{abb}$	A_1	0	0	-12	-6	-2
	B_1	0	0	0	18	6
	C_1	0	0	6	0	0
$\mathcal{A}^{aSpSp}$	A_2	0	0	0	0	0
	B_2	0	0	0	3	1
	C_2	0	0	0	0	0
$\mathcal{A}^{agg}$		0	0	0	0	0

Table 9.4.: U(1) anomalies of the supersymmetric three family model published in [13].

- $\frac{Q_3}{3}$ corresponds to the Baryon number.
- Q_1 corresponds to the Lepton number.

Since $Q_3 + 3Q_1$, or equivalently $\frac{Q_3}{3} + Q_1$, become massive we have a pertubartive symmetry corresponding to the conversation of the sum of Baryon and Lepton number.

9.3. Higgs Sector

9.3.1. Location And Quantum Numbers

Recall the properties of the Higgs doublets as listed in Table 1.2. Such particles appear in the A_1B_1 and $A_1B'_1$ sector. We list the corresponding string states in Table 9.5.

9.3.2. Mass For Higgs Particles

Let us first consider the Higgs particles arising in the A_1B_1-sector. To this end we display the branes A_1 and B_1 in Figure 9.2. Note that these branes are not parallel in one of the tori. So in comparision to the non-supersymmetric model discussed in chapter 7, one does not obtain mass terms that depend on a separation $Z_I^{A_1B_1}$. Rather the lightest bosonic excitations in this sector have masses [4]

$$\alpha' M^2_{A_1B_1} = \frac{1}{2} \cdot \left[\frac{1}{2} \pm \left(\left| \vartheta^3_{A_1B_1} \right| - \left| \vartheta^2_{A_1B_1} \right| \right) \right] \tag{9.6}$$

[4] We used $\vartheta^1_{A_1B_1} = \frac{1}{2}$.

Sector	Higgs Doublet	Representation	Q_8	Q'_8	Q_2	Q_Y
A_1B_1	H_U	$3 \times \left(1, \overline{2}, 1, 1, 1\right)$	1	0	-1	$\frac{1}{2}$
	H_D	$3 \times (1, 2, 1, 1, 1)$	-1	0	1	$-\frac{1}{2}$
	H'_U	$3 \times \left(1, \overline{2}, 1, 1, 1\right)$	0	1	-1	$\frac{1}{2}$
	H'_D	$3 \times (1, 2, 1, 1, 1)$	0	-1	1	$-\frac{1}{2}$
$A_1B'_1$	$\widetilde{H}_D$	$3 \times \left(1, \overline{2}, 1, 1, 1\right)$	-1	0	-1	$-\frac{1}{2}$
	$\widetilde{H}_U$	$3 \times (1, 2, 1, 1, 1)$	1	0	1	$\frac{1}{2}$
	$\widetilde{H}'_D$	$3 \times \left(1, \overline{2}, 1, 1, 1\right)$	0	-1	-1	$-\frac{1}{2}$
	$\widetilde{H}'_U$	$3 \times (1, 2, 1, 1, 1)$	0	1	1	$\frac{1}{2}$

Table 9.5.: Higgs doublets in the supersymmetric three family model first published in [13]. The representations are written as $SU(3)_C \times SU(2)_W \times USp(2,\mathbb{C})_A \times USp(2,\mathbb{C})_B \times USp(4,\mathbb{C})$.

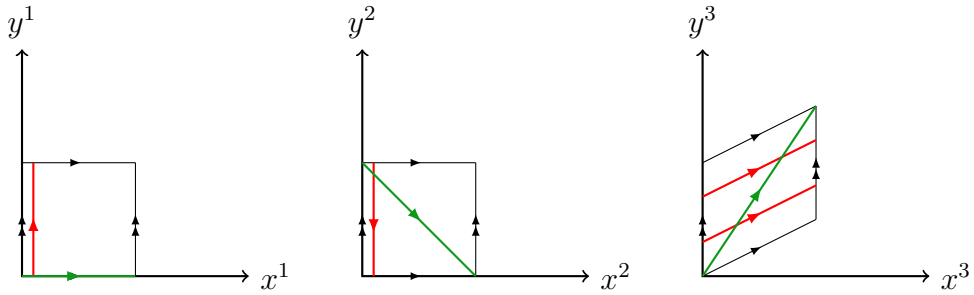

Figure 9.2.: The A_1 (red) and B_1 (green) branes in the three family supersymmetric model first published in [13]. For illustrational reasons we have separated the A_1 brane from the y^I axis in the first two tori.

Similarly one finds for the lightest bosonic excitations in the $A_1B'_1$ sector

$$\alpha' M^2_{A_1B'_1} = \frac{1}{2} \cdot \left[\frac{1}{2} \pm \left(\left|\vartheta^3_{A_1B'_1}\right| - \left|\vartheta^2_{A_1B'_1}\right|\right)\right] \tag{9.7}$$

9.3.3. Multiplicity Of Higgs Doublets

In the A_1B_1 sector we find three Higgs doublets H_U and three Higgs doublets H'_U. They only differ in the sense that the former are charged under Q_8 and the latter under Q'_8, whilst the associated Higgs particles have the same masses. In this sense there are six Higgs doublets in the A_1B_1 sector. The same is true for the $A_1B'_1$ sector, where we find another six Higgs doublets. Therefore the total number of Higgs doublets in this three family supersymmetric model is twelve.

9.4. Summary

Our discussion of this supersymmetric model proceeded in the same way as the discussion of the non-supersymmetric model in chapter 7. Again we considered basic properties of the model in section 9.1 which includes the construction of the brane picture displayed in Figure 9.1. It allows for an intuitive picture of the entire situation.
Subsequently we discussed the massless spectrum and the $U(1)$ gauge bosons in section 9.2. The massless fermionic spectrum is given in Table 9.2. From it we deduced, that there are three generations of left-handed quarks and leptons in this model. However there are only two generations of right-handed up- and down-quarks as well as right-handed charged and neutral leptons. In this sense one right-handed generation is missing. Nevertheless we found that there is a massless $U(1)$ gauge boson that gives the correct Standard Model hypercharge. Also we found that two $U(1)$ combinations become massive, namely Q_2 and $\frac{Q_3}{3} + Q_1$. The latter has an interpretation as conservation of the sum of lepton and baryon number. This statement is weaker than individual baryon and lepton number conservation, which we obtained for the non-supersymmetric model in chapter 7. However conservation of $B+L$ rules out a number of possible decays for the proton.
We concluded the discussion of this supersymmetric model in section 9.3 where we pointed out that twelve Higgs doublets appear in this model. We also worked out their masses. In comparison to the non-supersymmetric model in which only one or two Higgs doublets appear, the appearance of twelve such doublets makes the discussion of the possible Yukawa couplings more challenging and lengthy. For this reason we do not present this analysis here.

10. Supersymmetric GUT Model

We will now discuss the basic properties of a GUT model that was first published in [13]. It is built on

$$\mathbb{O} = \mathcal{O}/\left(\overline{\sigma} \times \Omega\right), \qquad \mathcal{O} = \mathcal{M}/\left(\mathbb{Z}_2 \times \mathbb{Z}_2\right) \tag{10.1}$$

where the third torus is tilted. So put shortly this model is built on precisely the same background as the three family supersymmetric model that we discussed back in chapter 9.

10.1. General Features Of The Setup

10.1.1. The Branes

Table 10.1 lists the branes that form this intersecting D6-brane model, as well as their images under $\overline{\sigma}$. This brane setup is supersymmetric if we choose [1]

$$\arctan\left(u^1\right) - \arctan\left(u^2\right) + \arctan\left(\frac{u^3}{2}\right) = 0 \bmod 2\pi \tag{10.2}$$

The orientifold plane for the current model is given by [2]

$$\pi^o_{O6} = 4\prod_{i=1}^{3}\left[a^{i,o}\right] - 2\left[a^{1,o}\right]\left[b^{2,o}\right]\left[b^{3,o}\right] - 2\left[a^{2,o}\right]\left[b^{1,o}\right]\left[b^{3,o}\right] - 4\left[a^{3,o}\right]\left[b^{1,o}\right]\left[b^{2,o}\right] \tag{10.3}$$

10.1.2. Intersection Numbers And Brane Picture

The topological intersection number of two 3-cycles is given by

$$\pi_a \circ \pi_b = \prod_I \left(n_a^I \widetilde{m}_b^I - n_b^I \widetilde{m}_a^I\right) \tag{10.4}$$

The brane picture of this situation is given in Figure 10.1, which includes the absolute value of the intersection numbers. Moreover we use the following convention.

- $I_{ab} < 0$, then **left-handed, massless** fermions stretch from a to b.
- $I_{ab} > 0$, then **left-handed, massless** fermions stretch from b to a.

[1] Recall our definition $u^i = \frac{R^i_y}{R^i_x}$.

[2] Use Equation 8.26 and note that in the current setup only the third torus is tilted. Therefore it holds $b^1 = b^2 = 0$ and $b^3 = \frac{1}{2}$.

Label	N_a	Wrapping numbers	Gauge group	$U(1)$ Gauge boson
A_5	5	$(1,1)\times(1,-1)\times\left(1,\widetilde{\frac{1}{2}}\right)$	$SU(5)\times U(1)$	Q_5
A_5'	5	$(1,-1)\times(1,1)\times\left(1,\widetilde{-\frac{1}{2}}\right)$		
A_3	3	$(1,1)\times(1,-1)\times\left(1,\widetilde{\frac{1}{2}}\right)$	$SU(3)\times U(1)$	Q_3
A_3'	3	$(1,-1)\times(1,1)\times\left(1,\widetilde{-\frac{1}{2}}\right)$		
B	8	$(0,1)\times(1,0)\times\left(0,\widetilde{-1}\right)$	$USp(16,\mathbb{C})$	✗
B'	8	$(0,-1)\times(1,0)\times\left(0,\widetilde{1}\right)$		

Table 10.1.: Branes, image branes as well as their gauge groups in the supersymmetric GUT model first published in [13].

10.1.3. Check Of The Various Constraints

This is a supersymmetric model and therefore has to satisfy three sets of constraints, namely

- the Supersymmetry constraints.
- the R-R tadpole constraints.
- the K-theory constraints.

One readily verifies that all these constraints are satisfied by this GUT model. In particular note that Equation 10.2 ensures that the model is supersymmetric.

10.2. Massless Spectrum And U(1) Gauge Bosons

10.2.1. Gauge Groups

The brane stacks A_5 and A_3 are not invariant under $\overline{\sigma}$. Therefore they carry a $U(N)$ gauge group. The brane stack B carries the gauge group $USp(2N_b,\mathbb{C})$ since it is invariant under $\overline{\sigma}$. These findings are summarized in Table 10.1.

10.2.2. Massless Fermionic Spectrum

The massless fermionic spectrum for intersecting D6-brane models is given in Table 5.1. Note in particular that in this GUT model massless fermionic excitations in $U(N)-USp(2N,\mathbb{C})$ bifundamental representations arise at the insections of the brane stack B with A_3 and A_5, respectively.
Moreover we obtain massless fermions from strings in the $\mathrm{A}_5\mathrm{A}_5'$-sector as well as the $\mathrm{A}_3\mathrm{A}_3'$-sector. The bifundamental representations in which these strings transform can be decomposed into symmetric and antisymmetric representations of $U(5)$ and

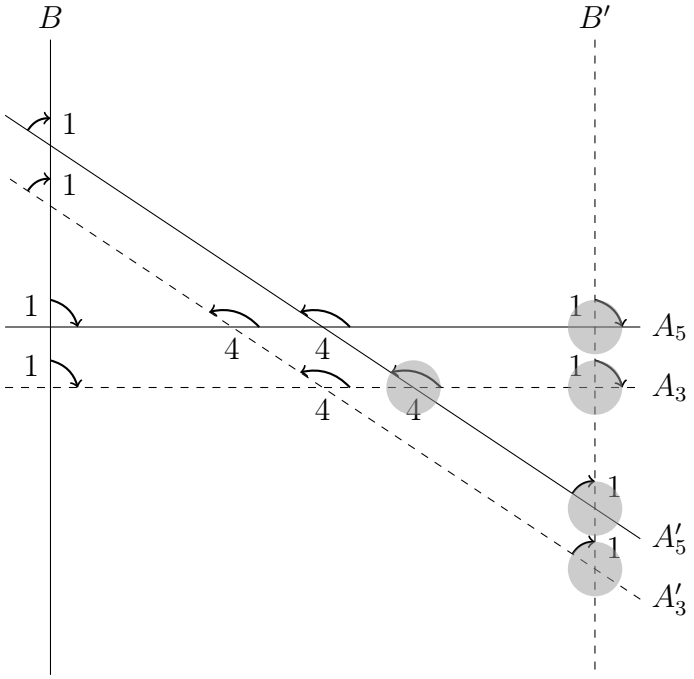

Figure 10.1.: Brane setup of the supersymmetric GUT model first published in [13]. Arrows along arcs describe the orientation of the open strings stretching between the corresponding branes and giving rise to left-handed chiral fermions. Shadows mark image particles.

$U(3)$, respectively. The multiplicites of the so-obtained symmetric and antisymmetric representations are given in Table 5.1. In this GUT model we have

- $\pi^o_{O6} \circ A_5 = \pi^o_{O6} \circ A_3 = -4$
- $A'_5 \circ A_5 = A'_3 \circ A_3 = -4$

So Table 5.1 tells us that the multiplicity for the symmetric representations vanishes. So we are left with antisymmetric representations only. Their dimensionalities are

- $\begin{smallmatrix}\square\\\square\end{smallmatrix}$ of $U(5)$ has $\begin{pmatrix} 5 \\ 2 \end{pmatrix} = 10$ degrees of freedom.
- $\begin{smallmatrix}\square\\\square\end{smallmatrix}$ of $U(3)$ has $\begin{pmatrix} 3 \\ 2 \end{pmatrix} = 3$ degrees of freedom.

We summarize these results in Table 10.2.

10.2.3. Massless Bosonic Spectrum

We list the massless bosonic spectrum of this GUT model in Table 10.3. As in the models discussed previously, the massless bosons arise in the aa-sector and can therefore be identified with the gauge bosons of the corresponding gauge groups.

Sector	Chirality	$U(5) \times U(3) \times USp(16, \mathbb{C})$	Q_5	Q_3
A_3B	L	$1 \times \left(1, 3, \overline{16}\right)$	0	1
	R	$1 \times \left(1, \overline{3}, 16\right)$	0	-1
$A_3'B$	L	$1 \times (1, 3, 16)$	0	1
	R	$1 \times \left(1, \overline{3}, \overline{16}\right)$	0	-1
A_5B	L	$1 \times \left(5, 1, \overline{16}\right)$	1	0
	R	$1 \times \left(\overline{5}, 1, 16\right)$	-1	0
$A_5'B$	L	$1 \times (5, 1, 16)$	0	1
	R	$1 \times \left(\overline{5}, 1, \overline{16}\right)$	0	-1
A_5A_3'	L	$4 \times \left(\overline{5}, \overline{3}, 1\right)$	-1	-1
	R	$4 \times (5, 3, 1)$	1	1
A_5A_5'	L	$4 \times \left(\overline{10}, 1, 1\right)$	2	0
	R	$4 \times (10, 1, 1)$	2	0
A_3A_3'	L	$4 \times \left(1, \overline{3}, 1\right)$	0	-2
	R	$4 \times (1, 3, 1)$	0	2

Table 10.2.: Massless fermionic spectrum in the supersymmetric GUT model first published in [13]. The branes forming this model are specified in Table 10.1.

10.2.4. U(1) Gauge Bosons

Anomalous U(1) Gauge Bosons

The $U(1)$ anomalies are summarized in Table 6.2. By using these results one derives the $U(1)$ anomalies, that we list in Table 10.4. From this table we deduce that $3Q_5 - 5Q_3$ remains anomaly free, whilst $3Q_5 + 5Q_3$ is anomalous.

Masses For Anomalous U(1) Gauge Bosons

To see whether $3Q_5 - 5Q_3$ remains massless we calculate M^2 by using Equation 6.20. Thereby we obtain

$$M^2 = \begin{array}{c} \begin{array}{cc} Q_3 & Q_5 \end{array} \\ \left(\begin{array}{cc} -3 & -5 \\ 6 & 10 \\ -6 & -10 \\ 3 & 5 \end{array} \right) \end{array} \tag{10.5}$$

This matrix has

$$\ker(M) = \text{span}\left[\begin{pmatrix} 5 \\ -3 \end{pmatrix} \right] \tag{10.6}$$

which tells us that indeed $3Q_5 - 5Q_3$ remains massless, whilst the anomalous combination $3Q_5 + 5Q_3$ aquires mass. As already anticipated one can therefore hope to

Sector	$U(5) \times U(3) \times USp(16, \mathbb{C})$
A_1A_1	$3 \times (25, 1, 1)$
A_2A_2	$3 \times (1, 9, 1)$
BB	$3 \times (1, 1, 136)$

Table 10.3.: Massless bosonic spectrum of the GUT model first published in [13]. Note that the bosons transform in the adjoint representations and that we used $\dim_{\mathbb{R}}(USp(2N, \mathbb{C})) = N \cdot (2N + 1)$ (for more details on $USp(2N, \mathbb{C})$ see Appendix A).

		Q_3	Q_5
$\mathcal{A}^{abb}$	A_3	-6	-10
	A_5	-6	-10
$\widetilde{\mathcal{A}}^{abb}$	Q_3	-36	-60
	Q_5	-60	-100
$\mathcal{A}^{aSpSp}$	B	3	5
$\mathcal{A}^{agg}$		-36	-60

Table 10.4.: U(1) anomalies in the supersymmetric GUT model first published in [13].

obtain a massless $U(1)$ combination after splitting $U(5)$, which gives the Standard Model hypercharge.

Part IV.

Computation Of Supersymmetric Models

11. Introduction

In Part II we have discussed a class of models on the $\mathcal{M}/(\overline{\sigma} \times \Omega)$ orientifold, that was first published in [21]. This class of models was derived under very general assumptions, among which the most important is to obtain the massless fermionic spectrum of the Standard Model. As was noted in our discussion of these models, they are not supersymmetric. Therefore one is lead to consider different orientifolds to built supersymmetric models on, whose massless fermionic spectrum is as close as possible to the matter particles in the Standard Model.
A possible orientifold with structure similar to $\mathcal{M}/(\overline{\sigma} \times \Omega)$ is $\mathcal{O}/(\overline{\sigma} \times \Omega)$. In [13] supersymmetric models on this orientifold were constructed. The corresponding three family and GUT model were discussed in chapter 9 and chapter 10, respectively.
To arrive at these models, certain assumptions have been made in [13]. In particular it was pointed out that these assumptions proved very restricting, giving rise to a unique three family supersymmetric model - namely the one that we discussed in detail in chapter 9. This restrictive character arises because the combination of R-R tadpole cancelation conditions (including K-theory constraints) and supersymmetry conditions form a strong constraint. In particular this observation raises the question whether the number of supersymmetric intersecting D-brane models on $\mathcal{O}/(\overline{\sigma} \times \Omega)$ is finite for a given number of brane stacks.
This question has been adressed in [15]. Here we will take up this analysis. In chapter 12 we will discuss symmetries of the wrapping numbers and a classification of the D6-branes. Subsequently we will consider a supersymmetric model made of N brane stacks [1]. By applying the knowledge from chapter 12 we will then find bounds for the wrapping numbers of branes forming a supersymmetric model that also satisfies R-R tadpole cancelation. This is presented in chapter 13.
In particular we will show that these bounds are independent on the moduli j, k and l. Given a number of brane stacks it is therefore possible to count the number of wrapping number combinations that give a brane setup which satisfies R-R tadpole cancelation and K-theory constraints. To obtain the supersymmetric configurations for given moduli j, k and l only those configurations need to be checked for supersymmetry.
To demonstrate this task we designed a C++ program which counts the number of one-stack models that undersaturate the R-R tadpole but satisfy the K-theory constraints. We will discuss this topic in chapter 14. For further reference the major part of the code of the program as well as the numerical results for $T \leq 20$ are given in Appendix C.

[1] N is arbitary but fixed.

12. Structures

12.1. Restriction To Simple Models

Given a fixed number of brane stacks, our aim is to show that the wrapping numbers of the branes forming a setup which satisfies R-R tadpole cancelation, K-theory constraints and supersymmetry, are bounded. [1]
Both R-R tadpole and K-theory constraints include the number of coincident branes N_a that form the brane stack a, as well as prefactors of the form 2^{2b^I} resulting from tilted tori. So the more coincident branes and the more tori are tilted, the more the wrapping numbers are restricted by these constraints. Conversely, models with single branes (i.e. $N_a = 1$) on three rectangular tori give the least restrictive conditions for the wrapping numbers. For that reason it is sufficient to find bounds on the wrapping numbers for models with the following properties.

- All three tori are rectangular, i.e. $b^I = 0$ for $I = 1, 2, 3$.
- $N_a = 1$ for all brane stacks.

We term such models **simple models**.

12.2. Summary On Constraints

We now give a summary on the constraints, that supersymmetric simple models have to satisfy.

12.2.1. R-R Tadpole Cancelation

The R-R Tadpole constraints on $\mathcal{O}/\left(\overline{\sigma} \times \Omega\right)$ are [2]

$$\begin{aligned} 8 &= \sum_a n_a^{1,o} n_a^{2,o} n_a^{3,o} \\ 8 &= -\sum_a \left(n_a^{I,o} m_a^{J,o} m_a^{K,o} \right), \qquad I \neq J \neq K \neq I \end{aligned} \tag{12.1}$$

[1] Recall that R-R tadpole constraints together with the K-theory constraints ensure cancelation of R-R tadpoles. Then NS-NS tadpoles cancel precisely if the brane setup is supersymmetric [7]. Therefore models that satisfy R-R tadpole, K-theory and supersymmetry conditions have no uncanceled tadpoles and are therefore stable.
[2] For more details see section 8.6.

12.2.2. K-Theory Constraints

The K-Theory constraints on $\mathcal{O}/\left(\overline{\sigma}\times\Omega\right)$ are [3]

$$\begin{aligned}&\sum_a\left(m_a^{1,o}m_a^{2,o}m_a^{3,o}\right)\in 2\mathbb{Z}\\&\sum_a\left(m_a^{I,o}n_a^{J,o}n_a^{K,o}\right)\in 2\mathbb{Z},\qquad I\neq J\neq K\neq I\end{aligned}\tag{12.2}$$

12.2.3. Supersymmetry Constraints

As discussed in chapter 4, there are two non-trivial supersymmetry conditions - namely

$$\begin{aligned}0&<n_a^{1,o}n_a^{2,o}n_a^{3,o}-n_a^{1,o}m_a^{2,o}u^2m_a^{3,o}u^3-n_a^{2,o}m_a^{1,o}u^1m_a^{3,o}u^3-n_a^{3,o}m_a^{1,o}u^1m_a^{2,o}u^2\\0&=m_a^{1,o}m_a^{2,o}m_a^{3,o}-m_a^1\cdot\frac{n_a^2n_a^3}{u^2u^3}-m_a^2\cdot\frac{n_a^1n_a^3}{u^1u^3}-m_a^3\cdot\frac{n_a^1n_a^2}{u^1u^2}\end{aligned}\tag{12.3}$$

12.3. New Notation

12.3.1. Definition

We define

$$\begin{aligned}P_a&:=n_a^{1,o}n_a^{2,o}n_a^{3,o}&\qquad Q_a&:=-n_a^{1,o}m_a^{2,o}m_a^{3,o}\\R_a&:=-m_a^{1,o}n_a^{2,o}m_a^{3,o}&\qquad S_a&:=-m_a^{1,o}m_a^{2,o}n_a^{3,o}\end{aligned}\tag{12.4}$$

From now on we will refer to these four terms as **tadpoles**. Moreover we define [4]

$$j:=\frac{1}{u^2u^3},\quad k:=\frac{1}{u^1u^3},\quad l:=\frac{1}{u^1u^2}\tag{12.5}$$

Also we define

$$\Xi_a:=P_a+\frac{Q_a}{j}+\frac{R_a}{k}+\frac{S_a}{l}\tag{12.6}$$

12.3.2. Revision Of The Constraints

With the above definitions at hand, we can always rewrite the R-R tadpole constraints as well as the supersymmetry positivity constraint as

$$\begin{aligned}T:=8=\sum_a P_a=\sum_a Q_a=\sum_a R_a=\sum_a S_a\\0<\Xi_a=P_a+\frac{Q_a}{j}+\frac{R_a}{k}+\frac{S_a}{l}\end{aligned}\tag{12.7}$$

[3] More details to be found in section 8.7.

[4] Recall that $u^I:=\frac{R_y^I}{R_x^I}\neq 0$.

Given that all tadpoles [5] are non-zero, we can also rewrite the supersymmetry reality constraint as

$$0 = \frac{1}{P} + \frac{j}{Q} + \frac{k}{R} + \frac{l}{S} \tag{12.8}$$

12.4. Classification Of Branes

12.4.1. Symmetries

Symmetry I

A 3-cycle on $\mathcal{O}$ is given by

$$\pi_a^o = \prod_{I=1}^{3} \left(n_a^{I,o} \left[a^{I,o} \right] + \widetilde{m}_a^{I,o} \left[b^{I,o} \right] \right) \tag{12.9}$$

If we change the signs of the n's and m's in two of the two-tori, the 3-cycle remains unchanged. This symmetry allows for any 3-cycle to choose two of the n's to be non-negative. Our choice is therefore to always arrange non-negative $n_a^{1,o}, n_a^{2,o}$.

Symmetry II

The involution $\overline{\sigma}$ acts by changing the signs of all $\widetilde{m}_a^{I,o}$. The so-obtained image branes are not summed over in R-R tadpole and K-theory constraints. Given a brane and its image brane we may therefore interchange the role of brane and image brane, such as to sum over the original image brane in R-R tadpole and K-theory constraints. In particular this enables us to always choose two m's non-negative.
Note however that we have already fixed the sign of $n_a^{1,o}$ and $n_a^{2,o}$. Therefore we can not pick two arbitary m's and render them non-negative, rather it depends on the given wrapping numbers which particular m's can be chosen non-negative.

Symmetry III

Given a brane π_a with tadpoles (P_a, Q_a, R_a, S_a) one can think of mapping this brane to another brane π_b with tadpoles (P_b, Q_b, R_b, S_b), such that

$$(P_a, Q_a, R_a, S_a) \overset{\tau \in S_4}{\to} (P_b, Q_b, R_b, S_b) \tag{12.10}$$

In particular one can extend this S_4 symmetry to act on the moduli j, k, l also [15]. To this end one first replaces the moduli via

$$(j, k, l) \to \left(\frac{j}{h}, \frac{k}{h}, \frac{l}{h} \right) \tag{12.11}$$

where $h \in \mathbb{R} \backslash \{0\}$. Then one can extend the above S_4 symmetry to act on the numbers j, k, l, h. In particular one may therefore assume without loss of generality $1 \leq j \leq k \leq l$, which we will use later.

[5] By which we mean P,Q,R and S, as defined in subsection 12.3.1.

12.4.2. Brane Types

Classification

We classify branes by the number of non-vanishing tadpoles. In particular we define

- A-Type branes - 4 non-vanishing tadpoles.
- B-Type branes - precisely 2 non-vanishing tadpoles.
- C-Type branes - precisely 1 non-vanishing tadpole.

Completeness

For a brane with three non-vanishing tadpoles, all wrapping numbers must be non-zero. Consequently the fourth tadpole is non-zero and the brane under consideration is an A-type brane. A brane with four vanishing tadpoles violates the supersymmetry condition $0 < P + \frac{Q}{j} + \frac{R}{k} + \frac{S}{l}$ and can consequently not exist in a supersymmetric model. For these reasons every brane in a supersymmetric model is either an A-, a B- or a C-type brane. So the above classification is complete.

Summary On Brane Types

By applying the symmetries I and II presented in subsection 12.4.1 and analyzing the supersymmetry conditions, one can decide on the signs of the wrapping numbers and tadpoles of the various brane types. The results of these deductions are given in Table 12.1 [6] Note in particular that the C-type branes are the probe branes, that were used to derive the K-theory constraints in section 8.7.

Canonical Form

The branes in Table 12.1 were obtained without using symmetry III - the extended S_4 symmetry. The latter allows to order the tadpoles and thereby to obtain the canonical form for the various branes. Let us demonstrate in detail how to obtain this canonical form by considering A-type branes.
First we agree on the convention for the canonical forms.

- A1: $Q \leq R \leq S$
- A2: $P \leq R \leq S$
- A3: $P \leq Q \leq S$
- A4: $P \leq Q \leq R$

[6] For further detais we refer the reader to the original literature [15].

Brane Type	Label	(P,Q,R,S)	$(n_a^{1,o}, n_a^{2,o}, n_a^{3,o})$	$(m_a^{1,o}, m_a^{2,o}, m_a^{3,o})$
A	A1	$(-,+,+,+)$	$(+,+,-)$	$(+,+,-)$
	A2	$(+,-,+,+)$	$(+,+,+)$	$(+,-,-)$
	A3	$(+,+,-,+)$	$(+,+,+)$	$(-,+,-)$
	A4	$(+,+,+,-)$	$(+,+,+)$	$(-,-,+)$
B	B1	$(+,+,0,0)$	$(1,+,+)$	$(0,+,-)$
	B2	$(+,0,+,0)$	$(+,1,+)$	$(+,0,-)$
	B3	$(+,0,0,+)$	$(+,+,1)$	$(+,-,0)$
	B4	$(0,+,+,0)$	$(+,+,0)$	$(-,-,1)$
	B5	$(0,+,0,+)$	$(+,0,+)$	$(-,1,-)$
	B6	$(0,0,+,+)$	$(0,+,+)$	$(1,-,-)$
C	C1	$(1,0,0,0)$	$(1,1,1)$	$(0,0,0)$
	C2	$(0,1,0,0)$	$(1,0,0)$	$(0,1,-1)$
	C3	$(0,0,1,0)$	$(0,1,0)$	$(1,0,-1)$
	C4	$(0,0,0,1)$	$(0,0,1)$	$(1,-1,0)$

Table 12.1.: Classification of D6-branes on $\mathcal{O}$ internal space.

So an A1-type brane is canonically ordered if $Q \leq R \leq S$. Note however that in the case of equal tadpoles, the extended S_4 symmetry allows to order the associated n's. For example $Q = R$ implies

$$n_a^{1,o} m_a^{2,o} m_a^{3,o} = n_a^{2,o} m_a^{1,o} m_a^{3,o} \tag{12.12}$$

and we can order $n_a^{1,o}$ and $n_a^{2,o}$ such as to obtain

$$n_a^{1,o} \leq n_a^{2,o} \tag{12.13}$$

Note in particular that neither P nor Q is changed by this ordering.
For the B-type branes the two non-vanishing tadpoles can be ordered in the same manner. But note that for B-type branes two tadpoles vanish. The symmetry transformations that interchange these tadpoles then also need to be taken into account, in order to obtain the canonical form for B-type branes. Finally note that up to S_4 symmetry there is only a single C-type brane.

13. Bounds For The Wrapping Numbers

13.1. A-Type Branes In Further Detail

Let us consider an A1-type brane. It has negative S_a tadpole. From the supersymmetry condition in Equation 12.8 we learn

$$S_a = -\frac{l}{\frac{1}{P_a} + \frac{j}{Q_a} + \frac{k}{R_a}} \tag{13.1}$$

By applying the elementary inequality $\frac{1}{x} + \frac{1}{y} + \frac{1}{z} > \frac{3}{x+y+z}$ [1] we find

$$S_a > -\frac{l}{3}\left(P_a + \frac{Q_a}{j} + \frac{R_a}{k}\right) \tag{13.2}$$

By using this equation to replace S_a in Ξ_a we find

$$\Xi_a > \frac{2}{3}\left(P_a + \frac{Q_a}{j} + \frac{R_a}{k}\right) \tag{13.3}$$

But we can also use Equation 13.2 to replace $P_a + \frac{Q_a}{j} + \frac{R_a}{k}$. In this case we first obtain $-\frac{3}{l}S_a < P_a + \frac{Q_a}{j} + \frac{R_a}{k}$ which then yields

$$\Xi_a > -\frac{2}{l}S_a > 0 \tag{13.4}$$

So we found bounds for Ξ_a that can either be expressed entirely in terms of positive tadpoles or with negative tadpoles only.
The above strategy can be applied to the remaining A-type branes A2, A3 and A4 in precisely the same manner.

[1] For $x, y, z > 0$ it holds $(x+y)\,xy + (x+z)\,xz + (y+z)\,yz > 0$. This implies

$$(x+y+z)\,xy + (x+y+z)\,xz + (x+y+z)\,yz > 3xyz$$

This implies the above inequality.

13.2. Bounds For Tadpoles And Wrapping Numbers

Let us now consider a setup of N brane stacks, which is supersymmetric and satisfies the R-R tadpole constraints. In particular each brane satisfies the supersymmetry positivity constraint. For each brane we have

$$0 < P_a + \frac{Q_a}{j} + \frac{R_a}{k} + \frac{S_a}{l} = \Xi_a \tag{13.5}$$

Consequently we must also have

$$0 < \sum_a \Xi_a = T \cdot \left(1 + \frac{1}{j} + \frac{1}{k} + \frac{1}{l}\right) \tag{13.6}$$

where we used the R-R tadpole constraint to obtain the equality.

13.2.1. Upper Bound

For each A-type brane we now use the inequalities (similar to) 13.3. This yields

$$0 < \frac{2}{3} \cdot \sum_{A+} \Xi_a + \frac{2}{3} \cdot \sum_B \Xi_a + \frac{2}{3} \cdot \sum_C \Xi_a < \sum_a \Xi_a = T \cdot \left(1 + \frac{1}{j} + \frac{1}{k} + \frac{1}{l}\right) \tag{13.7}$$

where $\sum_{A+}$ corresponds to summing the positive tadpoles of all A-type branes. But recall that for B-type and C-type branes, all tadpoles are non-negative. For that reason we can write

$$0 < \frac{2}{3} \cdot \sum_{a+} \Xi_a < T \cdot \left(1 + \frac{1}{j} + \frac{1}{k} + \frac{1}{l}\right) \tag{13.8}$$

where $\sum_{a+}$ corresponds to summing the positive tadpoles of all branes in the setup.

13.2.2. Lower Bound

Instead of Equation 13.3 we can also use the inequalities (similar to) 13.4 for A-type branes. Similar arguments then yield

$$0 > \sum_{A-} \Xi_a \geq \frac{1}{2} \sum_B \Xi_a + \frac{1}{2} \sum_C \Xi_a - \frac{T}{2} \cdot \left(1 + \frac{1}{j} + \frac{1}{k} + \frac{1}{l}\right) \geq -\frac{T}{2} \cdot \left(1 + \frac{1}{j} + \frac{1}{k} + \frac{1}{l}\right) \tag{13.9}$$

13.2.3. Final Bounds

As pointed out in subsection 12.4.1, without loss of generality we can restrict to $1 \leq j \leq k \leq l$. This allows to reformulate the bounds on the tadpoles as

$$0 < \sum_{a+} \Xi_a < 6T, \qquad -2T \leq \sum_{a-} \Xi_a < 0 \tag{13.10}$$

Note that the tadpoles are obtained by multiplying three wrapping numbers, which themselves are integer valued. So these wrapping numbers must be bounded (and the bounds are independ of j, k and l). This is what we wanted to proof. □

14. Computation Of One-Stack Models

As our final task we want to consider one stack models. Such models are made of single A-type, B-type or C-type branes. In particular the S_4 symmetry allows to restrict attention to A1-, B1- and C1-type branes.
C-type branes are special, because they do not give contributions to the K-theory constraints, are supersymmetric for any set of modules (j,k,l) but add 1 to one of the four tadapoles. Therefore any brane model that undersaturates the R-R tadpole condition and satisfies the K-theory constraints can be completed uniquely by C-type branes, so that the final setup satisfies the R-R tadpole condition as well as the K-theory constraints [15].
For that reason we restrict our attention to A1- and B1-type branes which undersaturate the R-R tadpole but satisfy the K-theory constraints. To compute their number we designed a C++ program. For further reference we outline the major part of the code in Appendix C. For $T \leq 20$ we display the numbers calculated by the program in Table C.1, but plot these numbers for greater ranges of T in Figure 14.1.
In [15] bounds for the number of A1- and B1-type branes were derived, namely

$$\begin{aligned} \mathcal{N}_a(T) &\lesssim \frac{1}{6}\left(\frac{\pi^2}{6}\right)^3 T^3, \qquad \mathcal{N}_b(T) \lesssim \frac{1}{4}T^2\left(\ln(T)\right)^2 \\ \widetilde{\mathcal{N}}_a(T) &\sim \frac{1}{6}\left(\frac{\pi^2}{6\zeta(3)}\right)^3 T^3, \qquad \widetilde{\mathcal{N}}_b(T) \sim \frac{1}{4}\left(\frac{6}{\pi^2}\right)^2 T^2\left(\ln(T)\right)^2 \end{aligned} \tag{14.1}$$

These bounds are also displayed in Figure 14.1.
In [15] the exact number of A1-type and B1-type branes is given for $T = 8$. These results match with our calculations. Also our plots match phenomenologically with the one given in [15]. Unfortunately the numberical values that lead to the plots in [15] were not given, so that the results can not be compared further. To allow for such comparisons we present the numerical results for $T \leq 20$ in Table C.1.

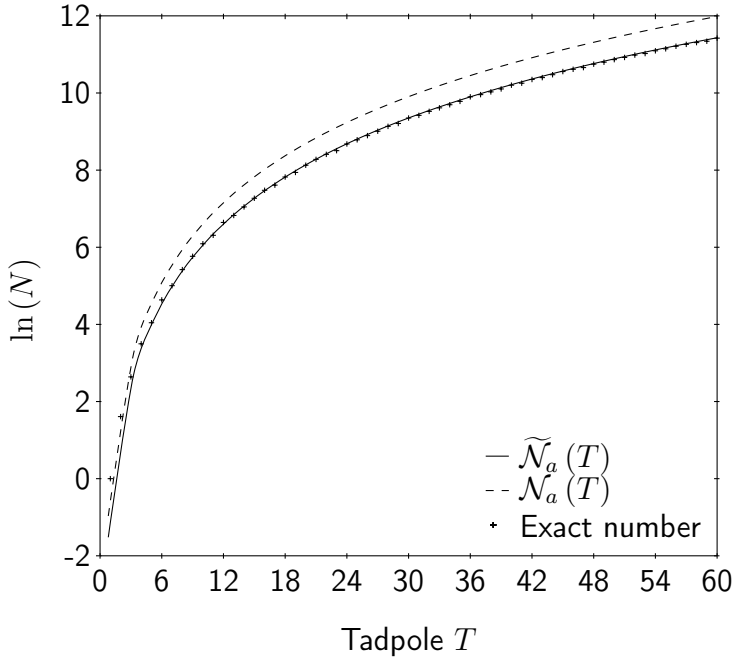

(a) Number of A1-type branes.

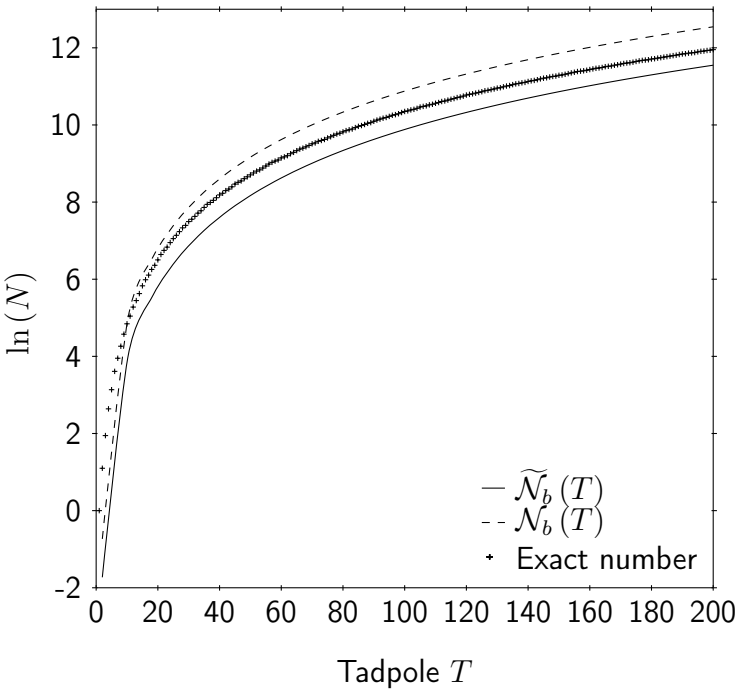

(b) Number of B1-type branes.

Figure 14.1.: Exact number of A1-type and B1-type branes plotted against the number of tadpoles T. Also the coresponding estimates are displayed.

Part V.

Conclusion, Outlook And Appendix

15. Conclusion And Outlook

In this thesis we have presented an analysis of intersecting D6-brane models on the orientifolds $\mathcal{M}/(\overline{\sigma} \times \Omega)$ as well as $\mathcal{O}/(\overline{\sigma} \times \Omega)$. In particular we have discussed three different models built on these internal spaces.
In chapter 7 a class of non-supersymmetric models on the orientifold $\mathcal{M}/(\overline{\sigma} \times \Omega)$ was discussed. It turned out that the massless fermionic spectrum is in one-to-one correspondance with the Standard Model matter particles, that a massless $U(1)$ gauge boson can be achieved such that it gives the Standard Model hypercharge and that Higgs doublets can appear in this model. Also the Yukawa couplings were briefly discussed. From a phenomenological point of view, this class of models is therefore a very tempting setup. Unfortunately these models are not supersymmetric. For that reason they will in general suffer from uncanceled NS-NS tadpoles which may trigger instabilities [7].
To stay on firm ground we therefore abandoned this class of models and instead considered supersymmetric models built on the orientifold $\mathcal{O}/(\overline{\sigma} \times \Omega)$. In chapter 9 we discussed such a supersymmetric three family model. Note however that only two right-handed familes appeared in the massless fermionic spectrum. Also additional exotic matter appeared in the massless fermionic spectrum. Even though Higgs doublets can be incorporated into this model, the appearance of exotic matter as well as the lack of one generation of right-handed particles is not completely satisfactory from a phenomenological point of view. This raises the need to extend the search for supersymmetric models with massless fermionic spectrum as close as possible to the Standard Model matter particles.
We therefore followed the approach of [15] and first classified the various D6-branes on the orientifold $\mathcal{O}/(\overline{\sigma} \times \Omega)$. Based on this classification we found bounds on the wrapping numbers of D6-branes that form supersymmetric models on $\mathcal{O}/(\overline{\sigma} \times \Omega)$. For given moduli j, k and l this allows to find a bound on the number of supersymmetric models by counting the number of intersecting D6-brane models that satisfy R-R tadpole cancelation and the K-theory constraints. This analysis will need computational methods. Therefore we designed a C++ program to determine the number of one-stack simple models.
The implementation of R-R tadpole cancelation and K-theory constraints in a C++ program is relatively easy. Difficulties arise when two or more brane stacks are considered. In this case permutations of brane configuations have to be compared to avoid overcounting. Also brane configurations exchanged by the extended S_4 symmetry must be figured out to avoid overcounting.
Still the major difficulty arrises when one tries to obtain all supersymmetric models. Then the above analysis must be performed for any set of moduli j, k and l. By using

the extended S_4 symmetry one can restrict attention to mouli with $1 \leq j \leq k \leq l$. Nevertheless these moduli need neither be integers nor rational numbers. So a scan over all possible moduli is a very challenging task in computational physics.
A detailed analysis of intersecting D6-brane models on $\mathcal{O}/\left(\overline{\sigma} \times \Omega\right)$ by computational methods was presented in [15]. The authors found agreement with many former publications. Unfortunately a completely satisfactory model is so far missing [7]. For that reason it is natural to extend the search of realistic intersecting D6-brane models to interal spaces, different from $\mathcal{M}/\left(\overline{\sigma} \times \Omega\right)$ and $\mathcal{O}/\left(\overline{\sigma} \times \Omega\right)$.
A possible generalisation is to consider orientifolds such as $\mathcal{M}/\left(G \times \overline{\sigma} \times \Omega\right)$ with G some finite group. This has been studied for $G = \mathbb{Z}_4$ [8], $G = \mathbb{Z}_4 \times \mathbb{Z}_2$ [19] [17] [18] and $G = \mathbb{Z}_6$ [20].
An unattractive phenomenological feature of toroidal models is that they give rise to too many scalars in the adjoint representation [7]. This appearance is related to too many deformations of 3-cycles π_a. Thus it is desirable to consider more general internal spaces.
As we noted in chapter 3 general assumptions on both internal and external space together with the requirement of at least $\mathcal{N} = 1$ supersymmetry restrict the internal spaces to Calabi-Yau three-folds [4]. General features of Calabi-Yau compactifications can be found in [16].
For general algebraic Calabi-Yau manifolds, knowledge about special Lagrangian 3-cycles, which branes must wrap to allow for at least $\mathcal{N} = 1$ supersymmetry, is very restricted [7]. One possible approach is therefore to consider Gepner models. Such models were studied in [14] and lead to a large class of three-family Standard-like Models without exotic chirals.

Acknowledgements

The author thanks Timo Weigand for the many encouragements and enlightening discussions.

A. Symplectic Group

A.1. General Features

Be $\mathbb{F}$ a field [1] with $\mathrm{char}(\mathbb{F}) \neq 2$ and $N \in \mathbb{N}$ [2]. Then we define

$$USp(2N,\mathbb{F}) := \left\{ T \in GL(2N,\mathbb{F}) \;;\; T^t I_{2N} T = I_{2N} \right\}, \qquad I_{2N} = \begin{pmatrix} 0 & E_N \\ -E_N & 0 \end{pmatrix} \tag{A.1}$$

A.2. Generators

Be $A \in USp(2N,\mathbb{F})$ an element, situated close to the identity $\mathbb{1}_{2N}$. Then there exists $T \in M(2N \times 2N, \mathbb{F})$ and $\alpha \in \mathbb{F}$ close to $1_{\mathbb{F}}$ such that

$$\begin{aligned} A &= \exp(i\alpha T) = 1 + i\alpha T + \mathcal{O}\left(\alpha^2\right) \\ A^t &= \left(\exp(1 + i\alpha T)^t\right) = 1 + i\alpha T^t + \mathcal{O}\left(\alpha^2\right) \end{aligned} \tag{A.2}$$

But since $A \in USp(2N,\mathbb{F})$ we have $A^t I_N A = I_N$. Using the above equalities we find

$$\mathbb{1}_{2N} = I_{2N} + i\alpha\left(T^t I_{2N} + I_{2N} T\right) + \mathcal{O}\left(\alpha^2\right) \tag{A.3}$$

Consequently it holds

$$I_{2N} T + T^t I_{2N} = 0 \tag{A.4}$$

So the generators $T \in M(2N \times 2N, \mathbb{F})$ are *Hamiltonian matrices*. Note in particular that $\mathbb{1}_{2N}$ is not a generator of $Sp(2N,\mathbb{C})$. Therefore there exists no $U(1)$ subgroup of $Sp(2N,\mathbb{C})$.
Let us now examine the generators T a bit further. To this end we write them out explicitely as

$$T = \begin{pmatrix} A & B \\ C & D \end{pmatrix} \tag{A.5}$$

Then one readily confirmes that Equation A.4 requires

$$T = \begin{pmatrix} A & B \\ C & -A^t \end{pmatrix} \quad B,C \text{ symmetric} \tag{A.6}$$

[1] Here we talk about the algebraic structure called field, not scalar fields, spinor fields or similar constructions.

[2] Our convention is that $\mathbb{N}$ does not include 0. So the symplectic groups are $USp(2,\mathbb{F})$, $USp(4,\mathbb{F})$ and so on.

In particular we have

$$\mathrm{tr}\,(T) = \mathrm{tr}\,(A) + \mathrm{tr}\left(-A^t\right) = \mathrm{tr}\,(A) - \mathrm{tr}\,(A) = 0 \tag{A.7}$$

So the generators of the symplectic group are traceless.

A.3. Dimension Of The Symplectic Group

From Equation A.6 one can easily deduces

$$\dim_{\mathbb{F}}\left(USp\left(2N,\mathbb{F}\right)\right) = \underbrace{\frac{N\cdot(N+1)}{2}}_{\text{d.o.f. of } B} + \underbrace{\frac{N\cdot(N+1)}{2}}_{\text{d.o.f. of } C} + \underbrace{N^2}_{\text{d.o.f. of } A} = N\cdot(2N+1) \tag{A.8}$$

A.4. A Special Subgroup

One defines

$$USp\left(2N,\mathbb{C}\right) = Sp\left(2N,\mathbb{C}\right)\cap U\left(2N\right) \subset Sp\left(2N,\mathbb{C}\right) \tag{A.9}$$

The generators of $USp\left(2N,\mathbb{C}\right)$ are then still of the form given in Equation A.6, but in addition must be Hermitian. This implies

$$\widetilde{T} = \begin{pmatrix} A & B \\ B^\dagger & -A^t \end{pmatrix} \tag{A.10}$$

where B is symmetric and A Hermitian. Therefore B has $\frac{N(N+1)}{2}$ complex degrees of freedom, whilst A has $\frac{N^2}{2}$ complex degrees of freedom. So

$$\dim_{\mathbb{C}}\left(USp\left(2N,\mathbb{C}\right)\right) = \frac{1}{2}\cdot N\cdot(2N+1) = \frac{1}{2}\dim_{\mathbb{C}}\left(USp\left(2N,\mathbb{C}\right)\right) \tag{A.11}$$

Equivalently

$$\dim_{\mathbb{R}}\left(USp\left(2N,\mathbb{C}\right)\right) = N\cdot(2N+1) = \dim_{\mathbb{C}}\left(USp\left(2N,\mathbb{C}\right)\right) \tag{A.12}$$

Finally note that the generators of $USp\left(2N,\mathbb{C}\right)$ are traceless.

B. Anomalies

In this chapter we give a detailed derivation for all $U(1)$ anomalies, that arise from the massless fermionic spectrum on the $\mathcal{M}/(\overline{\sigma} \times \Omega)$ orientifold. This spectrum is listed in Table 5.1. A summary of all $U(1)$ anomalies that we are going to calculate during this chapter is given in Table 6.2.

B.1. U(1) - SU(N) - SU(N) Anomalies

The $U(1)_a$ - $SU(N_a)^2$ anomalies arise from

$$\mathcal{A}^{aaa} = Tr\left(Q^a \left(T^a\right)^A \left(T^a\right)^B\right) \tag{B.1}$$

In this case Q^a and $(T^a)^A$ have matching dimensions and we do not split the trace. We then sum over all states in Table 5.1 that are charged under both $U(1)_a$ and $SU(N_a)$. Consequently we find

$$\begin{aligned}\mathcal{A}^{aaa} = &\frac{\left(\pi_a^{U\prime} \circ \pi_a^U + \pi_{O6} \circ \pi_a^U\right)}{2} \cdot \mathrm{tr}_A\left(\left(T^a\right)^A \left(T^a\right)^B\right) \\ &+ \frac{\left(\pi_a^{U\prime} \circ \pi_a^U - \pi_{O6} \circ \pi_a^U\right)}{2} \cdot \mathrm{tr}_S\left(\left(T^a\right)^A \left(T^a\right)^B\right) \\ &+ \sum_{b \neq a} N_b \cdot \left(-\pi_a^U \circ \pi_b + \pi_a^{U\prime} \circ \pi_b\right) \cdot \mathrm{tr}_F\left(\left(T^a\right)^A \left(T^a\right)^B\right)\end{aligned} \tag{B.2}$$

By using the quadratic casimir coefficients for $SU(N)$, which are listed in Table 6.1, we can rewrite this expression as

$$\begin{aligned}\mathcal{A}^{aaa} = &\frac{N_a - 2}{2}\left(\pi_a^{U\prime} \circ \pi_a^U + \pi_{O6} \circ \pi_a^U\right)\delta^{AB} + \frac{N_a + 2}{2}\left(\pi_a^{U\prime} \circ \pi_a^U - \pi_{O6} \circ \pi_a^U\right)\delta^{AB} \\ &+ \frac{1}{2} \cdot \sum_{b \neq a} N_b \cdot \left(-\pi_a^U + \pi_a^{U\prime}\right) \circ \pi_b \cdot \delta^{AB}\end{aligned} \tag{B.3}$$

By using R-R tadpole cancelation we finally arrive at

$$\mathcal{A}^{aaa} = \frac{N_a}{2}\pi_a^{U\prime} \circ \pi_a^U \cdot \delta^{AB} \tag{B.4}$$

We now move on to calculate the $U(1)_a$ - $SU(N_b)^2$ anomalies for $b \neq a$. This means that we have to sum over all states that are charged unter both $U(1)_a$ as well as

$SU(N_b)$. The only such states are strings stretching between the branes π_a^U and π_b^U (as well as their images). Note alo that for $a \neq b$, Q^a and $(T^a)^A$ are in general not of the same dimension. This makes it necessary to split the trace. Consequently we obtain

$$\begin{aligned}\mathcal{A}^{abb} &= \pi_a \circ \pi_b^U \cdot (-1) \cdot N_a \cdot \frac{\delta^{AB}}{2} + \pi_a' \circ \pi_b^U \cdot (1) \cdot N_a \cdot \frac{\delta^{AB}}{2} \\ &= \frac{N_a}{2} \left(-\pi_a + \pi_a'\right) \circ \pi_b^U \cdot \delta^{AB}\end{aligned} \tag{B.5}$$

In particular note that this reduces to Equation B.4 for $a = b$.

B.2. U(1) - USp(2N, ℂ) − USp(2N, ℂ) Anomalies

These anomalies are obtained in precisely the same way as the $U(1)_a - SU(N_b)^2$ anomalies for $a \neq b$. Consequently one obtains

$$\mathcal{A}^{aUSpUSp} = \frac{N_a}{2} \left(-\pi_a^U + \pi_a^{U\prime}\right) \circ \pi_b^{USp} \tag{B.6}$$

B.3. U(1) - U(1) - U(1) Anomaly

The $U(1)_a - U(1)_b - U(1)_c$ anomalies arise from

$$\widetilde{\mathcal{A}}^{abc} = \mathrm{tr}\left(Q^a Q^b Q^c\right) \tag{B.7}$$

But open strings have just one starting and one ending point, for which reason they can be charged under at most two different gauge fields. Consequently this anomaly vanishes for $a \neq b \neq c \neq a$. Let us therefore move on to calculate

$$\widetilde{\mathcal{A}}^{abb} = \mathrm{tr}\left(Q^a Q^b Q^b\right) \tag{B.8}$$

for $b \neq a$. This anomaly is obtained similar to the $U(1)_a - SU(N_b)^2$ anomalies, for which reason one obtains

$$\widetilde{\mathcal{A}}^{abb} = N_a \cdot N_b \left(\pi_a^U + \pi_a^{U\prime}\right) \circ \pi_b^U \tag{B.9}$$

If we take $b = a$ we have to calculate a $U(1)_a^3$ anomaly. One finds

$$\begin{aligned}\widetilde{\mathcal{A}}^{aaa} &= \frac{1}{2}\left(\pi_a^{U\prime} \circ \pi_a^U - \pi_{O6} \circ \pi_a^U\right) \cdot 2^3 \cdot \frac{N_a(N_a+1)}{2} \\ &\quad + \frac{1}{2}\left(\pi_a^{U\prime} \circ \pi_a^U + \pi_{O6} \circ \pi_a^U\right) \cdot 2^3 \cdot \frac{N_a(N_a-1)}{2} \\ &\quad + \sum_{b\neq a} N_b \cdot \left(\pi_a^U \circ \pi_b\right) \cdot (-1)^3 \cdot N_a \\ &\quad + \sum_{b\neq a} N_b \cdot \left(\pi_a^{U\prime} \circ \pi_b\right) \cdot (1)^3 \cdot N_a \\ &= 2N_a \cdot \left[2N_a \cdot \left(\pi_a^{U\prime} \circ \pi_a^U\right) - 2\pi_{O6} \circ \pi_a^U\right] - N_a \pi_a^U \circ \sum_{b\neq a} N_b \left[\pi_b + \pi_b'\right]\end{aligned} \tag{B.10}$$

R-R tadpole cancelation requires $\sum_b N_b (\pi_b + \pi_b') = 4\pi_{O6}$. In particular this allows to rewrite $\sum_{b\neq a} N_b [\pi_b + \pi_b']$ to find

$$\widetilde{\mathcal{A}}^{aaa} = 3N_a^2 \pi_a^{U\prime} \circ \pi_a^U \tag{B.11}$$

Here a slight subtlety appears. If three $U(1)_a$ gauge bosons couple in a triangle diagram, the associated Feynman diagram has symmetry factor $S = 3!$ (see Figure 6.1). Conversely the $U(1)_a - U(1)_b^2$ diagram just has $S = 2!$. When evaluating expressions for Feynman diagrams one has to divide by S. Strictly speaking this means to devide the result for $\widetilde{\mathcal{A}}^{aaa}$ by $6 = 3!$ and the result for $\widetilde{\mathcal{A}}^{abb}$ by $2!$.
For our purposes however, only the relative values of the various anomalies matter, as this is all we need in order to determine whether or not a $U(1)$ gauge field is anomaly free. Therefore we leave all results but the one for $\widetilde{\mathcal{A}}^{aaa}$ unchanged. The latter is changed by including an additional factor $\frac{1}{3}$ [22]. So our final result for this anomaly is

$$\widetilde{\mathcal{A}}^{aaa} = N_a^2 \pi_a^{U\prime} \circ \pi_a^U \tag{B.12}$$

B.4. Gravitational Anomalies

We conclude this chapter by calculating the gravitational anomaly, given by

$$\mathcal{A}^{agg} = \mathrm{tr}\,(Q^a) \tag{B.13}$$

So we have to sum over all states that are charged under $U(1)_a$. Baring Table 5.1 in mind this anomaly is given by

$$\begin{aligned}
\mathcal{A}^{agg} = Tr\,(Q^a) = &\frac{1}{2}\left(\pi_a^{U\prime} \circ \pi_a^U + \pi_{O6} \circ \pi_a^U\right) \cdot 2 \cdot \frac{N_a (N_a - 1)}{2} \\
&+ \frac{1}{2}\left(\pi_a^{U\prime} \circ \pi_a^U - \pi_{O6} \circ \pi_a^U\right) \cdot 2 \cdot \frac{N_a \cdot (N_a + 1)}{2} \\
&+ \sum_{b\neq a} N_b \left(\pi_a^U \circ \pi_b\right) \cdot (-1) \cdot N_a + \sum_{b\neq a} N_b \left(\pi_a^{U\prime} \circ \pi_b\right) \cdot 1 \cdot N_a \\
= &\, N_a^2 \pi_a^{U\prime} \circ \pi_a^U - N_a \cdot \pi_{O6} \circ \pi_a^U - N_a \cdot \pi_a^U \circ \sum_{b\neq a} N_b (\pi_b + \pi_b')
\end{aligned} \tag{B.14}$$

Finally we use R-R tadpole cancelation to rewrite the gravitational anomaly as

$$\mathcal{A}^{agg} = 3N_a \cdot \pi_{O6} \circ \pi_a^U \tag{B.15}$$

C. C++ Program

C.1. Brane Class

C.1.1. Declaration

```
class Brane{
public:
    Brane(); Brane(int N); ~Brane();
    virtual bool check();
    bool checkrp();
    /* various gets and sets ... */
protected:
    // wrapping numbers
    int n1,n2,n3,m1,m2,m3;
    // limits for the wrapping numbers
    int n1U, n1B, n2U,n2B, n3U, n3B;
    int m1U,m1B, m2U, m2B, m3U, m3B;
    // wrapping numbers relatively prime?
    bool rp1(); bool rp2(); bool rp3();
};
```

C.1.2. Implementation

```
#include "branes.h"
#include <math.h>
*/ constructor, destructor, sets and gets ... */
bool Brane::check(){ return true; }

int gcd(int i, int x){ // gcd of two positive integers
    if(x \% i == 0){return(i);}
    else{return( gcd( x , i \% x ) );}
}

bool Brane::checkrp(){ // wrapping numbers relatively prime?
     if (rp1() && rp2() && rp3()){return true;}
     else{return false;}
}
```

```
bool Brane::rp1(){
      bool A = false;
      if ((n1 == 0) && (abs(m1) == 1)){A = true;}
      else if ((abs(n1) == 1)&&(m1 == 0)){A = true;}
      else if((n1 != 0)&&(m1 != 0)){
               A = (gcd(abs(n1),abs(m1))==1);
      }
      return A;
}
/* same routine for second and third torus ... */
```

C.2. A1 Brane Class

C.2.1. Declaration

```
#include "Branes.h"
class A1Brane: public Brane {
public:
      A1Brane(int B, int U, int N); ~A1Brane();
      bool check();
};
```

C.2.2. Implementation

```
#include "A1Branes.h"

A1Brane::A1Brane(int B, int U, int N): Brane(N) {
   // ranges for A1-type wrapping numbers
   n1B = 1; n1U = U; n2B = 1; n2U = U; n3B = -B; n3U = -1;
   m1B = 1; m1U = U; m2B = 1; m2U = U; m3B = -B; m3U = -1;
}
/* destructor ... */

bool A1Brane::check(){
      // obtain Q,R,S tadpoles
      int q = getQ(); int r = getR(); int s = getS();
      // A1-brane in canonical form?
      bool res = false;
      if ((0 < q) && (q <= r) && (r <= s)){
           if ((q < r) && (r < s)){res = true;}
           else if ((q == r) && (r<s)){
                if (n1 <= n2){res = true;}
           }
           else if ((q < r) && (r == s)){
```

```
            if (n2 <= n3){res = true;}
        }
        else if ((q == r) && (r == s)){
            if ((n1 <= n2) && (n2 <= n3)){
                res = true;
            }
        }
    }
    return res;
}
```

C.3. B1 Brane Class

C.3.1. Declaration

```
#include "Branes.h"
class B1Brane: public Brane {
public:
    B1Brane(int B, int U, int N); ~B1Brane();
    bool check();
private:
    bool checkp(); // P,Q permuted or canonically ordered?
    bool checkRS(); // R,S tadpole permutations?
};
```

C.3.2. Implementation

```
#include "B1Branes.h"
B1Brane::B1Brane(int B, int U, int N): Brane(N) {
    // ranges for wrapping numbers of B1-type brane
    n1B = 1; n1U = 1; n2B = 1; n2U = U; n3B = 1; n3U = U;
    m1B = 0; m1U = 0; m2B = 1; m2U = U; m3B = -B; m3U = -1;
}
/* destructor ... */

// P,Q canonically ordered?
bool B1Brane::checkp(){
    int p = getP(); // get P tadpole
    int q = getQ(); // get R tadpole
    bool res = false;
    if ((0 < p) && (p <= q)){
        if (p < q){res = true;}
        else if(p == q){
            if(n2 <= n3){res = true;}
```

```
            }
        }
        return res;
}

// R<->S exchange possible -> avoid overcounting
bool B1Brane::checkRS(){
        int n21 = n1; // n1 for P<->Q interchanged brane
        int m21 = m1; // m1 for P<->Q interchanged brane
        int n22 = n3;
        int m22 = -m3;
        int n23 = n2;
        int m23 = -m2;
        bool res = true;
        if (n21 < n1){res = false;}
        else if (n21 == n1){
                if (n22 < n2){res = false;}
                else if (n22 == n2){
                        if (n23 < n3){res = false;}
                        else if(n23 == n3){
                                if (m21 < m1){res = false;}
                                else if (m21 == m1){
                                        if (m22 < m2){res = false;}
                                        else if (m22 == m2){
                                                if (m23 < m3){res = false;}
                                        }
                                }
                        }
                }
        }
        return res;
}

bool B1Brane::check(){
        return (checkp() && checkRS());
}
```

C.4. Counting Branes

C.4.1. Counting A1-Branes

```
#include <iostream>
#include <A1Brane.h>
```

```
bool KTheory1(A1Brane *A1){
     int i = A1->getnB() * A1->getm1()
             * A1->getm2() * A1->getm3();
     if(i \% 1){ // i is odd
        return false;
     }
     else { return true; }
}
/* same routine for the other K-theory constraints */

bool KTheory(A1Brane *A1){
     if (KTheory1(A1) && KTheory2(A1)
         && KTheory3(A1) && KTheory4(A1)){
         return true;
     }
     else{ return false; }
}

int main(){
    int T = 8; // total tadpole
    A1Brane *A = new A1Brane(T,T,1); // create new A1 brane
    int counter = 0; // count branes
    // loop over wrapping numbers of brane A
    for (int n1=A->getn1B(); n1<=A->getn1U(); n1++){
     for (int n2=A->getn2B(); n2 <=A->getn2U(); n2++){
      for (int n3=A->getn3B(); n3 <=A->getn3U();n3++){
       for (int m1=A->getm1B(); m1<=A->getm1U(); m1++){
        for (int m2=A->getm2B(); m2<=A->getm2U(); m2++){
         for (int m3=A->getm3B(); m3<=A->getm3U(); m3++){
              // set wrapping numbers
              A->setwn(n1,m1,n2,m2,n3,m3);
              if (A->check() && A->getS() <= T
                  && A->checkrp() && KTheory(A)){
                   counter++; // found solution
              }
         }
        }
       }
      }
     }
    }
    std::cout<<counter; // return result to cmd
    return 0;
}
```

C.4.2. Counting B1-Branes

By minor changes the code presented in subsection C.4.1 also allows to count B1-type branes. We list the so-obtained number of A1-type and B1-type branes as well as their estimates from [15] for tadpoles $T \leq 20$ in Table C.1.

T	A1 branes			B1 branes		
	$\widetilde{\mathcal{N}}_a(T)$	Exact number	$\mathcal{N}_a(T)$	$\widetilde{\mathcal{N}}_b(T)$	Exact number	$\mathcal{N}_b(T)$
1	0.43	1	0.74	0	1	0
2	3.42	5	5.93	0.18	3	0.48
3	11.53	14	20.03	1.00	7	2.72
4	27.34	33	47.48	2.84	14	7.69
5	53.40	57	92.73	5.98	23	16.19
6	92.28	103	160.23	10.68	37	28.89
7	146.53	149	254.44	17.14	52	46.39
8	218.73	226	379.81	25.57	71	69.19
9	311.43	319	540.78	36.13	97	97.76
10	427.20	442	741.81	48.98	127	132.55
11	568.54	550	987.35	64.28	155	173.93
12	738.12	768	1281.85	82.15	196	222.29
13	938.45	920	1629.76	102.73	232	277.96
14	1172.24	1149	2035.53	126.12	278	341.27
15	1441.63	1437	2503.62	152.45	340	412.51
16	1749.81	1767	3038.46	181.82	398	491.98
17	2098.59	2020	3644.53	214.34	449	579.96
18	2491.43	2493	4326.25	250.08	520	676.69
19	2929.82	2807	5088.09	289.17	579	782.44
20	3417.60	3384	5934.50	331.66	666	897.44

Table C.1.: Exact number of A1-type and B1-type branes in canonical form which undersaturate the R-R tadpole constraints but satisfy the K-theory constraints. For the estimates two decimal places are displayed.

D. Bibliography

[1] G. Aldazabal, S. Franco, Luis E. Ibanez, R. Rabadan, and A.M. Uranga. D = 4 chiral string compactifications from intersecting branes. *J.Math.Phys.*, 42:3103–3126, 2001. arXiv:hep-th/0011073, doi:10.1063/1.1376157.

[2] G. Aldazabal, S. Franco, Luis E. Ibanez, R. Rabadan, and A.M. Uranga. Intersecting brane worlds. *JHEP*, 0102:047, 2001. arXiv:hep-ph/0011132.

[3] H. Arfaei and M.M. Sheikh Jabbari. Different d-brane interactions. *Phys.Lett.*, B394:288–296, 1997. arXiv:hep-th/9608167, doi:10.1016/S0370-2693(97)00022-1.

[4] K. Becker, M. Becker, and J.H. Schwarz. *String Theory And M-Theory: A Modern Introduction*. Cambridge University Press, 2007.

[5] Micha Berkooz and Robert G. Leigh. A D = 4 N=1 orbifold of type I strings. *Nucl.Phys.*, B483:187–208, 1997. arXiv:hep-th/9605049, doi:10.1016/S0550-3213(96)00543-3.

[6] Ralph Blumenhagen, Volker Braun, Boris Kors, and Dieter Lust. Orientifolds of K3 and Calabi-Yau manifolds with intersecting D-branes. *JHEP*, 0207:026, 2002. arXiv:hep-th/0206038.

[7] Ralph Blumenhagen, Mirjam Cvetic, Paul Langacker, and Gary Shiu. Toward realistic intersecting D-brane models. *Ann.Rev.Nucl.Part.Sci.*, 55:71–139, 2005. arXiv:hep-th/0502005, doi:10.1146/annurev.nucl.55.090704.151541.

[8] Ralph Blumenhagen, Lars Gorlich, and Tassilo Ott. Supersymmetric intersecting branes on the type 2A T6 / Z(4) orientifold. *JHEP*, 0301:021, 2003. arXiv:hep-th/0211059.

[9] Ralph Blumenhagen, Boris Kors, Dieter Lust, and Stephan Stieberger. Four-dimensional String Compactifications with D-Branes, Orientifolds and Fluxes. *Phys.Rept.*, 445:1–193, 2007. arXiv:hep-th/0610327, doi:10.1016/j.physrep.2007.04.003.

[10] D. Cremades, L.E. Ibanez, and F. Marchesano. SUSY quivers, intersecting branes and the modest hierarchy problem. *JHEP*, 0207:009, 2002. arXiv:hep-th/0201205.

[11] Mirjam Cvetic, Paul Langacker, and Gary Shiu. A Three family standard - like orientifold model: Yukawa couplings and hierarchy. *Nucl.Phys.*, B642:139–156, 2002. arXiv:hep-th/0206115, doi:10.1016/S0550-3213(02)00684-3.

[12] Mirjam Cvetic, Paul Langacker, and Gary Shiu. Phenomenology of a three family standard like string model. *Phys.Rev.*, D66:066004, 2002. arXiv:hep-ph/0205252, doi:10.1103/PhysRevD.66.066004.

[13] Mirjam Cvetic, Gary Shiu, and Angel M. Uranga. Three family supersymmetric standard - like models from intersecting brane worlds. *Phys.Rev.Lett.*, 87:201801, 2001. arXiv:hep-th/0107143, doi:10.1103/PhysRevLett.87.201801.

[14] T.P.T. Dijkstra, L.R. Huiszoon, and A.N. Schellekens. Supersymmetric standard model spectra from RCFT orientifolds. *Nucl.Phys.*, B710:3–57, 2005. arXiv:hep-th/0411129, doi:10.1016/j.nuclphysb.2004.12.032.

[15] Michael R. Douglas and Washington Taylor. The landscape of intersecting brane models. *JHEP*, 01:031, 2007. arXiv:hep-th/0606109, doi:10.1088/1126-6708/2007/01/031.

[16] M.B. Green, J.H. Schwarz, and E. Witten. *Superstring Theory: Introduction.* Cambridge Monographs on Mathematical Physics. Cambridge University Press, 1988.

[17] Gabriele Honecker. Chiral supersymmetric models on an orientifold of Z(4) x Z(2) with intersecting D6-branes. *Nucl.Phys.*, B666:175–196, 2003. arXiv:hep-th/0303015, doi:10.1016/S0550-3213(03)00540-6.

[18] Gabriele Honecker. Supersymmetric intersecting D6-branes and chiral models on the T**6 / (Z(4) x Z(2)) orbifold. pages 191–198, 2003. arXiv:hep-th/0309158.

[19] Gabriele Honecker. Chiral N=1 4-D orientifolds with D-branes at angles. *Mod.Phys.Lett.*, A19:1863–1879, 2004. arXiv:hep-th/0407181, doi:10.1142/S0217732304015087.

[20] Gabriele Honecker and Tassilo Ott. Getting just the supersymmetric standard model at intersecting branes on the Z(6) orientifold. *Phys.Rev.*, D70:126010, 2004. arXiv:hep-th/0404055, doi:10.1103/PhysRevD.70.126010,10.1103/PhysRevD.71.069902.

[21] Luis E. Ibanez, F. Marchesano, and R. Rabadan. Getting just the standard model at intersecting branes. *JHEP*, 0111:002, 2001. arXiv:hep-th/0105155.

[22] Fernando G. Marchesano Buznego. Intersecting D-brane models. 2003. Ph.D. Thesis (Advisor: D.Luis E. Ibanez Santiago). arXiv:hep-th/0307252.

[23] M. Nakahara. *Geometry, topology and physics.* 2003. Bristol, UK: Hilger (1990) 505 p. (Graduate student series in physics).

[24] Michael E. Peskin and Dan V. Schroeder. *An Introduction To Quantum Field Theory (Frontiers in Physics)*. Westview Press, 1995.

[25] J.G. Polchinski. *String Theory: Superstring theory and beyond*. Number Bd. 2 in Cambridge Monographs on Mathematical Physics. Cambridge University Press, 2005.

[26] Angel M. Uranga. D-brane probes, RR tadpole cancellation and K theory charge. *Nucl.Phys.*, B598:225–246, 2001. `arXiv:hep-th/0011048`, `doi:10.1016/S0550-3213(00)00787-2`.

[27] B. Zwiebach. *A First Course in String Theory*. Cambridge University Press, 2004.

Erklärung

Ich versichere, dass ich diese Arbeit selbstständig verfasst und keine anderen als die angegebenen Quellen und Hilfsmittel benutzt habe.

Heidelberg, 14. Mai 2012

Martin Bies